University of North Dakota
UND Scholarly Commons

Theses and Dissertations | Theses, Dissertations, and Senior Projects

1997

Chemistry and environmental implications of thio-red and 2,4,6-trimercaptotriazine compounds

Kevin R. Henke
University of North Dakota

Follow this and additional works at: https://commons.und.edu/theses

 Part of the Geology Commons

Recommended Citation
Henke, Kevin R., "Chemistry and environmental implications of thio-red and 2,4,6-trimercaptotriazine compounds" (1997). *Theses and Dissertations*. 135.
https://commons.und.edu/theses/135

This Dissertation is brought to you for free and open access by the Theses, Dissertations, and Senior Projects at UND Scholarly Commons. It has been accepted for inclusion in Theses and Dissertations by an authorized administrator of UND Scholarly Commons. For more information, please contact zeineb.yousif@library.und.edu.

CHEMISTRY AND ENVIRONMENTAL IMPLICATIONS OF THIO-RED® AND 2,4,6-TRIMERCAPTOTRIAZINE COMPOUNDS

by

Kevin R. Henke
Master of Science, University of North Dakota, 1984

A Dissertation

Submitted to the Graduate Faculty

of the

University of North Dakota

in partial fulfillment of the requirements

for the degree of

Doctor of Philosophy

Grand Forks, North Dakota
December
1997

Copyright 1997 Kevin R. Henke

GEOL-
T1997
H388

This dissertation, submitted by Kevin R. Henke in partial fulfillment of the requirements for the Degree of Doctor of Philosophy from the University of North Dakota, has been read by the Faculty Advisory Committee under whom the work has been done and is hereby approved.

Dexter Perkins
(Chairperson)
Richard W. Lesser
Ronald C. McPherson
Philip J. Gerla
Richard J. Baltisberger

This dissertation meets the standards for appearance, conforms to the style and format requirements of the Graduate School of the University of North Dakota, and is hereby approved.

Dean of the Graduate School

Date

PERMISSION

Title Chemistry and Environmental Implications of Thio-Red® and 2,4,6-Trimercaptotriazine Compounds

Department Geology

Degree Doctor of Philosophy

In presenting this dissertation in partial fulfillment of the requirements for a graduate degree from the University of North Dakota, I agree that the library of this University shall make it freely available for inspection. I further agree that permission for extensive copying for scholarly purposes may be granted by the professor who supervised my dissertation work or, in his absence, by the chairperson of the department or the dean of the Graduate School. It is understood that any copying or publication or other use of this dissertation or part thereof for financial gain shall not be allowed without my written permission. It is also understood that due recognition shall be given to me and to the University of North Dakota in any scholarly use which may be made of any material in my dissertation.

Signature Kevin R. Hardy

Date November 18, 1997

TABLE OF CONTENTS

LIST OF FIGURES

LIST OF TABLES

ACKNOWLEDGMENTS

I greatly appreciate the efforts and patience of my committee chair, Dr. Dexter Perkins III, and my other committee members: Drs. Richard D. LeFever, Philip J. Gerla, Ronald K. Matheney, and Richard Baltisberger. Through the kind efforts of Dr. Perkins, I was able to obtain a vital EPSCoR Fellowship. I also thank Dr. Richard D. LeFever, Dr. Patricia Kelley and the Geology Department at the University of North Dakota for support through teaching assistantships. I am very grateful for Dr. Ralph R. Turner and personnel at the Y-12 Nuclear Weapons Plant for providing a two-year appointment to the Postgraduate Research Program administered by the Oak Ridge Institute for Science and Education. Dr. Turner inspired my research and was extremely generous with his funds, laboratory facilities, equipment, and time. The Division of Chemical Sciences in the Office of Basic Energy Sciences and the Environmental Restoration Division of the U.S. Department of Energy under contract with Lockheed Martin Energy Systems, Inc. also provided support for this study. Drs. Greg J. McCarthy and David A. Atwood at the Chemistry Department at North Dakota State University were very generous with advice, technical assistance, and funds. John Harju, Dr. Frank Beaver, Ed Steadman, and Dr. David Charlton of the Energy & Environmental Research Center of the University of North Dakota provided encouragement and financial support. Many chemists, crystallographers, and other professionals were extremely generous with their time and

advice, including: Gail R. Hutchens, Mary Beth Norris, Dr. L. P. Keller, Dr. David Canada, Doyle Hembree, Dean Grier, Ryan Winburn, Bryan R. Jarabek, Terry Munson, Dr. C. L. (Jan) Ma, Dr. Mark Elless, Dr. Leon Maya, Jeffrey Bryan, Norm Smyrl, Rick Slayle, Q. Grindstaff, Dr. David Mogk, Sam Lewis, and others. I also thank Mark Barnett and Dr. S.Y. Lee for their comments on my manuscripts and ideas. Ernest W. Haug of Degussa Corporation and Richard Dunkel of ETUS, Inc. generously provided samples and helpful advice.

I wish especially to thank my wife, Yvonne, and my children, Erin and Kyle, for their love and patience through some very difficult times. They made many sacrifices for my education. I also especially thank my generous parents for their love and financial support over the years.

ABSTRACT

Many compounds, including Thio-Red® and 2,4,6-trimercaptotriazine, trisodium salt (TMT-55), have been marketed to precipitate mercury and other heavy metals from water, including contaminated ground waters. For the products to be effective, information is needed on the chemistry of the products, how they precipitate metals from aqueous solutions, and the chemistries and stabilities of the precipitates.

CS_3^{2-}, HS^-, and S^{2-} are the dominant sulfur species in Thio-Red®. They precipitate heavy metals from water as sulfides (*e.g.*, HgS, PbS, and ZnS). Thio-Red® also contains traces of poisonous carbon disulfide (CS_2). Additional CS_2 could form from reactions between dissolved heavy metals and CS_3^{2-}. Large volumes of undiluted Thio-Red® should not be injected into low oxygen environments for *in situ* restoration until studies eliminate the possibility of contamination from CS_2 or H_2S.

TMT-55 is $Na_3C_3N_3S_3 \cdot 9H_2O$. The crystallographic data at 25°C are $R\bar{3}$, $Z = 6$, a = 17.600(1) Å, c = 9.720(2) Å, V = 2607.5(5) Å^3, and a density of 1.55 g/cm^3.

The precipitation of divalent mercury with TMT-55 may produce one or more mercury 2,4,6-trimercaptotriazine (HgTMT) compounds, including white, greenish yellow to greenish brown, gray, or yellow varieties. The white variety probably contains mercury(I). White HgTMT is monoclinic with a = 5.904(3) Å, b = 6.966(1) Å, c = 4.572(1) Å, β = 104.85(2)°, and V = 181.79 Å^3. Within three months, white HgTMT may

decompose in air or aerated water to the yellow or gray varieties. In batch leachates with distilled and deionized water, white HgTMT may release more than 3 milligrams/liter of mercury. Mercury concentrations in water leachates of gray and bright yellow samples are relatively low (3.3 - 53 micrograms/liter). The gray, yellow and greenish varieties still require extensive chemical analyses and leaching studies to identify any leachable organic compounds. TMT-55 should not be used in the *in situ* restoration of mercury contaminated sites until the resulting precipitates are known to be stable.

Studies of $Ba_3(C_3N_3S_3)_2 \bullet 8H_2O$ and $BaH_4(C_3N_3S_3)_2 \bullet 4.5H_2O$ (BaTMT compounds) were initiated to determine if TMT-55 could be used to remove barium from water. However, the aqueous solubilities of both compounds are probably too high (around 5 grams/liter) for effective barium removal.

The results of powder XRD analyses show that $Ba_3(C_3N_3S_3)_2 \bullet 8H_2O$ is either hexagonal or orthorhombic. The results of a single crystal analysis of $BaH_4(C_3N_3S_3)_2 \bullet 4.5H_2O$ at 25°C state that the compound is monoclinic ($P2_1/c$) with $Z = 4$, calculated density = 2.077 g/cm^3, $a = 8.5576(4)$ Å, $b = 21.028(1)$ Å, $c = 20.276(1)$ Å, $\beta = 96.440(1)°$, and $V = 3625.6(3)$ Å^3.

CHAPTER 1

INTRODUCTION

During the last few decades, federal and state governments have instituted environmental regulations to protect the quality of surface and ground waters from divalent "heavy metal" pollutants, such as barium, copper, lead, mercury, and zinc (*e.g.*, 40 Code of Federal Regulations [CFR] 141, 261.24, and 268.40). In response to the regulatory requirements, manufacturers have developed and marketed chemical products to precipitate heavy metals from waste waters. Additionally, some of the chemicals have been used to remove heavy metals from contaminated surface waters and ground waters. Contaminated ground waters, for example, may be pumped to the surface and treated or, in some cases, the products may be injected into the subsurface for *in situ* restoration (ETUS, Inc., 1994).

The efficient use of any commercial chemical treatment product requires basic information on the chemistry of the product, the precipitation reactions associated with the product, and the chemistry of the resulting precipitates. Furthermore, if the precipitates ultimately reside in the subsurface, which would be the case in *in situ* ground water treatment applications, information on the chemistry and crystallinity of the precipitates would be useful to assure environmental regulators that the precipitates will not deteriorate over time and release heavy metals back into the environment.

Thio-Red® (manufactured and distributed by ETUS, Inc. of Sanford, Florida) and 2,4,6-trimercaptotriazine, trisodium salt (TMT-55, a product of Degussa Corporation USA of Allendale, New Jersey) are commercial products that are widely used to remove divalent heavy metals from water. Thio-Red® is a red aqueous solution and TMT-55 is a white powder. Degussa Corporation also sells TMT-15, which is a 15-weight percent (wt%) aqueous solution of TMT-55.

Many papers discuss the effectiveness of TMT-55 or Thio-Red® in removing copper, mercury, and other heavy metals from waste waters (*e.g.*, Tarabocchia and Karg, 1990). Degussa Corporation (1993) and Ayoub et al. (1995) also summarize studies on the toxicity of TMT-55. However, inadequate information is available on the chemistry of the commercial products, how they precipitate heavy metals from aqueous solutions, and the chemistry of the precipitates. The major objectives of this dissertation study are to: 1) better define the chemical composition of Thio-Red® without revealing proprietary information on the exact concentrations of the constituents in the product; 2) identify the chemical reactions involved in the precipitation of mercury, copper, lead, and zinc with Thio-Red®; 3) determine the chemistry and crystalline properties of TMT-55, mercury 2,4,6-trimercaptotriazine (HgTMT), and barium 2,4,6-trimercaptotriazine (BaTMT) compounds; 4) discuss some batch leaching properties of HgTMT compounds in distilled and deionized water; and 5) comment on the potential environmental impacts on natural water quality from the use of the commercial products. Once these goals are achieved, future laboratory and field investigations can verify and better define any environmental impacts.

CHAPTER 2

MATERIALS AND METHODS

Introduction

This chapter discusses the materials and methods that were frequently used in the research presented in this dissertation. Chapters 3-7 contain information on materials and methods that were only used with specific compounds or experiments. Unless otherwise specified, the experimental conditions were 22+/-3°C and normal atmospheric pressure.

Materials

Mr. Ernest W. Haug of Degussa Corporation and Mr. Richard Dunkel of ETUS, Inc. generously supplied samples of TMT-55 and Thio-Red®. Mr. Haug supplied some TMT-15, although most samples were prepared by dissolving 15 grams (g) of TMT-55 into every 100 g of distilled or distilled and deionized water.

The experiments used two different batches of Thio-Red®. The first batch, which was prepared in 1993 (an unknown lot), had a volume of only 100 milliliters (ml) and a pH of 13.4. A small number of analyses and experiments quickly depleted the pH 13.4 Thio-Red®. The experiments and analyses were later duplicated with a fresh and less alkaline second batch. The second batch of Thio-Red® (lot 2567-155) had an initial volume of 19 liters (five gallons) and was first used within a few days after its preparation on February

13, 1995. The initial pH of the second batch after arrival from ETUS, Inc. was 12.0. During the next three months, the pH slowly increased and finally stabilized at 12.2.

Several powder x-ray diffraction (XRD) standards were used to calibrate the *d*-values of the previously unstudied 2,4,6-trimercaptotriazine (TMT) compounds. Fluorophlogopite (National Bureau of Standards [NBS] Standard Reference Material SRM-675) and gypsum (Sigma lot number 94H0320) (XRD data from Powder Diffraction File [PDF] 21-816) were especially useful in calibrating *d*-values above 4.00 Å. Silicon (NBS Standard Reference Material SRM-640b) was used to calibrate *d*-values below 1.00 Å. For intermediate *d*-values between 1.00 and 4.00 Å, corundum (Baker-analyzed reagent grade, lot number 32435) (PDF 42-1468) and silicon were sometimes useful. Powder XRD confirmed the purities of the standards.

Routine powder XRD identification of compounds in samples, such as precipitates from solutions treated with Thio-Red®, used Vaseline® or alcohol mounts. The identification and calibration of previously unstudied 2,4,6-trimercaptotriazine (TMT) compounds used Vaseline®, acetone, alcohol or side mounts. A side mount is prepared by clamping a slotted aluminum slide between two glass slides and carefully packing a dry finely ground sample into the slot. The glass slides are then removed and the aluminum slide with the packed sample is placed in the diffractometer for analysis. Although side mounts require a large amount of sample, they have many advantages. Specifically, they usually result in particles with adequate random orientations, which are critical in determining the relative intensities of XRD peaks in new compounds. They also use no acetone or other mounting liquids that may react with the sample and chemically alter it.

All experiments used reagent grade compounds, which included: Mallinckrodt copper(II) sulfate pentahydrate ($CuSO_4 \cdot 5H_2O$) (an unknown lot), Fisher Scientific copper(II) chloride dihydrate ($CuCl_2 \cdot 2H_2O$) (lot 712305), Mallinckrodt red mercury(II) oxide (HgO) (lot 1426 KBJS), "Baker Analyzed" mercury(II) chloride ($HgCl_2$) (lot 243348), Mallinckrodt lead nitrate ($Pb[NO_3]_2$) (an unknown lot), EM Science zinc(II) chloride ($ZnCl_2$) (lot 31149318), Matheson Coleman & Bell zinc acetate dihydrate ($Zn[CH_3CO_2]_2 \cdot 2H_2O$) (lot A10F20), "Baker Analyzed" barium chloride dihydrate ($BaCl_2 \cdot 2H_2O$) (lot 32562), and Strem Chemicals barium hydroxide octahydrate ($Ba(OH)_2 \cdot 8H_2O$) (lot 138929-S). Homogeneous dark brown anhydrous copper(II) chloride ($CuCl_2$) was prepared by heating several grams of bluish green $CuCl_2 \cdot 2H_2O$ in an oven at 100°C over several days.

The distilled and deionized water was at least 16 megaohms•cm (Mohm•cm), whereas the resistivity of the distilled, nondeionized water was unknown. In some experiments, the distilled and deionized water was deaerated with ultrapure (99.999%) nitrogen gas.

Acids included 37.8 to 37.9 volume percent (v%) (various lots) Baker-Instra hydrochloric acid (HCl) and 70.8 v% (lot H22039) Baker-Instra nitric acid (HNO_3). Mercury analyses of water samples used reagent grade acids, because frequently ultrapure acids become contaminated with significant amounts of mercury during the distillation process (Henke et al., 1993, p. 46). Stannous chloride ($SnCl_2$) solutions were produced by mixing 200.0 g of stannous chloride dihydrate ($SnCl_2 \cdot 2H_2O$) with 100 ml of Baker-Instra HCl and diluting the mixture to one liter with distilled and deionized water. The

$SnCl_2$ solutions were then bubbled with ultrapure nitrogen gas for 24 hours to remove any trace amounts of mercury and to guarantee that the $SnCl_2$ had entirely dissolved. Bromine monochloride (BrCl) was produced by dissolving 5.4 g of potassium bromide in 500 ml of concentrated HCl. The solution was stirred for one hour and then 7.6 g of $KBrO_3$ were added while stirring continued. Batches of trithiocyanuric acid ($H_3C_3N_3S_3$) were prepared by adding 40 ml of Baker-Instra HCl to a 500-ml aqueous solution of 59.0 g of TMT-55. The solid $H_3C_3N_3S_3$ was recovered, thoroughly washed with distilled water to remove sodium and chloride, and allowed to air dry. Table 1 lists the chemical results for a $H_3C_3N_3S_3$ sample. The analysis was done on a Perkin Elmer Series II 2400 CHNS/O analyzer with an acetanilide ($CH_3CONHC_6H_5$) standard. The results in Table 1 suggest that the acid is structurally anhydrous.

Table 1. Chemical results of trithiocyanuric acid ($H_3C_3N_3S_3$). Sulfur was not analyzed. The results are normalized on the ideal sulfur concentration. The ideal chemistry of anhydrous $H_3C_3N_3S_3$ is also listed.

Parameters	Measured Concentrations (wt%)	Ideal Concentrations (wt%)
Carbon	20.42	20.33
Hydrogen	1.60	1.71
Nitrogen	23.28	23.71
Sulfur	54.26 (not measured)	54.26
Total	99.56	100.01
Formula	$H_{2.9}C_{3.1}N_{3.0}S_{3.0}$	$H_3C_3N_3S_3$

Analytical Methods

Mass measurements were usually made on either a Sartorius balance to the nearest 0.01 g or a Mettler AE 163 balance to the nearest 0.0001 g. Both balances were checked with standard weights several times per week and calibrated every six months. The mass measurements mentioned in Chapters 6 and 7 were normally done on another Sartorius balance to the nearest 0.01 g. The calibration history of this balance was not well defined.

Gilson volume adjustable pipettes were used to measure microliter (μl) and ml volumes up to 5 ml. The pipettes were checked daily either on the well-calibrated Sartorius or Mettler AE 163 balances. Volumes more than 5 ml were either measured with a graduated cylinder to the nearest 0.5 ml or determined by mass to the nearest 0.01 g with a Sartorius balance.

Approximate pH values were sometimes obtained with paper strips. All other pH measurements were done with an Orion model 710A pH/ISE meter. The meter was calibrated with pH 4.00, 7.00, and 10.00 +/- 0.01 VWR Scientific buffers. Additionally, the calibrations were periodically checked against pH 1.79 - 2.00 HCl solutions.

Details on the chemical analyses are presented in Chapters 3-7. Unless otherwise stated, the author analyzed his own samples. However, usually, the analyses were done by technicians and professional analytical chemists at a commercial laboratory (Materials Engineering and Testing [ME&T] Corporation) and two federal research facilities (Oak Ridge National Laboratory [ORNL] and the Y-12 Nuclear Weapons Plant [Y-12]). These laboratories are in Oak Ridge, Tennessee.

Powder XRD analyses were done at ORNL, in the Department of Chemistry at North Dakota State University (NDSU), Fargo, North Dakota, and in the Department of Geology and Geological Engineering at the University of North Dakota (UND), Grand Forks, North Dakota. The ORNL diffractometer was a Scintag DMS 2000 equipped with cobalt $K\alpha_1$ ($\lambda = 1.78896$ Å) radiation, whereas the NDSU and UND instruments were Philips diffractometers with copper $K\alpha_1$ ($\lambda = 1.540598$ Å) radiation. For routine identifications, samples (such as metal sulfides) were typically step scanned from 2.00 to 90.00° 2θ (when measured with $CuK\alpha_1$ radiation) using 0.02° 2θ steps at one second per step. The *d*-values of sodium thiocarbonate samples and previously unstudied TMT compounds were calibrated using 0.0125 to 0.02° 2θ steps at one to two seconds per step over $CuK\alpha_1$ 2θ ranges as large as 2.00 to 140.00°. Patterns produced at ORNL were compared with reference patterns in the International Centre for Diffraction Data (ICDD) (Newtown Square, Pennsylvania, USA) Mineral PDF computer database. NDSU had copies of the ICDD Mineral and Organic PDF computer databases. A PDF card catalog of inorganic and some organic compounds was available at the UND laboratory.

Several computer programs, including TREOR90 (updated version of Werner et al., 1985), DICVOL91 (Boultif and Louer, 1991), PIRUM (updated version of Werner, 1969), NBS*AIDS83 (expanded version of Mighell et al., 1981), LSUCRI (Garvey, 1986 after Appleman and Evans, 1973), and Micro-POWD (Smith and Smith, 1993) were used to calculate theoretical XRD powder patterns and identify the crystal systems and unit cell parameters of previously unstudied compounds. Some programs and their user's manuals are public domain software and copies are available from web sites on the Internet.

Accuracy and Precision of Methods

Personnel at ME&T Corporation, ORNL, and Y-12 provided only limited information on the accuracy and precision of their analyses. As shown in Table 1 and several tables in Chapters 4-7, the reliability of chemical analyses of solid samples may be estimated by comparing the results with ideal compositions, which are often based on formulas from single crystal XRD analyses. The reliability of the chemical data also may be evaluated by how closely the results sum to 100 wt%. Except for mercury and carbon measurements of the light gray and medium yellow HgTMT samples in Chapter 6, differences between the measured values and ideal concentrations were no more than 8% and rarely exceeded 4%. Personnel at ME&T Corporation provided duplicate analyses of the sodium concentration for pH 12.2 Thio-Red® and the nitrogen concentration for the white HgTMT sample in Chapter 6. The original concentrations and their duplicates were within ±2% of their averages.

For $H_3C_3N_3S_3$ (Table 1) and the BaTMT compounds in Chapter 7, carbon, nitrogen, and nonaqueous hydrogen analyses were done at NDSU. The acetanilide standard was analyzed before and after the sample measurements. Analyses of the acetanilide standard were always within ±0.5% of the required concentrations for carbon (71.09 wt%), hydrogen (6.71 wt%), and nitrogen (10.36 wt%). As shown in tables in Chapter 7, duplicate and original analyses of the BaTMT compounds were within ±3% of their averages.

A chemist at Y-12 analyzed the carbon disulfide (CS_2) concentration of pH 12.2 Thio-Red® with a Finnigan 5100 ion/mass chromatograph. The analysis easily detected

CS_2, but the analytical chemist claimed that the measurements were only semiquantitative because the accuracy was about ±50%. There were also accuracy errors of approximately ±50% associated with the sulfite concentration in the pH 12.2 Thio-Red®. The sulfite errors resulted from the partial oxidation to sulfate of the sulfite compounds used to produce the analytical standards. Because of the large errors, the sulfur concentrations of CS_2 and sulfite are reported in Chapter 3 as single digit "less than" percentages of the total sulfur concentration in pH 12.2 Thio-Red® (*i.e.*, <0.1% and <2%, respectively).

An Orion silver/sulfide electrode measured the total free sulfide (*i.e.*, $H_2S^\circ + HS^- + S^{2-}$) and S^{2-} concentrations of the pH 12.2 Thio-Red®. Orion Research Inc. (1991, p. 47) states that the electrode has a reproducibility of ±4%. A duplicate analysis was done on the S^{2-} concentration of undiluted pH 12.2 Thio-Red®. The duplicate and original analyses were within ±3% of their average.

As discussed in Chapter 6, the mercury concentrations of HgTMT leachates were measured with a method developed by Dr. Ralph R. Turner at ORNL (Kriger and Turner, 1995; Šolc et al., 1997). Based on mercury standards and blanks, the accuracy of the mercury analyses was approximately ±12%. Initial and duplicated concentrations were always within ±12% of their averages. For replicate measurements of water samples with their method, Kriger and Turner (1995, p. 1297) report a typical standard deviation of about 10%.

The pH 13.4 Thio-Red® was analyzed for total carbon and sodium. As discussed in Chapter 3, the precision of multiple sodium measurements of a sample was always within ±1% of the average. However, multiple carbon measurements varied as much as ±

6% from the average. The accuracies of the carbon and sodium measurements were more difficult to determine because the small volume of pH 13.4 Thio-Red® prevented a thorough chemical examination. Based on measurements of the standards, the accuracy of the sodium analyses for the pH 13.4 Thio-Red® was estimated at ±1%, whereas the accuracy of the carbon results was approximately ±8%.

ME&T personnel measured the sodium, sulfur, and potassium concentrations of the pH 12.2 Thio-Red®. Duplicate and original sodium analyses were within ±2% of their average. Furthermore, as discussed in Chapter 3, the concentrations were consistent with the chemical composition of Thio-Red®, as stated in ETUS, Inc. (1994) and by an XRD analysis of dried solid residues of pH 12.2 Thio-Red® (Chapter 4).

A technician at ORNL analyzed both batches of Thio-Red® for sulfate. He used an ion chromatography method from Clesceri et al. (1989). He also stated that the accuracy and precision data in this reference would apply to the Thio-Red® measurements. In Clesceri et al. (1989, p. 4-6), the chromatography method was tested by spiking reagent water with 0.51 mg/l of sulfate and distributing the sample to 15 laboratories. The sulfate concentration in the sample was similar to the sulfate concentrations in the analyzed dilutions of the two Thio-Red® samples. The average of the sulfate measurements from the 15 laboratories was 0.52 mg/l, which was only 2% greater than the actual value. The precision of the values from the 15 laboratories was 0.07 mg/l or less than 14% of the concentration.

CHAPTER 3

CHEMICAL COMPOSITION OF THIO-RED®

Introduction

Thio-Red® is an orange-red to red liquid with a pH of around 12 when freshly prepared. Although the absolute concentrations of the dissolved species in Thio-Red® are proprietary, ETUS, Inc. (1994) and the results of chemical analyses by the author state that the liquid is an aqueous solution of sodium (with or without potassium) thiocarbonate ($[Na,K]_2CS_3 \bullet nH_2O$, where $n \geq 0$). At the request of the manufacturer, the exact concentrations of the various dissolved species in Thio-Red® will not be discussed.

Materials and Methods

Both batches of Thio-Red® were chemically analyzed. ETUS, Inc. (1994) states that the only abundant chemical components in Thio-Red® should be sodium, carbon, and sulfur. The small volume of pH 13.4 Thio-Red® only allowed for a few chemical analyses. Sodium and carbon concentrations were obtained with an IRIS Thermo Jarrell Ash inductively coupled argon plasma spectrometer (ICP) at ORNL. The measurements were done under guidelines established by Thermo Jarrell Ash and the supervising analytical chemist. The calibration curve was produced from a distilled water blank and two standards: one containing 9.8 mg/l of carbon and 9.4 mg/l of sodium and the other

consisting of 100 mg/l of carbon and 96 mg/l of sodium. Carbon was measured at a wavelength (λ) of 193.090 nanometers (nm), whereas sodium used two wavelengths at 330.2 and 588.9 nm. For every standard, blank, and sample, the sodium and carbon concentrations were measured three times and averaged. The triple sodium measurements were always within ±1% of their averages. Carbon stuck to the plasma torch and, when compared with sodium, the torch required longer rinsing with distilled water between analyses to remove the carbon. The carbon adherence caused the triple carbon measurements to vary by as much as ±6% from their averages. Based on measurements of the standards, the sodium analyses for the pH 13.4 Thio-Red® had an estimated accuracy of ±1%, whereas the accuracy of the carbon results was approximately ±8%.

The second batch of Thio-Red® (pH 12.2) with its larger volume allowed for more extensive characterization studies. Professional chemists at ME&T Corporation measured the sodium, potassium, and total sulfur concentrations. Sodium and potassium were analyzed with a Leeman Labs, Inc. Model PS Spec ICP using U.S. Environmental Protection Agency (U.S. EPA) method 6020 (U.S. EPA, 1990). The total sulfur concentration of the pH 12.2 Thio-Red® was determined by oxygen bomb combustion (American Society for Testing Materials [ASTM] method D808) followed by analysis with the Model PS Spec ICP using U.S. EPA method 6020 (ASTM, 1992; U.S. EPA, 1990).

A professional technician at ORNL analyzed both batches of Thio-Red® for sulfate and semiquantitative sulfite. The sulfate and sulfite analyses were done on a Dionex ion chromatograph with revised methods from Clesceri et al. (1989) and ASTM D4327 (1991). A professional chemist at Y-12 measured the carbon disulfide (CS_2)

concentrations in several aliquots of the pH 12.2 Thio-Red® with a Finnigan 5100 ion/mass chromatograph. Total free sulfide measurements on the pH 12.2 Thio-Red® used a combination of an Orion 94-16 silver/sulfide electrode, an Orion 90-20 double junction reference electrode, and an Orion 710A pH/ISE meter (Orion Research, Inc., 1991). Orion Research Inc. (1991, p. 47) states that the silver/sulfide electrode can measure sulfide concentrations between 0.003 and 32,000 mg/l with ±4% reproducibility at 0-80°C.

The sulfide analysis included a sulfide antioxidant buffer (SAOB), which converted HS^- and H_2S to S^{2-} and allowed for the measurement of the total free sulfide concentration. The composition of the SAOB, which was derived from an older than 1991 version of the instructions for the Orion silver/sulfide electrode, consisted of 16.0 g of EM Science NaOH, 64.0 g of J.T. Baker sodium salicylate and 14.4 g of "Baker Analyzed" ascorbic acid diluted in 200 ml of deaerated, distilled and deionized water. Durst (1969, p. 179, 430), Moody and Thomas (1971, p. 60), Orion Research, Inc. (1991) and conversations with a technical person at Orion Research, Inc. state that sulfur species (*e.g.*, thiosulfate, sulfate, thiocarbonates, and even polysulfides) and other dissolved forms expected in Thio-Red® should not significantly interfere with the measurement of total free sulfide as S^{2-} with a silver/sulfide electrode.

Results and Discussion

A comparison of the sodium concentrations of the two batches of Thio-Red® found that the molarity of the sodium thiocarbonate in the first batch was about 30%

higher than the molarity in the second batch. The second batch also contained significant amounts of potassium, although sodium was much more abundant. Variations in the concentrations of sodium thiocarbonate are probably related to the unknown proprietary process used to produce Thio-Red®. The molar ratio of the sulfur to the combined sodium and potassium concentrations for the second batch (S/Na+K) was 1.5, which is consistent with an aqueous solution of $(Na,K)_2CS_3 \cdot nH_2O$.

The total carbon concentration of the pH 13.4 Thio-Red® was about 30% higher than predicted from its $(Na,K)_2CS_3 \cdot nH_2O$ concentration. The excess carbon may result from the tendency of aqueous $Na_2CS_3 \cdot nH_2O$ solutions to react with carbon dioxide in the atmosphere (Ingram and Toms, 1957).

Information on the composition of Thio-Red® and discussions in ETUS, Inc. (1994) suggest that the reduced sulfur species in the liquid should control the precipitation of heavy metals in aqueous solutions. As shown in Table 2, the concentrations of sulfur in various species in pH 12.2 Thio-Red® are expressed as percentages of the total sulfur concentration. The percentages were determined by calculating the number of moles of sulfur in each species (*e.g.*, moles of sulfur in sulfate), dividing the value by the total sulfur concentration in moles, and multiplying by 100 to convert to a percentage. Measurements with a silver/sulfide electrode suggest that about 19 wt% of the total sulfur concentration in pH 12.2 Thio-Red® is associated with total free sulfide. Although Thio-Red® has a noticeable H_2S odor, at pH 12.2 the H_2S^o concentration would be insignificant when compared with the HS^- and S^{2-} concentrations (Faure, 1991, p. 198-199). Using dissociation constants from Faure (1991, p. 198-199), the activity ratio of HS^- to S^{2-}, or

$[HS^-]/[S^{2-}]$, at pH 12.2 is 5.13. Without using the SAOB to convert H_2S^o and HS^- to S^{2-}, the silver/sulfide electrode measured that the S^{2-} concentration of the undiluted pH 12.2 Thio-Red® as 6.2 wt% of the total sulfur concentration (Table 2). The ratio of the absolute concentrations of HS^- to S^{2-}, *i.e.*, $(HS^-)/(S^{2-})$, in the undiluted Thio-Red® is 2.0, which is reasonable for a high ionic strength pH 12.2 solution.

Table 2. Percent of the total sulfur concentration in various species in undiluted pH 12.2 Thio-Red®.

Sulfur Species	Percentage of Total Sulfur Concentration	Analysis Method
CS_3^{2-}	75	Titrations, X-ray diffraction
HCS_3^-	<0.1	Estimated from activity calculations
$H_2CS_3^o$	<0.1	Estimated from activity calculations
CS_2	<0.1	Ion/mass chromatography
$H_2S^o + HS^- + S^{2-}$	19	Sulfide electrode
S^{2-}	6.2	Sulfide electrode
HS^-	13	Sulfide electrode
H_2S^o	<0.1	Estimated from activity calculations
SO_3^{2-}	<2	Ion chromatography
SO_4^{2-}	0.06	Ion chromatography
Polysulfides, thiosulfate, COS, $HCOS_2^-$, $H_2CS_2O_2^{2-}$, others	4-6	Calculated by difference from the other percentages
Total	100	ASTM D808; U.S. EPA method 6020

The ionic strength of pH 12.2 Thio-Red® was estimated at 1.4-2.6 by three different methods. The usual method for estimating ionic strength involves summing the concentrations and charges of the major ions as shown in equation 1 (Faure, 1991, p. 214):

1) $I = 0.5 \Sigma m_i z_i^2$

where:

I = ionic strength

m_i = concentrations in moles of ionic species

z_i = charge of ionic species.

Although the concentrations of some species, such as CS_3^{2-}, could only be estimated, this approach provided an ionic strength of about 1.8. Snoeyink and Jenkins (1980, p. 76) provide two other equations that estimate ionic strength from the total dissolved solids (TDS) concentration in milligrams/liter (mg/l) and the conductivity (SC) of the solution in μmho/cm:

2) $I \approx 2.5 \times 10^{-5} \times \text{TDS}$

3) $I \approx 1.6 \times 10^{-5} \times \text{SC}$

The ionic strength based on TDS was 2.6, whereas the conductivity of the solution provided a value of 1.4. Ionic strengths of 2 are high enough so that the activities and concentrations of most dissolved species in Thio-Red® should not be equal. That is, their activity coefficients (γ) would not equal one (Krauskopf, 1979, p. 60; Faure, 1991, p. 214). The high ionic strength of Thio-Red® and the charge differences in HS^- and S^{2-} explains why $[HS^-]/[S^{2-}]$ and $(HS^-)/(S^{2-})$ are different.

Sulfate and sulfite were not very abundant in either batch of Thio-Red®, which suggested that the samples were not well oxidized. Sulfate concentrations for both the pH 12.2 and 13.4 Thio-Red® samples represented less than 1 wt% of the total sulfur in the solutions, whereas the sulfite concentrations in both batches were estimated to represent less than 2 wt% of the total sulfur (Table 2).

Thiocarbonate, like carbonate, exists in three dissolved forms (*i.e.*, CS_3^{2-}, HCS_3^-, and $H_2CS_3^\circ$) in aqueous solutions. The relative activities of CS_3^{2-}, HCS_3^-, and $H_2CS_3^\circ$ in Thio-Red® may be calculated by using dissociation constants and pH. Gattow and Krebs (1963) concluded that $H_2CS_3^\circ$, like $H_2CO_3^\circ$, will dissociate in water through two steps:

4) $H_2CS_3^\circ = HCS_3^- + H^+$

5) $HCS_3^- = CS_3^{2-} + H^+$

In reality, as discussed in Krauskopf (1979, p. 24), hydronium (H^+) is hydrated and exists as H_3O^+, as well as other relatively minor species, including: $H_5O_2^+$ and $H_7O_3^+$. For simplicity, the hydronium ion is normally written as H^+, but it is understood that water is involved in both sides of a reaction (*e.g.*, $HCS_3^- + H_2O = CS_3^{2-} + H_3O^+$, $H_5O_2^+$, $H_7O_3^+$, etc.).

The dissociation constant (K_{a1}) for Reaction 4 was measured by Gattow and Krebs (1963) as 2.1×10^{-3} at 20°C, while they estimated the K_{a2} for Reaction 5 as 6×10^{-9} at the same temperature. At equilibrium, the K_a values provide activity ratios of $[CS_3^{2-}]/[HCS_3^-] = 9000$ and $[HCS_3^-]/[H_2CS_3^\circ] = 3 \times 10^9$ for pH 12.2 Thio-Red®. These calculations show that the activities of $H_2CS_3^\circ$ and HCS_3^- in Thio-Red® should be negligible compared with the activity of CS_3^{2-}.

Although many laboratories were contacted about measuring the concentrations of thiocarbonate species in Thio-Red®, none of them could do the analyses. As alternatives, the CS_3^{2-} abundance was estimated by titrating pH 12.2 Thio-Red® into $CuCl_2$ and $Pb(NO_3)_2$ solutions and by boiling dry approximately 400 ml of pH 12.2 Thio-Red® and analyzing the solid residues by XRD. The next chapter discusses the details of the titration and XRD studies. The XRD analyses detected abundant anhydrous Na_2CS_3 (PDF 14-598) in the solid residues. The titrations suggest that about 75 wt% of the total sulfur in Thio-Red® is probably associated with CS_3^{2-} (Table 2). The data in Table 2 still leave about 4-6 wt% of the total sulfur unspeciated. Ingram and Toms (1957) and Adewuyl and Carmichael (1987) state that thiocarbonates in aqueous solutions may react with CO_2, O_2, HS^-, and OH^- to form many complex sulfur species (*e.g.*, COS, $HCOS_2^-$, and $H_2CS_2O_2^{2-}$). The proprietary process used to prepare Thio-Red® could also generate many unidentified sulfur species. The identities and concentrations of these potentially diverse species could not be determined at this time because many of them have properties that are poorly understood and analytical standards and reliable methods are generally not available.

Most treatment applications with Thio-Red® would involve adding small amounts of the liquid to large volumes of slightly alkaline or slightly acidic waste waters. Under such conditions, the relative concentrations of most of the sulfur species in the Thio-Red® dose would rapidly change as the dose enters the waste water. The nature of the changes would depend upon the contaminant concentrations and speciation, oxygen levels, pH and other properties of the waste water. Nevertheless, as discussed in the next chapter and in

ETUS, Inc. (1994), Thio-Red® consistently and effectively precipitates heavy metals from aqueous solutions with very different heavy metal concentrations and pH values.

CHAPTER 4

REACTIONS BETWEEN THIO-RED® AND AQUEOUS SOLUTIONS OF DIVALENT HEAVY METALS

Previous Investigations

Few documents discuss the compositions of precipitates that result from reacting Thio-Red® or more dilute aqueous solutions of $Na_2CS_3 \bullet nH_2O$ or $K_2CS_3 \bullet nH_2O$ with aqueous solutions containing dissolved heavy metals. ETUS, Inc. (1994) states that Thio-Red® precipitates stable metal thiocarbonates (MCS_3, where $M = Pb^{2+}$, Cu^{2+}, Ni^{2+}, Cd^{2+}, Zn^{2+}, or other divalent heavy metals), which may be produced through the following general reaction:

6) $CS_3^{2-} + M^{2+} \rightarrow MCS_3\downarrow$.

Some metal thiocarbonates form from mixing metal salts with trithiocarbonic acid (H_2CS_3), which should be present as a minor hydrolysis product in Thio-Red®. Metal thiocarbonates may also develop from adding metal salts to $Na_2CS_3 \bullet nH_2O$ or $K_2CS_3 \bullet nH_2O$ solutions that are more dilute than Thio-Red®. As examples, Johri et al. (1970) obtained $PbCS_3$, $CdCS_3$, $CuCS_3$, $NiCS_3$, and $ZnCS_3$ by adding metal salts to 0.1 molar (M) solutions of $K_2CS_3 \bullet nH_2O$. However, Johri et al. (1970) obtained metacinnabar (black isometric HgS) rather than $HgCS_3$ by adding $HgCl_2$ to a 0.1 M $K_2CS_3 \bullet nH_2O$ solution.

References to $HgCS_3$ were not found in the peer-reviewed literature. O'Donoghue and Kahan (1906) produced bright crimson red $PbCS_3$, pale yellow and supposedly crystalline $ZnCS_3$, and possibly pale yellow or reddish yellow $CdCS_3$ by reacting unknown lead, zinc, and cadmium compounds with a solution containing H_2CS_3. However, all metal thiocarbonates described by O'Donoghue and Kahan (1906) were unstable and rapidly decomposed to metal sulfides (*i.e.*, PbS, CdS, and ZnS = *M*S) and flammable and poisonous liquid carbon disulfide (CS_2) in 30 minutes or less through this reaction:

7) $MCS_3 \rightarrow MS + CS_2$.

Ingram and Toms (1957, p. 4333) also obtained bright crimson red $PbCS_3$ by reacting a relatively dilute (0.001 M) $Na_2CS_3 \cdot 2H_2O$ solution with an unknown amount of $Pb(NO_3)_2$. The $PbCS_3$ also decomposed to PbS and CS_2 within a few hours through Reaction 7.

The crystallographic properties of metal thiocarbonates are largely unknown. The 1995 ICDD Inorganic database was searched for XRD reference patterns of silver, cadmium, copper, mercury, lead, and zinc thiocarbonates. Only two patterns were found, both of which were $PbCS_3$ (PDF 22-0382 and 23-0340).

Materials and Methods

A solid precipitate produced from adding pH 12.2 Thio-Red® to a $ZnCl_2$ solution was analyzed for zinc, carbon, sulfur, and hydrogen (for water) by personnel at ME&T Corporation. The zinc analysis was done with a Model PS Spec ICP using U.S. EPA method 6020 (U.S. EPA, 1990). ASTM methods E777 and D4239 were used to determine the carbon and sulfur contents, respectively (ASTM, 1992). The water content

was calculated from a hydrogen analysis using a modification of ASTM D3178 (ASTM, 1992). The modification in the ASTM procedure consisted chiefly of adjustments in the volumes of reagents to correspond with smaller sample sizes.

Approximately 400 ml of pH 12.2 Thio-Red® were boiled dry in air at 100°C. The solid residue was then analyzed by XRD. The *d*-values were calibrated with a fluorophlogopite standard.

Results

As part of the initial efforts to understand how Thio-Red® reacts with dissolved divalent metals, Thio-Red® was added to 15.0-300 ml aqueous solutions containing: $CuCl_2$, $CuSO_4 \cdot 5H_2O$, $Pb(NO_3)_2$, $HgCl_2$, red HgO, or $ZnCl_2$. Aqueous solutions with large concentrations of heavy metals were first used to guarantee that enough precipitates would form for XRD and other analyses (Table 3). The pH 12.2 Thio-Red® was added to the $Pb(NO_3)_2$ and $ZnCl_2$ solutions, whereas the other solutions used the older pH 13.4 Thio-Red®. A formula in ETUS, Inc. (1994) was used to calculate the dosages of Thio-Red® for the solutions:

8) $D = p \times V \times Y$

where:

D = dosage of Thio-Red® in ml

p = part per million (ppm) concentration of the metal contaminant

V = volume of the treated solution in gallons

Y = constant.

Table 3. Contents of initial heavy metal solutions treated with Thio-Red®.

Dissolved Compound	Volume of Water (ml)	Mass of Compound in Water (g)	Volume of Thio-Red® Added (ml)
$CuCl_2$	100	0.31	2.00
$CuSO_4 \cdot 5H_2O$	100	0.80	2.00
$Pb(NO_3)_2$	15.0	0.64	3.30
$ZnCl_2$	300	1.52	12.0
$HgCl_2$	100	0.61	6.10
HgO	100	0.20	2.00

Each metal has its own constant for Y (Table 4). The values of Y are inversely proportional to the atomic weights of the metals. ETUS, Inc. (1994) does not contain a Y value for mercury (Y_{Hg}), so an intermediate value of 0.04 was used in the experiments described in Table 3. Later experiments used an estimated Y_{Hg} of 0.02, which was calculated by using proportions based on the atomic weights and Y values of other elements.

In every case, the addition of Thio-Red® immediately produced precipitates. Black precipitates formed in the mercury and copper solutions. The $Pb(NO_3)_2$ solution produced black and silver solids, whereas the $ZnCl_2$ solution yielded a yellowish white precipitate. The solutions were centrifuged and the precipitates were recovered, air dried, and submitted for XRD. Initially, some precipitates were not washed with water so that any potential thiocarbonate compounds would not dissolve or possibly decompose through Reaction 7. Later, residues from the $CuSO_4 \cdot 5H_2O$ solution, which contained a

substantial amount of water soluble compounds, were washed with distilled and deionized water and reanalyzed by XRD.

Table 4. Values of *Y* for different metals, which are used to calculate the Thio-Red® dosage. Except for the estimated value for mercury, all other values are from ETUS, Inc. (1994).

Element	Atomic Weight	*Y*
Cadmium	112.40	0.0362
Copper	63.546	0.0641
Mercury	200.59	0.02 (estimated)
Nickel	58.71	0.0693
Lead	207.2	0.0196
Zinc	65.38	0.0622
Other metals or mixtures of different or unknown metals	-	0.04

Table 5 lists the XRD results. The unwashed precipitate from the $CuSO_4 \cdot 5H_2O$ solution contained a few minor unidentified XRD peaks, which may be associated with villamaninite (CuS_2). Overall, however, XRD scans for both the washed and unwashed samples easily matched the patterns of well-known sulfides, including metacinnabar (HgS), covellite (CuS), galena (PbS) and sphalerite (ZnS). Except for ZnS, the peaks were very sharp and intense. Figure 1 compares the XRD patterns of a highly crystalline PbS precipitate from the $Pb(NO_3)_2$ solution with the ZnS precipitate from the $ZnCl_2$ solution.

The ZnS peaks are broad, which may suggest that the sample is hydrated, unknown amorphous materials are also present, and/or the crystals are extremely small (*i.e.*, nanocrystalline). Observations with a binocular microscope show that the precipitate almost entirely consists of waxy yellow flakes with small amounts of black particles, which may be carbon. A chemical analysis of the precipitate shows that its composition is more consistent with ZnS than $ZnCS_3$ (Table 6). The water identified by the chemical analysis may be trapped between nanocrystals of ZnS rather than in the ZnS structure. The sample was only air dried, because even gentle heating could decompose any $ZnCS_3$.

Table 5. X-ray diffraction (XRD) results of precipitates from the addition of Thio-Red® to various aqueous solutions containing dissolved heavy metals. Table 3 lists the compositions of the aqueous solutions.

Dissolved Compound	Crystalline Compounds in Unwashed Precipitate	Crystalline Compounds in Water Washed Precipitate
$CuCl_2$	–	Covellite (CuS)
$CuSO_4 \cdot 5H_2O$	$CuSO_4 \cdot 3H_2O$; $Na_2Cu(SO_4)_2 \cdot 2H_2O$; Few unidentified peaks, perhaps CuS_2 (villamaninite)	Covellite (CuS)
$Pb(NO_3)_2$	–	Galena (PbS)
$ZnCl_2$	–	Sphalerite (ZnS)
$HgCl_2$	Metacinnabar (HgS)	–
HgO	Metacinnabar (HgS); Unreacted HgO	–

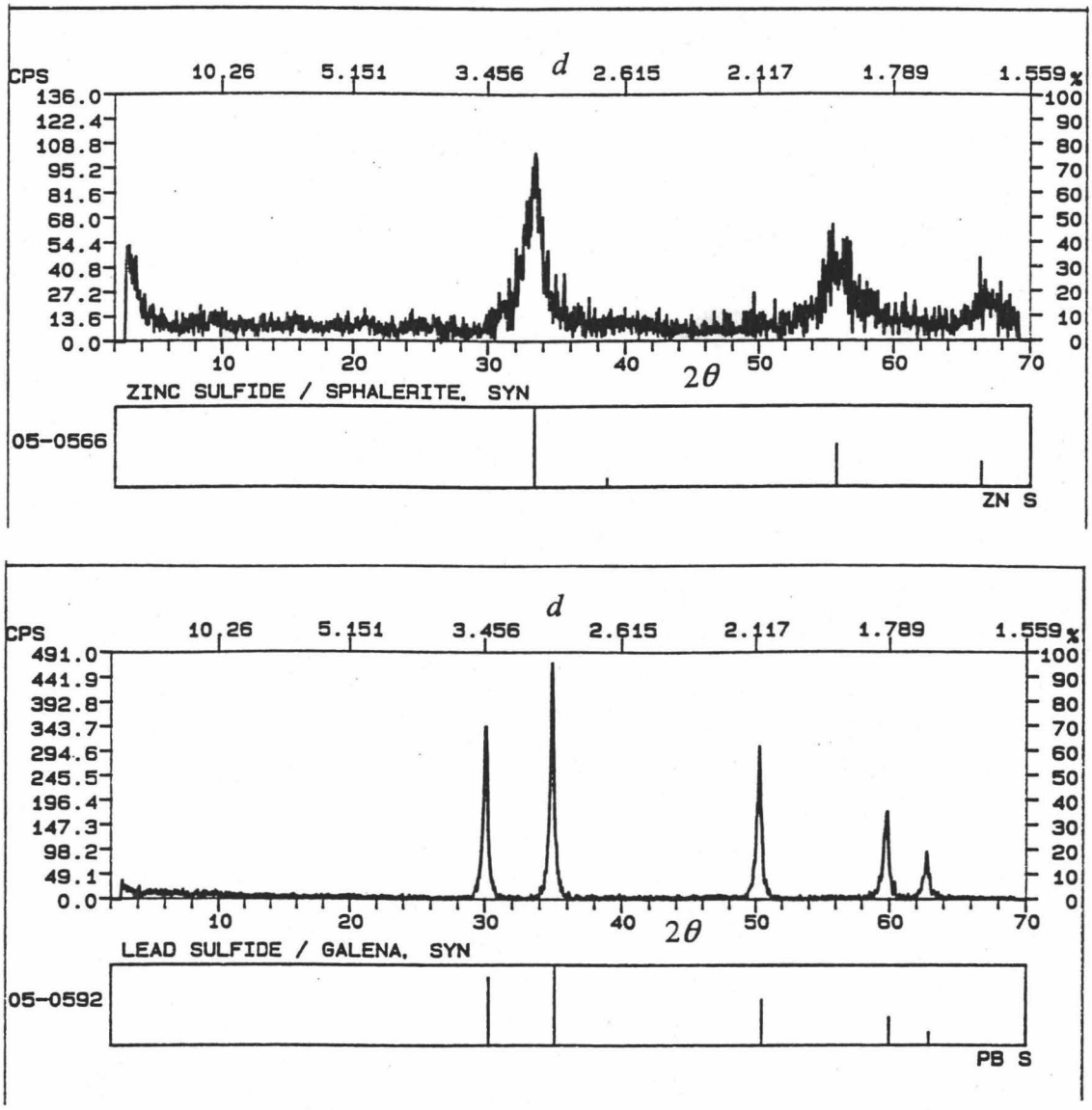

Figure 1. XRD patterns of sphalerite (ZnS) (top) and galena (PbS) (bottom) precipitates produced from adding Thio-Red® to aqueous solutions of $ZnCl_2$ and $Pb(NO_3)_2$, respectively. Relative intensities and counts per second (cps) are listed on the y axes, while the x axes list 2θ and *d*-values. The 2θ values in the patterns are based on cobalt $K\alpha_1$ ($\lambda = 1.78896$ Å) radiation. Table 3 lists the Thio-Red® dosages and the compositions of the $ZnCl_2$ and $Pb(NO_3)_2$ solutions.

Table 6. Chemical analysis of a zinc precipitate produced by adding Thio-Red® to a $ZnCl_2$ solution. The composition of the precipitate is compared with theoretical compositions for $ZnS \cdot nH_2O$ and $ZnCS_3 \cdot nH_2O$. Table 3 lists the concentration of the $ZnCl_2$ solution and the volume of the Thio-Red® dose.

Parameter	Measured Concentration in Precipitate (wt%)	Ideal Concentration of ZnS (wt%) + 12.69 wt% Water	Ideal Concentration of $ZnCS_3$ (wt%) + 12.69 wt% Water
Zinc	54.75	57.80	32.45
Carbon	2.09	0.00	5.96
Sulfur	29.31	28.35	47.74
Water	12.69	12.69	12.69
Total	98.84	98.84	98.84

The precipitation studies were repeated with laboratory aqueous solutions containing minimal metal concentrations that would still produce enough precipitates for powder XRD analyses. The purpose of the experiments was to verify whether metal sulfides were still significant precipitates at lower metal concentrations, *i.e.*, at concentrations that are somewhat closer to those of actual waste waters. ZnS was detected in precipitates produced from adding pH 12.2 Thio-Red® to solutions with as low as 22 mg/l (or 22,000 micrograms/liter [μg/l]) of Zn as $Zn(CH_3CO_2)_2 \cdot 2H_2O$ (Table 7). Because of the presence of broad and noisy XRD peaks, ZnS or any other crystalline zinc compound could not be detected in precipitates produced with lower zinc concentrations. Only CuS, HgS, and PbS were detected in precipitates that formed from adding Thio-Red® to aqueous solutions containing 152-193 μg/l of copper, mercury, or lead as $CuSO_4 \cdot 5H_2O$, $HgCl_2$, or $Pb(NO_3)_2$, respectively (Table 7). The Thio-Red® dosage for the

$HgCl_2$ solution used $Y_{Hg} = 0.02$. The pH values of the solutions were also measured before and after the addition of Thio-Red® (Table 7).

Table 7. XRD results of precipitates from relatively dilute aqueous solutions of metal salts treated with pH 12.2 Thio-Red®. The pH values of the solutions before and after the addition of Thio-Red® are also listed.

Dissolved Compound	Metal Conc. (μg/l)	Thio-Red® Dosage (μl)	pH before Thio-Red® Addition	pH after Thio-Red® Addition	Crystalline Compounds in Precipitate
$Zn(CH_3CO_2)_2 \cdot 2H_2O$	22,000	360	6.3	5.2	Sphalerite (ZnS)
$CuSO_4 \cdot 5H_2O$	172	11	5.7	6.8	Covellite (CuS)
$Pb(NO_3)_2$	152	5	5.8	6.5	Galena (PbS)
$HgCl_2$	193	5	6.0	6.4	Metacinnabar (HgS)

Mixing a few grains of $Pb(NO_3)_2$ with a few drops of Thio-Red® frequently produced bright crimson red solids. The crimson solids had the appearance of $PbCS_3$, but before they could be analyzed by XRD, they converted to black and silver PbS and released a dense volatile yellow liquid (CS_2?). The mixing of $Zn(CH_3CO_2)_2 \cdot 2H_2O$ or $ZnCl_2$ grains with a few drops of Thio-Red® produced bright yellow solids (perhaps, $ZnCS_3$). In seconds to minutes, the solids faded to yellowish white or white ZnS and also released a dense yellow liquid. Broad XRD peaks also existed in these ZnS precipitates.

No unusual precipitates, which could have been thiocarbonates, were detected in mixtures of Thio-Red® and various copper and mercury salts.

Titration Experiments

pH Effects

Titration experiments were done to better understand the relationships between dissolved copper or lead and HS^-, S^{2-}, and any CS_3^{2-}. If pH 12.2 Thio-Red® is slowly titrated into a $CuCl_2$ or $Pb(NO_3)_2$ solution, then thermodynamic data from Faure (1991, p. 551-603) show that essentially all of the HS^- and S^{2-} should precipitate as CuS or PbS through the following general reactions:

9) $HS^- + M^{2+} \rightarrow MS\downarrow + H^+$

10) $S^{2-} + M^{2+} \rightarrow MS\downarrow$

A total of one-third of the sulfur in CS_3^{2-} may form metal sulfides through a combination of Reactions 6 and 7 or the following general reaction:

11) $CS_3^{2-} + M^{2+} \rightarrow MS\downarrow + CS_2$

The initial titration experiments consisted of slowly adding 0.10 ml aliquots of pH 12.2 Thio-Red® into several 15-100 ml solutions of 0.09-0.13 M $CuCl_2$ and monitoring the pH and the formation of precipitates. The results shown in Table 8 are from a pH 4.38 0.09 M $CuCl_2$ solution. Multiple duplicate titrations with other 0.09 M $CuCl_2$ solutions obtained nearly identical results.

Table 8. Changes in pH values as Thio-Red® is added to a 0.09 M $CuCl_2$ solution. Calculated pH values are from the model MINTEQA2 (Allison et al., 1991). The calculated pH values only consider the effects of Reaction 9.

Total Volume of Thio-Red® Added (ml)	Measured pH	Color of Precipitates Observed Immediately after Adding Thio-Red® Aliquot	Calculated pH from MINTEQA2
0	4.38	None	4.35
0.10	2.65	Black	3.03
0.20	2.33	Black	2.73
0.30	2.18	Black	2.56
0.40	2.06	Black	2.44
0.50	1.96	Black	2.35
0.60	1.92	Black	2.27
0.70	1.85	Black	2.20
0.80	1.80	Black	2.15
1.40	1.58	Black	1.92
1.70	1.47	Black	1.85
1.80	1.43	Brown	1.82
1.90	1.42	Brown	1.80
2.00	1.49	Very little, brown	1.78
2.10	1.57	Yellow	1.76
2.20	1.67	None persisting	1.75
6.80	–	–	1.36
6.90	–	–	1.35
7.00	–	–	1.36

As aliquots of Thio-Red® were initially added to the $CuCl_2$ solution, black to brown solids (CuS) precipitated. Contrary to some expectations, the pH of the $CuCl_2$ solution did not increase after the addition of the first aliquot of pH 12.2 Thio-Red® (Table 8). The pH persistently declined and eventually minimized at 1.42, when CuS precipitation began to cease (Table 8). After the precipitation of CuS ceased, further addition of Thio-Red® aliquots increased the pH and produced unidentified yellow precipitates (perhaps dithioformic acids, Engler and Gattow, 1972). The yellow precipitates were unstable and dissolved within a few minutes.

The computer geochemical model, MINTEQA2 (Allison et al., 1991), was used to evaluate the effects of Reaction 9 on pH during the titrations. Table 8 compares the pH values of the laboratory results with those from MINTEQA2. The MINTEQA2 results were obtained by entering the HS^- and Na^+ concentrations for every 0.10 ml of Thio-Red® into the model and calculating the effects of those concentrations on the chemistry of the 0.09 M $CuCl_2$ solution. Because MINTEQA2 ignores the precipitation of CuS by S^{2-} and CS_3^{2-} through Reactions 10 and 11, CuS precipitation does not cease in the modeling results until 6.90 ml of the theoretical HS^- and Na^+ solution are added (Table 8). Although the laboratory and calculated pH values in Table 8 do not correspond exactly, both results show the same pH trend. The MINTEQA2 data suggest that Reaction 9 is primarily responsible for the initial pH decline in the laboratory titrations, although other unidentified reactions may also be influencing the pH values. Once essentially all of the dissolved copper has precipitated, Reaction 9 is no longer prominent and a potentially important source of H^+ is eliminated. Without the presence of significant concentrations

of dissolved copper, the addition of further aliquots of Thio-Red® results in an increase in pH. Any pH increase resulting from the precipitation of H^+ through the formation of dithioformic acids (?) would only be temporary because the precipitates rapidly decompose and any H^+ in them probably would be released back into the solution. Additional MINTEQA2 calculations suggest a likely cause for the pH increase. If additional aliquots of Thio-Red® are added to an acidic solution depleted of dissolved copper, the S^{2-} and HS^- from the Thio-Red® would react with H^+ to form H_2S^o as shown by the following reactions:

12) $S^{2-} + H^+ = HS^-$

13) $HS^- + H^+ = H_2S^o$

The volatilization of some of the H_2S^o from the solution would result in a further pH increase by forcing Reaction 13 to the right.

Estimating CS_3^{2-} Concentration in Thio-Red®

XRD Analyses

The likely presence of abundant CS_3^{2-} in the pH 12.2 Thio-Red® was indirectly confirmed by boiling dry approximately 400 ml of the liquid at 100°C in air and analyzing the solid residues by XRD. Because the residue samples were deliquescent, the XRD slides required no acetone, Vaseline®, or other mounting materials. The *d*-values of the residues were calibrated with a fluorophlogopite standard.

An XRD analysis was done on a partially moist sample. After the analysis, the entire sample eventually dried through a combination of low heating (about 40°C) and

exposure to moving air. Once the specimen completely dried, a second analysis was done as a comparison. As shown in Table 9, abundant Na_2CS_3 (PDF 14-598) was detected in the sample. The Na_2CS_3 PDF 14-598 reference analysis is from Maurin (1961, p. 1251). The small discrepancies (within ±0.01 Å) between the *d*-values of PDF 14-598 and the two analyses may be due to traces of potassium in the Na_2CS_3 of the residue or differences in the XRD methods. Preferred orientations in the crystals of the residue may explain the variations of some intensities in Table 9. The existence of abundant Na_2CS_3 in the residue suggests that CS_3^{2-} was abundant in the preheated pH 12.2 Thio-Red®.

XRD analyses of other samples of the residues found some evidence for the presence of $Na_2CS_3 \cdot 2H_2O$, $Na_2CS_3 \cdot 3H_2O$, and $Na_2CS_3 \cdot 4H_2O$. However, except for Na_2CS_3, no alkali thiocarbonates, sulfides, sulfates or other compounds were positively identified by XRD in any of the residue samples.

Table 9. XRD analyses of a sample of dried residues from pH 12.2 Thio-Red®. The sample contains abundant anhydrous Na_2CS_3 (PDF 14-598).

d-values (Å) of Na_2CS_3 (PDF 14-598)	Relative Intensities of Na_2CS_3 (PDF 14-598)	Corrected *d*-values (Å) of Damp Sample	Relative Intensities of Damp Sample	Corrected *d*-values (Å) of Dried Sample	Relative Intensities of Dried Sample
8.33	<10			8.47?	2
4.64	15				
3.476	15				
3.323	15	Overlap with standard[a]		Overlap with standard[a]	

Table 9 cont.

2.777	100	2.770	67	2.771	100
2.664	25	2.671	26	2.673	35
				2.669	59
2.330	20				
2.189	20	2.182	16	2.183	17
2.106	15			2.112?	5
2.083	<10				
1.971	20				
1.955	<10	1.954	5	1.955	5
1.871	<10			1.870	3
1.843	<10				
1.809	<10			1.811	3
1.744	<10	1.742	7	1.741	7
1.668	<10	Overlap with standard[a]		Overlap with standard[a]	
1.619	<10	1.618	18	1.617[b]	19
1.545	<10	1.546	6	1.546[b]	8
1.528	<10				
1.504	<10				
1.433	<10	1.434	6		

[a] The Na_2CS_3 *d*-values at 3.323 and 1.668 Å overlap values for the fluorophlogopite calibration standard.

[b] *d*-values are uncorrected.

Titrations to Estimate CS_3^{2-} Concentration

The CS_3^{2-} concentration in Thio-Red® may be quantitatively estimated by titrating $CuCl_2$ or $Pb(NO_3)_2$ solutions with Thio-Red® until metal sulfide precipitation ceases. The titration efforts make the following assumptions:

1. All sulfur species, except HS^-, S^{2-}, and CS_3^{2-}, total no more than 2 wt% of the total sulfur concentration in Thio-Red®. Because HS^- and S^{2-} represent 19 wt% of the total sulfur (Table 2), no more than about 79 wt% of the sulfur in Thio-Red® should exist as CS_3^{2-}.

2. The precipitates form through a combination of Reactions 9-11. Reaction 11 shows that one-third of the sulfur in CS_3^{2-} would precipitate as CuS or PbS and the remaining two-thirds would occur, at least initially, as CS_2.

3. When dried, the precipitates are pure and anhydrous CuS or PbS.

Under these assumptions, 45 wt% of the total sulfur in the titrated Thio-Red® would be expected to precipitate as metal sulfides, whereas the other 55 wt% should primarily exist as sulfite, sulfate and CS_2. If considerable amorphous $PbCS_3$ or $CuCS_3$ occur in the precipitates, the above assumptions would be false. That is, the actual mass of the precipitates would greatly exceed the predicted mass, which is based on pure metal sulfides consisting of all of the once dissolved copper or lead and an equal number of moles of sulfide.

Aqueous solutions consisting of 0.09 M $CuCl_2$ or 0.037 M $Pb(NO_3)_2$ were titrated with 0.10 ml aliquots of Thio-Red® until yellow precipitates (perhaps, dithioformic acids) formed instead of any further CuS or PbS precipitates. The metal sulfide precipitates were

then recovered, washed with distilled and deionized water, air dried, weighed, and analyzed by XRD. The percentage of total sulfur in the dose of Thio-Red® that precipitated as metal sulfides was calculated through two methods. In the first method, the percentage was determined by knowing the molarity of the dissolved copper or lead in the pretitrated solution, the volume of the Thio-Red® dose required to precipitate all of the dissolved copper or lead, and the molarity of the total sulfur in the dose. The second method involved weighing the dried precipitates and using XRD to verify within detection limits that the precipitates were only anhydrous CuS or PbS. The percentage of sulfur involved in the precipitation of the metal sulfides was then obtained by calculating the number of moles of sulfur in the CuS or PbS and comparing these values with the total sulfur concentration in the Thio-Red® dose.

The results in Table 10 show that the percentage of sulfur in pH 12.2 Thio-Red® that precipitates as metal sulfides is mostly 41-45 wt% of the total sulfur concentration or close to the 45 wt% predicted by the above assumptions. The low value of ≥39 wt% in Table 10 for the second $CuCl_2$ titration resulted from a small spill of the CuS sample during the drying and weighing process. Excluding the ≥39 wt% value, the average result for the percentages of sulfur precipitated as CuS or PbS is 43 wt%. Considering the second and third assumptions mentioned above, approximately 75 instead of 79 wt% of the total sulfur in Thio-Red® should exist as CS_3^{2-} (Table 2). The data in Table 2 still leave about 4-6 wt% of the total sulfur unspeciated. It is possible that some of the unspeciated sulfur is associated with $HCOS_2^-$, $H_2CS_2O_2^{2-}$, and other species mentioned in Ingram and Toms (1957) and Adewuyl and Carmichael (1987), whose thermodynamic

properties and potential to react with dissolved heavy metals are often unknown. The titration results essentially eliminate the possibility that substantial amounts of stable metal thiocarbonates could exist in the samples while remaining undetected by XRD or visual observations.

Table 10. The amount of pH 12.2 Thio-Red® required to precipitate essentially all of the dissolved metals in aqueous solutions of copper or lead. The percent of total sulfur in the Thio-Red® dose precipitated as metal sulfides was calculated with two methods as explained in the text.

Precipitate	Mass of Metal Salt (g) in Volume (ml) Water	Volume of Thio-Red® (ml) Added	Mass of Air Dried Metal Sulfide Precipitates (g)	Percent Sulfur from Thio-Red® Required to Precipitate Dissolved Cu or Pb	Percent Sulfur from Thio-Red® Precipitated as Metal Sulfide
Covellite (CuS)	0.1780 g $CuCl_2$ in 15 ml	2.00	0.1251	42	42
Covellite (CuS)	0.1784 g $CuCl_2$ in 15 ml	2.10	0.1225	41	≥39
Galena (PbS)	0.2951 g $Pb(NO_3)_2$ in 24 ml	1.30	0.2204	44	45

Solubilities of Metal Sulfides and Possible Environmental Impacts

Metal sulfide precipitation readily explains the effectiveness of Thio-Red® as a treatment agent. The solubilities of CuS, PbS, HgS (cinnabar and metacinnabar), and ZnS (sphalerite) are fairly well known and are extremely low when compared with most hydroxides, chlorides, sulfates, and carbonates of the heavy metals (Krauskopf, 1979, p.

416-418). The aqueous solubilities of metal sulfides have been studied in some detail over the years because the sulfides frequently occur as ore deposits and their solubilities are important in understanding the origins of the deposits (Krauskopf, 1979, p. 393-395, 405-410; Faure, 1991, p. 473-488).

As examples, Krauskopf (1979, p. 393-395) calculated Zn^{2+} concentrations of 1×10^{-7} to 1×10^{-10} M (approximately 7 to 0.007 μg/l) from the dissolution of sphalerite in water over a pH range of 5-9. Similar calculations could be done with MINTEQA2 for CuS, PbS and metacinnabar. Compared with sphalerite, CuS, PbS, and metacinnabar are even less soluble (Krauskopf, 1979, p. 552-553). However, as discussed in Chapter 6 with metacinnabar, the possible presence of abundant colloids of metal sulfides or surface oxidation of sulfides to more soluble sulfates may cause laboratory measurements of the aqueous solubilities of metal sulfides to exceed MINTEQA2 predictions by many orders of magnitude.

Krauskopf (1979, p. 414-423) further discusses how PbS, ZnS, and other metal sulfides may be oxidized under natural conditions to more soluble sulfates and carbonates. If any ground waters, soils or sediments have undergone *in situ* restoration with Thio-Red®, ground waters or other associated waters should be monitored for pH, heavy metal concentrations and reduction/oxidation conditions to guarantee that the sulfide precipitates have not oxidized.

CHAPTER 5

CHEMISTRY AND CRYSTALLINE STRUCTURE OF 2,4,6-TRIMERCAPTOTRIAZINE TRISODIUM SALT ($Na_3C_3N_3S_3 \bullet 9H_2O$)

Introduction

According to Degussa Inc. (1993), 2,4,6-trimercaptotriazine trisodium salt, also called TMT-55, precipitates univalent (*e.g.*, $M^+ = Ag^+$) and divalent (*e.g.*, $M^{2+} = Hg^{2+}$, Cd^{2+}, Pb^{2+}, and Cu^{2+}) heavy metals through the following reactions:

14) $Na_3C_3N_3S_3 \bullet nH_2O + H_2O \rightarrow 3Na^+ + (C_3N_3S_3)^{3-}$

15) $(C_3N_3S_3)^{3-} + 3M^+ \rightarrow M_3C_3N_3S_3 \bullet nH_2O\downarrow$

16) $2(C_3N_3S_3)^{3-} + 3M^{2+} \rightarrow M_3(C_3N_3S_3)_2 \bullet nH_2O\downarrow$

Figure 2 shows the structural formula of TMT-55. Additional data on TMT-55 are listed in Table 11, which are mostly derived from Degussa Corporation (1993).

Little else is known about the chemical and crystalline properties of TMT-55. As discussed in this chapter, TMT-55 was characterized by chemical and optical methods, and studied by powder XRD using an indexing code to provide a unit cell. Single-crystal structure determinations later confirmed the results from the powder diffraction study.

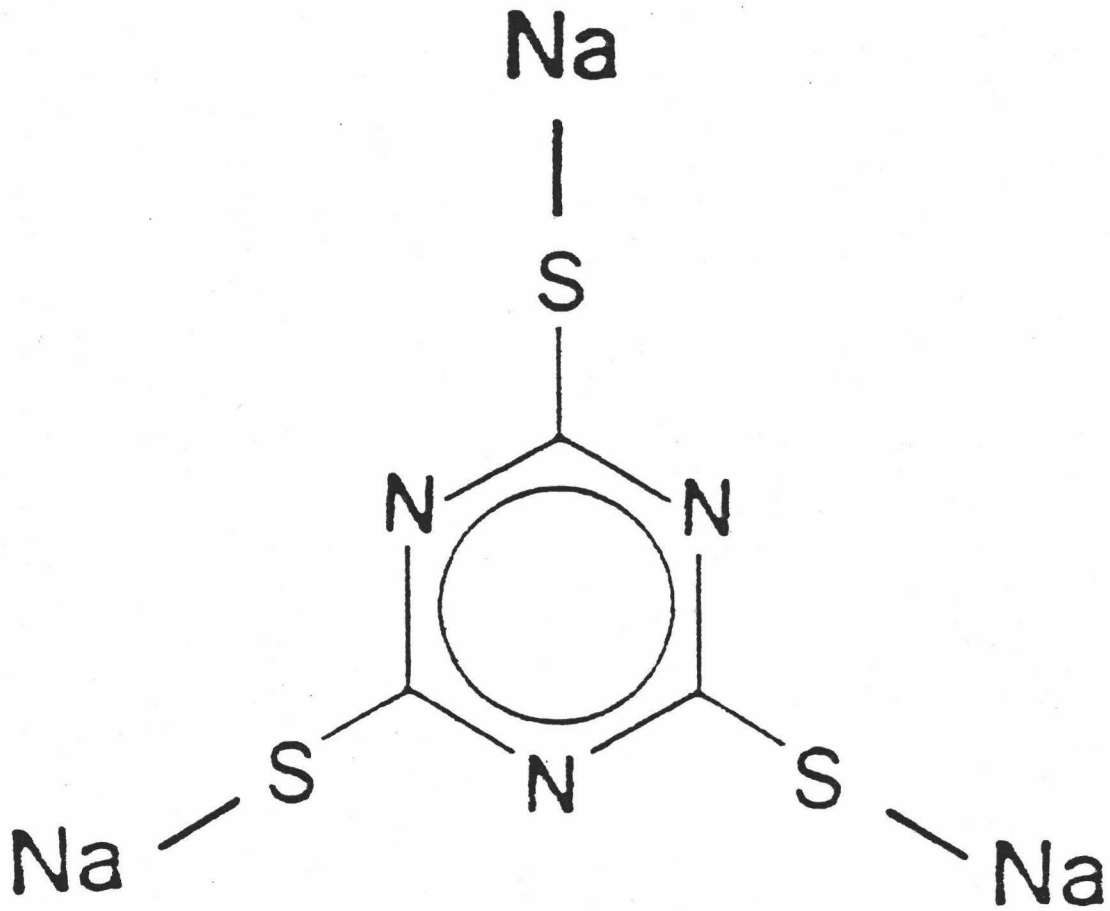

Figure 2. Structural formula of TMT-55 (after Degussa Corporation, 1993).

Table 11. Information on the chemistry and properties of TMT-55 (mostly derived from Degussa Corporation, 1993).

Property	Value
Name	TMT-55 or 2,4,6-Trimercaptotriazine, trisodium salt
Synonyms	2,4,6-Trimercapto-s-triazine, trisodium salt; 1,3,5-Triazine-2,4,6-(1H,3H,5H)-trithione, trisodium salt; Trithiocyanuric acid, trisodium salt
CAS No.	17766-26-6
Color	White powder, when dissolved in water forms pale yellow liquid
Density (25°C)	1.5 g/cm^3
Hazardous rating (health)	0
Hazardous rating (flammability)	0
Hazardous rating (reactivity)	0
Melting Point	>250°C
Molecular Weight	405.34
Odor	None
pH of 15% aqueous solution (*i.e.*, TMT-15)	12.0
Solubility in water (25°C)	540 g/l

Materials and Methods

The *d*-values for TMT-55 were calibrated with three mounts, each containing silicon, corundum, or gypsum standards and <38 micron (μm) TMT-55. The three standards provided enough intense peaks that all 33 measured TMT-55 peaks could be

reliably corrected. To reduce preferred orientations, the relative intensities of the powder XRD peaks for TMT-55 were determined from three Vaseline® mounts containing <45 μm particles. The TMT-55 was applied by placing Vaseline®-coated stubs inside a sieve pan and passing the TMT-55 through a 45 μm sieve by gently swirling the sieve assembly by hand.

Scans of the TMT-55 underwent background correction with the Scintag software. The software also reduced the noise in the diffraction peaks with three-point boxcar smoothing. Additionally, the Scintag "Profile Fitting" program was used to improve the reliability of the TMT-55 *d*-values.

Personnel at ME&T Corporation analyzed an aliquot of the TMT-55 sample for carbon, nitrogen, potassium, sodium, sulfur and water of hydration. Sodium and potassium were analyzed with a Leeman Labs, Inc. Model PS Spec ICP using U.S. EPA method 6020 (U.S. EPA, 1990). Sulfur was determined by modifying ASTM method D4239, whereas carbon and nitrogen were measured by a modification of ASTM D3187 (ASTM, 1992). The water of hydration for the sample was determined by a modification of ASTM D1744 (ASTM, 1992). The modifications in the ASTM procedures consisted chiefly of adjustments in the volumes of reagents to correspond with smaller sample sizes.

The indices of refraction of TMT-55 were determined with grain mounts and index of refraction oils at 22-23°C. The indices were corrected to 25°C by using recommended temperature correction factors for the oils. The indices of refraction of an acetone standard and several oils that were close or identical to the indices of refraction for TMT-55 were checked with a Milton Roy Company refractometer at 22.4-22.8°C.

Slowly evaporating a TMT-15 solution at 22°C produced significantly large single crystals of TMT-55. J. C. Bryan at ORNL mounted a clear rod, measuring 0.14 x 0.16 x 0.37 mm, on a glass fiber and transferred it to a single crystal diffractometer. The crystal was then cooled to -110°C to reduce errors in the atomic coordinates as well as the bond angles and lengths. All single crystal XRD measurements at -110°C were made on an Enraf Nonius CAD4 diffractometer. Cell constants and an orientation matrix were obtained by least-squares refinement using the setting angles of 25 reflections in the range $20°<2\theta<31°$ with molybdenum (Mo) $K\alpha_1$ ($\lambda = 0.71073$ Å) radiation (Henke et al., 1997, p. 8). Good crystal quality was also suggested by omega (ω) scans of several intense reflections. Omega scans at $4<2\theta<55°$ collected a total of 2036 reflections. The data were scaled for linear decay and corrected for Lorentz and polarization effects. No absorption correction was applied, owing to good crystal topography and its low absorption coefficient ($\mu = 5.5$ cm^{-1}). The data were averaged over $\bar{3}$ symmetry (R_{int} = 2.1%). The structure was solved by direct methods and expanded using Fourier techniques. All atoms were located in difference maps and all non-hydrogen atoms were refined anisotropically. Hydrogen atom positions were restrained such that all O–H bond lengths were equal (0.78[2] Å), and that all Na···H (2.76[4] Å) and H···H (1.23[2] Å, only for the two hydrogen atoms on each oxygen atom) distances were equal. Hydrogen atom isotropic displacement coefficients were constrained to a value 1.5 times the equivalent thermal parameter for the attached oxygen atom. Full-matrix least-squares refinement was carried out against F^2 using all independent reflections. Calculations were done with

SHELXTL version 5 (Siemens, 1994) on a Silicon Graphics INDIGO2 workstation (Henke et al., 1997, p. 8).

The mounted single crystal was also sent to Dr. David Atwood at NDSU for an independent analysis at 25°C. The analysis was done on a Siemens R3 m/V diffractometer with MoKα_1 radiation. Omega scans at $7<2\theta<45°$ obtained a total of 2141 reflections. Refinement efforts consisted of using a full-matrix least-squares method with 1645 (R_{int} = 2.6%) independent reflections (Henke et al., 1997, p. 8).

Results and Discussion

Chemistry

Table 12 lists the chemical composition of the TMT-55 sample. The nitrogen and sulfur analyses are slightly lower (*i.e.*, 4% or less) than their expected values. The lower values may be due to analytical errors or may result from the presence of oxygen or other trace impurities in the sample.

Degussa Corporation (1993) states that TMT-55 normally contains 45 wt% water, which would correspond to $n = 11$ (*i.e.*, $Na_3C_3N_3S_3 \bullet 11H_2O$) if all of the water was located in the crystalline structure. However, the results of the single crystal analyses state that the ideal crystalline structure should contain $n = 9$ or 40 wt% water of hydration. The chemical results in Table 12 state that the TMT-55 sample has 38.42 wt% water or n = 8.64. It is likely that the value of $n = 8.64$ is lower because the sample had a high surface area and was air dried at a humidity below 50%. The value of $n = 11$, reported by

Degussa Corporation, may result from not sufficiently drying the material before analysis. TMT-55 grains often become noticeably damp in the presence of humid (>50%) air.

Table 12. TMT-55 chemical analysis results.

Parameter	Measured Concentration (wt %)	Ideal Concentration (wt %)
Carbon	8.92	8.89
Nitrogen	10.05	10.37
Potassium	<0.1	0.00
Sodium	17.00	17.01
Sulfur	22.89	23.73
Water of hydration	38.42	40.00
Total	97.28	100.00
Formula for TMT-55	$Na_{3.0}C_{3.0}N_{2.9}S_{2.9}\bullet 8.64H_2O$	$Na_3C_3N_3S_3\bullet 9H_2O$

Optical Properties

Well-centered uniaxial negative optic axis figures were obtained from many TMT-55 grains with hexagonal basal cross sections. The indices of refraction and birefringence results for TMT-55 at 25°C are shown in Table 13. The birefringence (0.155) is quite high when compared with most minerals and inorganic compounds, but is still somewhat lower than that of calcite (0.172).

Powder X-ray Diffraction

The corrected *d*-values of 33 TMT-55 peaks and the relative peak intensities from three TMT-55 mounts are listed in Table 14. Comparisons between the measured *d*-values for the silicon, corundum, and gypsum standards and their expected results provided consistent correction factors for all of the TMT-55 peaks. For all three of the specimen mounts in Table 14, the most intense peak had a *d*-value of 4.63 Å and an *hkl* value of (012). Two peaks with *hkl* values of (303) ($d = 2.733$ Å) and (330) ($d = 2.935$ Å) varied as the second- and third-most intense values (Table 14).

Table 13. Optical properties and refined unit cell dimensions of TMT-55 at 25°C. Values in parentheses represent one standard deviation in the last digit.

Parameter	Value
Crystal System	Hexagonal (Rhombohedral Division)
Crystal Class	$\bar{3}$
Optical Sign	Uniaxial (−)
n_ϵ	1.520
n_ω	1.675
Birefringence	0.155
Length of *a* axis (Å)	17.600(1)
Length of *c* axis (Å)	9.720(2)
Unit cell volume, V (Å^3)	2607.5(5)
Rhombohedral unit cell: a_R (Å)	10.665(1)
Rhombohedral unit cell: α_R angle	111.20°
Space Group	$R\bar{3}$

Table 14. The corrected *d*-values for measured peaks of TMT-55, measured relative intensities from three specimen mounts, and average relative intensity. Calculated d-values and 2θ values based on the powder data are from NBS*AIDS83 (expanded version of Mighell et al., 1981). Calculated relative intensities based on single-crystal data at 25°C are from Micro-POWD version 2.31 (Smith and Smith, 1993).

d (Å)	*d* (Å) (calc.)	2θ (°)	2θ (°) (calc.)	*hkl*	*I1,I2,I3*	*I* (avg.)	*I* (calc.)
	8.80		10.04	110			1
6.00	6.00	14.75	14.76	021	9,7,7	8	10
4.95	4.96	17.91	17.88	211	5,6,4	5	6
4.63	4.63	19.15	19.15	012	100,100,100	100	100
4.098	4.098	21.67	21.67	202	4,4,5	4	3
3.877	3.877	22.92	22.92	131	15,21,17	18	20
3.548	3.548	25.08	25.08	401	11,15,13	13	13
3.326	3.326	26.78	26.78	410	3,3,4	3	4
3.290	3.290	27.08	27.08	321	9,11,9	10	11
	3.240		27.51	003			2
3.188	3.190	27.96	27.95	312	3,4,3	3	3
3.039	3.040	29.37	29.35	113	4,3,3	3	4
2.999	2.999	29.77	29.77	042	2,3,2	2	3
2.935	2.933	30.43	30.45	330	39,50,47	45	42
2.840	2.838	31.48	31.49	232	6,7,5	6	6
2.763	2.762	32.38	32.39	241	6,5,3	5	7
2.733	2.732	32.74	32.76	303	45,47,46	46	59
2.636	2.635	33.98	33.99	511	4,5,6	5	6
	2.609		34.34	223			2
2.582	2.582	34.72	34.71	502	2,2,2	2	3
2.541	2.540	35.29	35.30	600	9,11,9	10	13
2.441	2.441	36.79	36.79	520	7,7,4	6	6
2.400	2.400	37.44	37.45	104	6,8,7	7	11
2.385	2.385	37.69	37.68	152	9,5,5	6	9

Table 14 cont.

2.321	2.321	38.77	38.77	413	2,3,3	3	3
	2.315		38.87	024			1
2.261	2.261	39.84	39.84	161	4,5,4	4	5
2.239	2.239	40.25	40.25	214	2,3,2	2	3
2.227	2.227	40.47	40.47	342	5,6,4	5	8
	2.174		41.49	333			1
2.107	2.107	42.89	42.89	134	4,2,3	3	3
	2.065		43.80	621			2
2.018	2.019	44.88	44.86	710	2,2,2	2	2
1.9986	1.9991	45.34	45.33	603	14,13,12	13	27
1.9866	1.9871	45.63	45.62	072,532	3,4,5	4	3,3
1.9213	1.9203	47.27	47.30	630	2,3,3	3	5
	1.8574		49.00	244			2
1.8283	1.8289	49.83	49.82	271	2,2,2	2	1
	1.8110		50.34	452			2
	1.7738		51.48	802			2
	1.7662		51.72	315			2
1.7540	1.7546	52.10	52.08	811	2,2,3	2	4
	1.7444		52.41	434			3
	1.7388		52.59	722			3
	1.7208		53.19	461			1
	1.7134		53.43	713			4
	1.6888		54.28	731			4
1.6523	1.6520	55.57	55.59	633	2,2,2	2	3
	1.6216		56.72	704			1
	1.6200		56.78	006			4
	1.5766		58.49	191			2

The 33 corrected *d*-values from the powder XRD scans were first indexed using the version of TREOR90 provided with the Scintag/USA, Inc. (San Jose, California) software package (version 2.86, update of Werner et al., 1985). After the single-crystal structure determination confirmed the TREOR90 unit cell solution, the least squares unit cell refinement (LSUCRI) program implemented by Garvey (1986) after Appleman and Evans (1973) was used to refine the cell parameters, which are listed in Table 13.

De Wolff (1968) derived an M_{20} value or "figure of merit" to describe the reliability of the indexing of a powder pattern. M_{20} is defined by the following equation (de Wolff, 1968, p. 110):

17) $M_{20} = Q_{20}/2\grave{\varepsilon}N_{20}$

where:

Q for a line = $1/(d\text{-value in Å})^2$ of that line

$Q_{20} = 1/(d\text{-value})^2$ for the 20th observed and indexed line

$\grave{\varepsilon}$ = average discrepancy between the observed and calculated Q values for the 20 lines

N_{20} = number of different <u>calculated</u> Q values up to 20th <u>observed</u> Q line.

Comparisons between the indexed results of several powder patterns and corresponding, more definitive results from single crystal analyses demonstrate that powder patterns with $M_{20} < 6$ are unreliable. M_{20} values of 20 or higher are usually trustworthy (de Wolff, 1968, p. 108). De Wolff (1968, p. 108) even claims that if no more than two lines below Q_{20} are unindexed, an $M_{20} > 10$ "guarantees that the indexing is substantially correct." Smith and Snyder (1979) are not as optimistic. They state (p. 61) that the magnitude of

an M_{20} value depends on the crystal system and space group, that is, all other factors being equal, cubic compounds tend to have higher M_{20} values than triclinic compounds. Furthermore, they argue that $\grave{\varepsilon}$ is not a good measure of accuracy, since the Q values associated with $\grave{\varepsilon}$ are partially influenced by the size of the unit cell volume. Also, technically, M_{20} is undefined for compounds that have less than 20 diffraction lines. As an alternative, Smith and Snyder (1979, p. 60) propose a figure of merit, F_N, which is defined as:

18) $F_N = (1/|\Delta 2\theta|)(N/N_{poss})$

where:

$|\Delta 2\theta| =$ the absolute average discrepancy between the observed and calculated 2θ values.

$N =$ the 30th or, if the number of possible diffraction lines is less than 30, the last observed line.

$N_{poss} =$ the number of possible independent diffraction lines.

F_N has units of reciprocal degrees and is expressed in the following format (Smith and Snyder, 1979, p. 63):

19) $F_N =$ overall value given by Equation 18 ($|\Delta 2\theta|$, N_{poss})

F_N describes both the accuracy of the pattern (using $|\Delta 2\theta|$) and its completeness (N/N_{poss}). Unlike Q, Smith and Snyder (1979, p. 64) claim that errors given as $|\Delta 2\theta|$ are generally independent of the magnitude of 2θ and there is no reason to believe that the magnitude of $|\Delta 2\theta|$ would be affected by the crystal system or space group. Despite the

controversies associated with M_{20} values, both M_{20} and F_{30} figures of merit are widely used in the literature.

The 33 measured 2θ values of TMT-55 were no more than ±0.03° from their corresponding calculated values (Table 14). An NBS*AIDS83 (expanded version of Mighell et al., 1981) analysis of the powder data gave $M_{20} = 45$ and $F_{30} = 64$ (0.0093, 51), which suggest that the unit cell information and indexing in Tables 13 and 14 are reliable (de Wolff, 1968; Smith and Snyder, 1979).

Single Crystal X-ray Diffraction

The single crystal XRD data at -110 and 25°C were consistent with each other, and the cell parameters agreed with the data determined by the powder method (Tables 13 and 15). The largest discrepancies between the powder and single crystal data at 25°C dealt with the size of the *a* axis and the resulting unit cell volume. These discrepancies may be largely due to the fact that the single-crystal results were based on 1048 observed reflections, whereas the calculations with the powder data used 33 *d*-values with fewer significant digits. As expected, the lengths of the *a* and *c* axes and the unit cell volume are somewhat smaller at -110°C than at 25°C (Table 15). The two single-crystal structure solutions led to the rhombohedral space group $R\bar{3}$, which is consistent with the systematic absences in the indexed powder patterns. The residuals of the calculated versus observed peak intensities for the single-crystal data were good (Table 15).

The -110°C single-crystal data were used to determine the molecular structure of TMT-55, which is shown in Figure 3. A crystallographic threefold axis runs through the

centroid of the six-member carbon and nitrogen ring perpendicular to the plane of the ring. Therefore, only one-third of the molecule occupies the asymmetric unit and the remaining two-thirds are generated by symmetry. It is clear from the structure determination that there are three water molecules per sodium cation or nine water molecules per molecular formula (Henke et al., 1997, p. 11).

Table 15. Summary of single-crystal XRD data for TMT-55 at -110 and 25°C. One standard deviation in the value(s) of the last digit(s) is shown in parentheses.

Parameter	Value at -110°C	Value at 25°C
a (Å)	17.530(2)	17.595(1)
c (Å)	9.6312(13)	9.7190(10)
V (Å^3)	2563.1(5)	2605.8(5)
Number of formula units per unit cell (Z)	6	6
Calculated crystal density (D_i, g/cm^3)	1.58	1.55
Observed crystal density (D_m, g/cm^3)	_	1.5 (Degussa)
Absorption coefficient (μ, cm^{-1})	5.5	5.4
Residual $wR2$[a]	0.075	0.086
Residual $R1$[b]	0.028	0.058

[a] $wR2 = \{\Sigma|w(F_o^2 - F_c^2)^2]/\Sigma[w(F_o^2)^2]\}^{1/2}$, and is calculated by using all reflections.

[b] $R1 = (\Sigma||F_o| - |F_c||/\Sigma|F_o|)$, is presented here for comparison purposes only, and is calculated only for the observed reflections (*i.e.*, 1048 at 25°C and 1079 at -110°C) with $I > 2.0\sigma_I$.

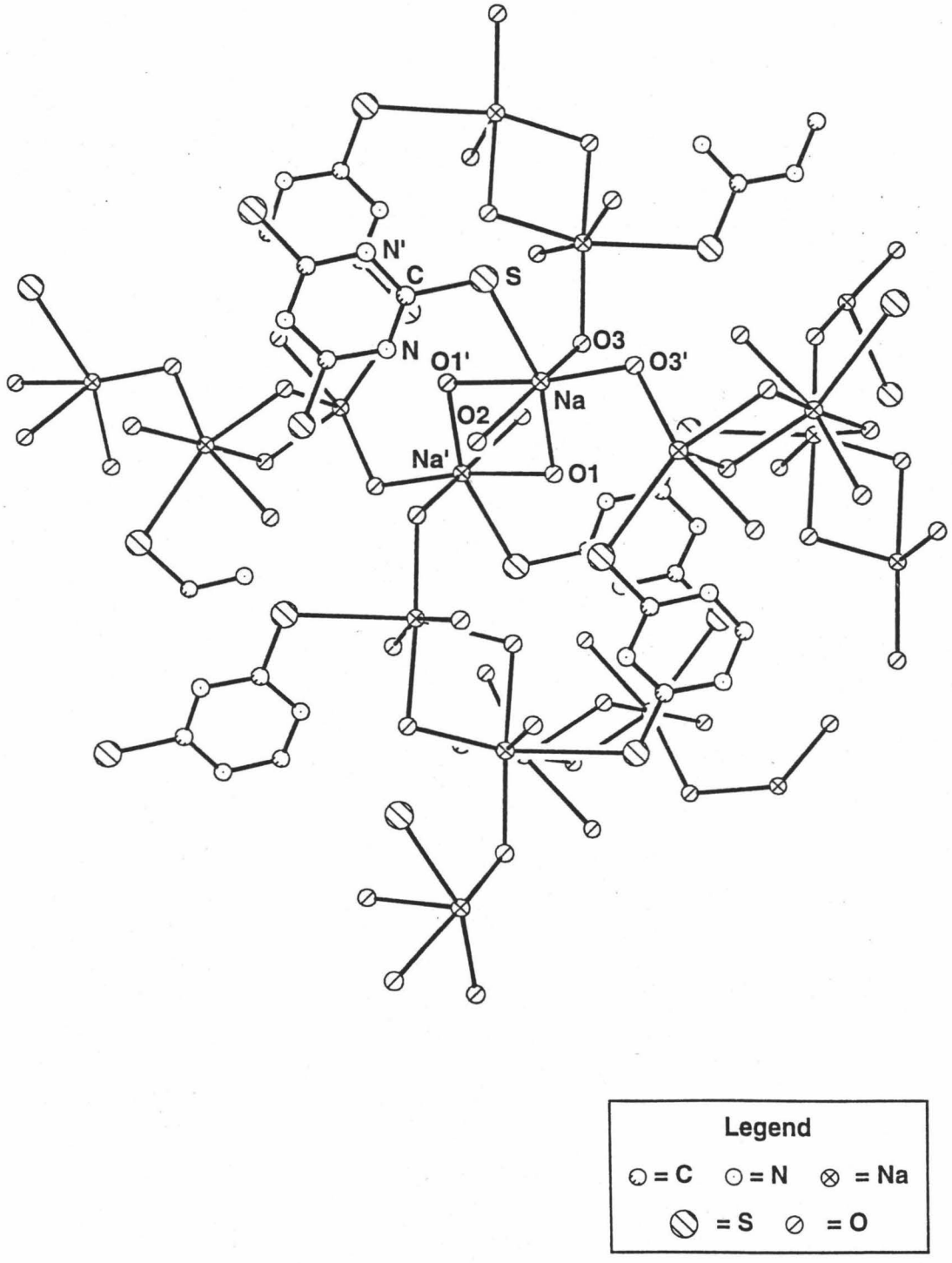

Figure 3. Ball and stick representation of the extended structure of TMT-55. Hydrogen atoms are omitted for clarity.

The structure forms an intricate three-dimensional network through the bridging of sodium ions by lone oxygen pairs (Figure 3). Each sodium ion has sixfold coordination with a coordination geometry that is roughly octahedral. One site of the octahedron is occupied by a sulfur atom. The other five sites are occupied by oxygen atoms: one terminal water molecule (O2), two symmetry equivalent, doubly bridging (both bridging the same two sodium ions) water molecules (O1), and two symmetry equivalent, singly bridging molecules (each bridging to a different sodium ion) (O3) (Figure 3). This network allows for the triazine units to stack along the *c* axis (Henke et al., 1997, p. 11).

Table 16 and the Appendix list selected bond lengths, atomic distances, and bond angles for TMT-55 at -110°C. The primed atoms are generated by symmetry from their corresponding atoms (*e.g.*, O1' from O1 in Figure 3).

Table 17 and the Appendix list the atomic coordinates (x, y, z) for the various atoms in the TMT-55 unit cell at -110°C. The similarity of the thermal parameters (U_{eq}) suggests that no significant impurities (*e.g.*, potassium or excess oxygen) were present in the measured crystal (Henke et al., 1997, p. 11).

The single-crystal data at 25°C were entered into Micro-POWD version 2.31 (Smith and Smith, 1993) to generate a list of theoretical peak height intensities for the TMT-55 powder pattern derived from a Scintag diffractometer. *B(iso)* values were calculated from the U_{eq} values at 25°C (Table 18). Neutral scattering factors were used and corrections were made for anomalous dispersion. To model the Scintag XRD results, the modeling conditions assumed the presence of a fixed slit, stripping of α_2 peaks, a

Pearson VII profile shape with an exponent of 1.5, and the absence of an incident or diffracted beam monochrometer.

Table 16. Selected bond lengths (Å), atomic distances (Å), and angles (degrees) for TMT-55 at -110°C. One standard deviation in the value(s) of the last digit(s) is shown in parentheses. Complete results are listed in the Appendix.

Bond or Atomic Distance	Length (Å)
S–C	1.727(2)
S–Na	2.9694(9)
Na–O1	2.3678(15)
Na–O1'	2.4609(15)
Na–O2	2.438(2)
Na–O3	2.420(2)
Na–O3'	2.357(2)
Na and Na'	3.6142(14)
C–N	1.354(2)
C–N'	1.352(2)

Angle	Degrees
C-S-Na	106.08(6)
O1-Na-O1'	83.10(5)
O1-Na-O2	79.62(5)
O1'-Na-O2	81.16(5)
O1-Na-O3	86.88(5)
O1-Na-O3'	103.11(5)
O1'-Na-O3	83.52(5)
O1'-Na-O3'	170.96(6)
O3-Na-O3'	90.20(3)

Table 16 cont.

O2-Na-O3'	106.26(5)
O2-Na-O3	160.65(5)
O1-Na-S	160.95(4)
O1'-Na-S	85.82(4)
O2-Na-S	83.41(4)
O3'-Na-S	89.86(4)
O3-Na-S	107.24(4)
N-C-N'	122.91(15)
N-C-S	118.34(12)
N'-C-S	118.74(12)
C-N-C'	117.08(15)

Micro-POWD identified 468 possible reflections. Overall, 71 reflections with relative intensities of ≥1 were identified at 55 unique *d*-values between 8.80 and 1.3657 Å. The *d*-values of all 33 major peaks were listed among the 55 Micro-POWD *d*-values.

At higher *d*-values, the average relative intensities from the three measured mounts were very similar to the calculated Micro-POWD intensities (Table 14). At lower *d*-values, however, the calculated and averaged measured intensities were less consistent, *e.g.*, (303), (104), and (603), which is probably due to a preferred orientation in the crystals of the measured mounts.

Table 17. Atomic coordinates and equivalent isotropic displacement for TMT-55 at -110°C. One standard deviation in the value(s) of the last digit(s) is shown in parentheses.

Atom	*x*	*y*	*z*	U_{eq} [a]
S	0.20090(3)	0.08723(3)	0.74665(4)	0.01503(13)
Na	0.24006(4)	-0.05894(4)	0.76188(7)	0.0186(2)
O1	0.22199(9)	-0.20198(9)	0.75017(13)	0.0196(3)
H1A	0.2249(14)	-0.2138(13)	0.6728(13)	0.029
H1B	0.2512(12)	-0.2163(13)	0.7900(19)	0.029
O2	0.12484(9)	-0.12551(9)	0.58631(14)	0.0216(3)
H2A	0.0951(12)	-0.1085(14)	0.6184(20)	0.032
H2B	0.1284(14)	-0.1129(14)	0.5087(13)	0.032
O3	0.32177(9)	-0.03952(9)	0.97401(14)	0.0210(3)
H3A	0.3574(11)	-0.0520(13)	0.9550(21)	0.03
H3B	0.2866(11)	-0.0806(11)	1.0153(21)	0.03
C	0.08756(10)	0.03819(10)	0.7409(2)	0.0128(3)
N	0.03926(9)	-0.05090(9)	0.74007(14)	0.0144(3)

[a] Equivalent isotropic (U_{eq}) is defined as one third of the trace of the orthogonalized U_{ij} tensor and is given in units of Å^2.

Micro-POWD also identified 22 peaks with *d*-values that were occasionally identified in one or two, but never all three, of the measured scans from the relative intensity mounts. Only five of the 22 unmeasured peaks had intensities of three or higher. Specifically, two calculated peaks with *d*-values of 1.7388 and 1.7444 Å had intensities of three (Table 14). Three other peaks with calculated relative intensities of four were located at 1.6200, 1.6888, and 1.7134 Å (Table 14).

Table 18. Atomic coordinates and equivalent isotropic displacement for TMT-55 at 25°C. One standard deviation in the value of the last digit is shown in parentheses. Standard deviations are not available for the positions of the hydrogen atoms.

Atom	*x*	*y*	*z*	U_{eq} [a]	B_{iso} [b]
S	0.7543(1)	0.2206(1)	0.0862(1)	0.027(1)	2.132
Na	0.6313(1)	-0.0941(1)	0.4048(2)	0.034(1)	2.685
O1	0.5350(2)	0.0916(2)	0.9140(3)	0.035(1)	2.763
H1A	0.4773	0.0638	0.9537	0.050	3.948
H1B	0.5776	0.1254	0.9831	0.050	3.948
O2	0.4592(2)	-0.0843(2)	-0.2478(4)	0.040(2)	3.158
H2A	0.4168	-0.0713	-0.2089	0.050	3.948
H2B	0.4343	-0.1217	-0.3265	0.050	3.948
O3	0.6274(2)	-0.0278(2)	-0.1408(4)	0.039(1)	3.079
H3A	0.5757	-0.0389	-0.1841	0.050	3.948
H3B	0.6039	-0.0909	-0.1231	0.050	3.948
C	0.7046(3)	0.2844(3)	0.0920(4)	0.021(1)	1.658
N	0.6158(2)	0.2433(2)	0.0923(4)	0.025(1)	1.974

[a] Equivalent isotropic (U_{eq}) is defined as one third of the trace of the orthogonalized U_{ij} tensor and is given in units of Å^2.

[b] $B_{iso} = 8\pi^2 U_{eq}$, Stout and Jensen (1989).

Very few structure determinations involving the 2,4,6-trimercaptotriazine trianion ($[C_3N_3S_3]^{3-}$) have been reported in the literature. One compound is $(Os_3H[CO]_{10})_3(C_3N_3S_3)$ from Ainscough et al. (1993). Ainscough et al. (1993) reported that $(Os_3H[CO]_{10})_3(C_3N_3S_3)$ consists of cluster cations of $(Os_3H[CO]_{10})^+$ that are bound to each sulfur atom through two of the osmium atoms. Unlike TMT-55,

$(Os_3H[CO]_{10})_3(C_3N_3S_3)$ is a discrete molecular unit in the solid state. That is, there is no bridging between the molecular units (Henke et al., 1997, p. 11).

CHAPTER 6

CHEMISTRIES, CRYSTALLINE PROPERTIES, AND LEACHING CHARACTERISTICS OF SELECTED MERCURY 2,4,6-TRIMERCAPTOTRIAZINE COMPOUNDS

Introduction

Mercury Toxicity

Mercury and its compounds are generally more toxic than most other heavy metals. The inhalation of elemental mercury vapors, for example, may damage the brains of humans and other animals (Clement Associates, 1989, p. 2-3). The release of mercury (I) and (II) compounds into aquatic environments may result in the transformation of the compounds by biogenic or abiogenic processes into highly toxic methylated forms (Stolzenburg et al., 1986, p. 47-48; Ramamoorthy et al., 1982; Andersson, 1979, p. 89-90; Henke et al., 1993, p. 28-29). Methylmercury may easily bioaccumulate up the food chain to threaten human health and life (Douglas, 1991; Cole et al., 1992; Henke et al., 1993, p. 14-17).

Precipitation of Mercury from Water with Aqueous Solutions of TMT-55

TMT-15 and TMT-55 remove dissolved mercury from contaminated water (Degussa Corporation, 1993). Only limited information is available on the chemistry of mercury precipitates that result from reactions between TMT and dissolved mercury. The most detailed study identified by a literature review is Chudy and Dalziel (1975), which contains information on infrared and chemical analyses of a single "pale cream colored" sample with the likely composition of $Hg^{2+}{}_3(C_3N_3S_3)_2$.

Formation of Mercury 2,4,6-Trimercaptotriazine Compounds

A clear to white gel initially forms when TMT-15 or other aqueous solutions of TMT-55 are mixed with aqueous solutions of $HgCl_2$ or red HgO. The results of a powder XRD analysis of the gel show that it is entirely amorphous. Once the gel dries in either air or ultrapure nitrogen gas, one or more solid mercury 2,4,6-trimercaptotriazine (HgTMT) compounds are produced, including chalky white, yellow, gray, or resinous greenish yellow to greenish brown varieties. Table 19 lists the conditions that produced several samples of the different varieties. Occasionally, mixtures of two or more varieties developed. As demonstrated by the information in Table 19, the conditions that cause one variety to develop rather than another are not clearly understood. That is, different varieties may develop under similar $Hg/(C_3N_3S_3)^{3-}$ molar ratios, water volumes, and mercury concentrations. The white variety often develops when mercury is in excess when compared with the TMT-55 dosage (*i.e.*, $Hg/[C_3N_3S_3]^{3-}$ molar ratio > 1). The recommended dosage in Degussa Corporation (1993) is 4.8 μl of TMT-15 for every mg/l

of Hg^{2+} and for every liter of waste water. That is, one million liters of waste water with 2 mg/l of Hg^{2+} would require a TMT-15 dosage of 9.6 liters. The dosage assumes that two moles of TMT-55 (not considering the mass of 9 H_2O) will remove three moles of Hg^{2+} through the formation of $Hg^{2+}{}_3(C_3N_3S_3)_2$. Under these assumptions, the recommended dosage results in a $Hg/(C_3N_3S_3)^{3-}$ molar ratio of about 2.8. In Table 19, both the recommended Degussa dosage and other dosages with $Hg/(C_3N_3S_3)^{3-}$ ratios of 0.05 to 3.4 were tested.

XRD Results and Stability of HgTMT Compounds

Different varieties of HgTMT are identified by powder XRD (Figure 4). The white variety is crystalline (Figure 4). White varieties from $HgCl_2$ or red HgO solutions have the same powder XRD pattern. As shown in Figure 4, the yellow variety contains the same major peaks as the white form. However, unlike white HgTMT, the yellow variety also contains a broad amorphous "hump" centered around 4.7 Å (22° 2θ for $CoK_{\alpha 1}$ radiation or 19° 2θ for $CuK_{\alpha 1}$ radiation). The resinous greenish yellow to greenish brown variety is entirely amorphous (Figure 4). XRD analyses of several gray samples suggest that their compositions are partially crystalline. As discussed below, the gray variety probably consists of mixtures of several compounds that result from the decomposition of white and yellow HgTMT. The compositions and concentrations of the compounds vary from sample to sample.

Table 19. Conditions used to produce several samples of different varieties of HgTMT.

Initial Variety Produced	g of $HgCl_2$ (or HgO)	g of TMT-55 usually in TMT-15	ml of Distilled, Deionized Water after TMT Addition	$Hg/(C_3N_3S_3)^{3-}$ Molar Ratio of Solution	Precipitates Dried by Heating? Dried under N_2 purge?
White	1.21	0.64[a]	204	2.8	No; No
White	2.39	1.05	200	3.4	Yes; No
White	11.91	6.60[a]	244	2.7	No; No
White	11.83	6.30[a]	242	2.8	No; No
White	1.56	1.40[b]	100	1.7	Yes; Yes
White	2.49 (HgO)	5.78	39	0.81	No; No
Pale yellowish white	0.16 (HgO)	39.96	40	0.05	No; No
Yellow-white	0.78 (HgO)	6.36	42	0.23	No; No
Yellow	4.80	8.00	150	0.90	No; No[c]
Yellow	1.37	0.75	205	2.7	No; Yes
Yellow	1.61	1.06	108	2.3	Yes; No
Greenish Yellow	0.54	0.28	52	2.9	No; No
Greenish Brown	5.26	5.80[b]	200	1.4	No; No
Greenish Brown	2.29	2.25	215	1.5	No; No
Gray, minor white and yellow	20.17	15.00	1100	2.0	No; No
Gray and Yellow	7.03	8.38	200	1.3	Yes; Yes

[a] The TMT-15 dosage was based on a formula in Degussa Corporation (1993).

[b] Solid TMT-55 was added rather than TMT-15.

[c] Sample was dried under a vacuum.

White HgTMT does not have long-term stability. It may convert to the yellow variety within three months in the presence of air at ambient temperatures. Continued exposure to air may result in the conversion of the yellow form to gray HgTMT within a year. If white HgTMT is left in water, it may alter to yellow HgTMT within a few days or to the gray variety within three months.

Chemistry of White and Other Varieties of HgTMT

Chemistry of White HgTMT

Extensive powder XRD studies and some chemical analyses were done on white HgTMT, because it is the most common variety. The white HgTMT sample produced from 2.39 g of $HgCl_2$ (Table 19) was analyzed for mercury, carbon, nitrogen, sulfur and water on the day after its formation and before it might convert to the yellow or gray varieties (Table 20). The sample had considerable water (Table 20). Table 20 also includes results that were adjusted to remove all of the water. Another white HgTMT sample made from 11.91 g of $HgCl_2$ (Table 19) had the typical XRD pattern, yet no water peaks were detected in the 3400 cm^{-1} region of its Raman spectrum and only an extremely broad and weak peak was present in the infrared spectrum (Figure 5; Nakamoto, 1986, p. 227-228; Anderson, 1973, p. 480). In comparison, Infrared (Figure 5) and Raman spectra of TMT-55 contain abundant water, which is consistent with the chemical and single crystal data in Chapter 5.

Table 20. Chemical analysis of white HgTMT precipitated from the addition of TMT-15 to an aqueous solution of 2.39 g of $HgCl_2$.

Parameter	Analysis of White HgTMT	Analysis of White HgTMT Normalized to Remove Water	Number of Moles Normalized on Three Carbons (without water)
Hg	58.86	69.22	1.98
C	5.33	6.27	3.00
H (nonaqueous)	0.40	0.47	2.68
N	5.94[a]	6.99	2.87
S	14.50	17.05	3.06
Water	15.30	0.00	–
Total	100.33	100.00	–

[a] This is an average of two nitrogen analyses: 5.88 and 6.01 wt%.

The HgTMT sample made from 11.91 g of $HgCl_2$ was later analyzed and only contained 0.49 wt% water. The absence of water in some white HgTMT samples suggests that the water described in Table 20 was not structural, but was probably on the surfaces of the freshly prepared compound.

Figure 4. Powder XRD patterns of different varieties of HgTMT compounds (see Table 19), including (from top to bottom): 1) white made from 1.56 g of $HgCl_2$, 2) yellow produced from the exposure to air of white HgTMT made from 1.21 g of $HgCl_2$, 3) originally pale yellowish white HgTMT made from 0.16 g of HgO and largely altered to gray and yellow varieties from drying in air, 4) mostly gray HgTMT produced from 20.17 g of $HgCl_2$, and 5) amorphous greenish yellow made from 0.54 g of $HgCl_2$. Relative intensity values (right) and counts per second (left) are listed on the y axes of the patterns. The x axes list 2θ values based on $CoK_{\alpha 1}$ radiation.

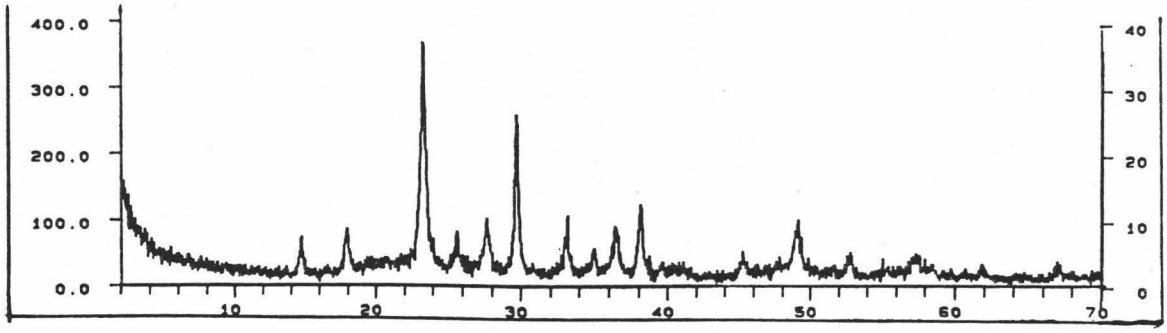
400.0
300.0
200.0
100.0
0.0
10
20
30
40
50
60
70
40
30
20
10
0

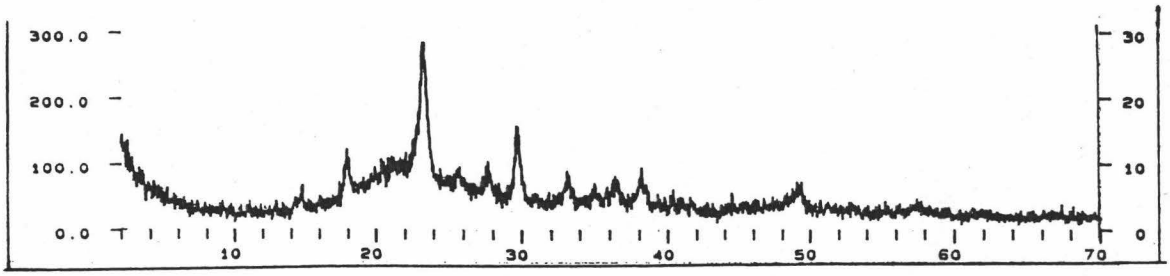
300.0
200.0
100.0
0.0
10
20
30
40
50
60
70
30
20
10
0

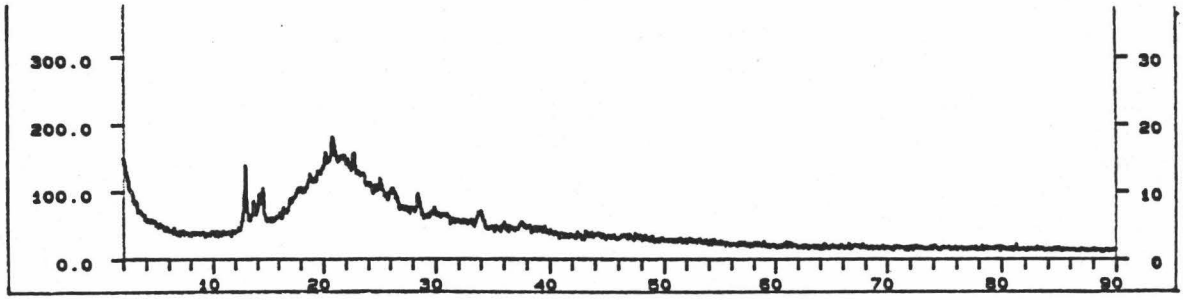
300.0
200.0
100.0
0.0
10
20
30
40
50
60
70
80
90
30
20
10
0

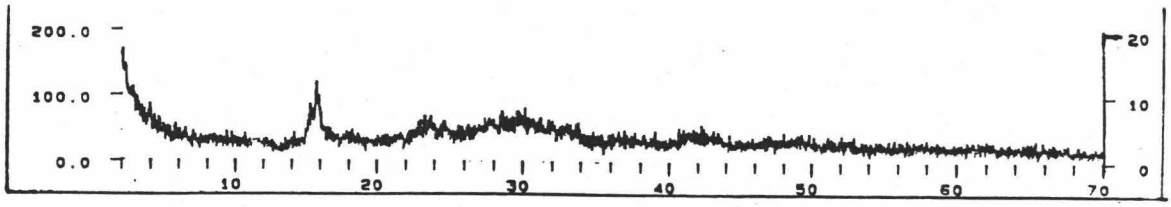
200.0
100.0
0.0
10
20
30
40
50
60
70
20
10
0

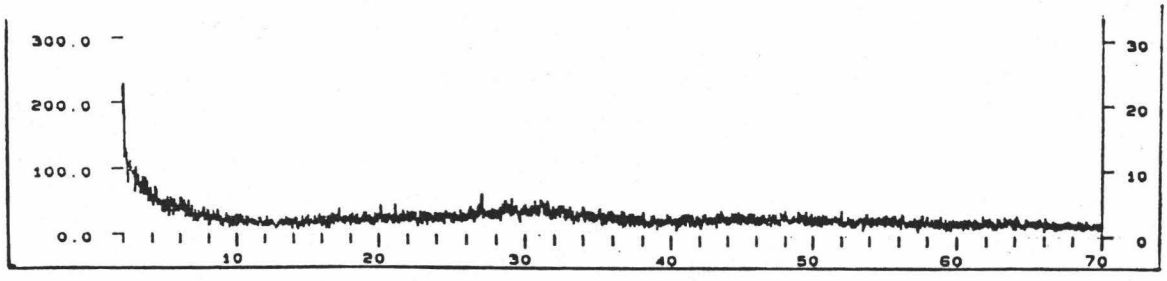
300.0
200.0
100.0
0.0
10
20
30
40
50
60
70
30
20
10
0

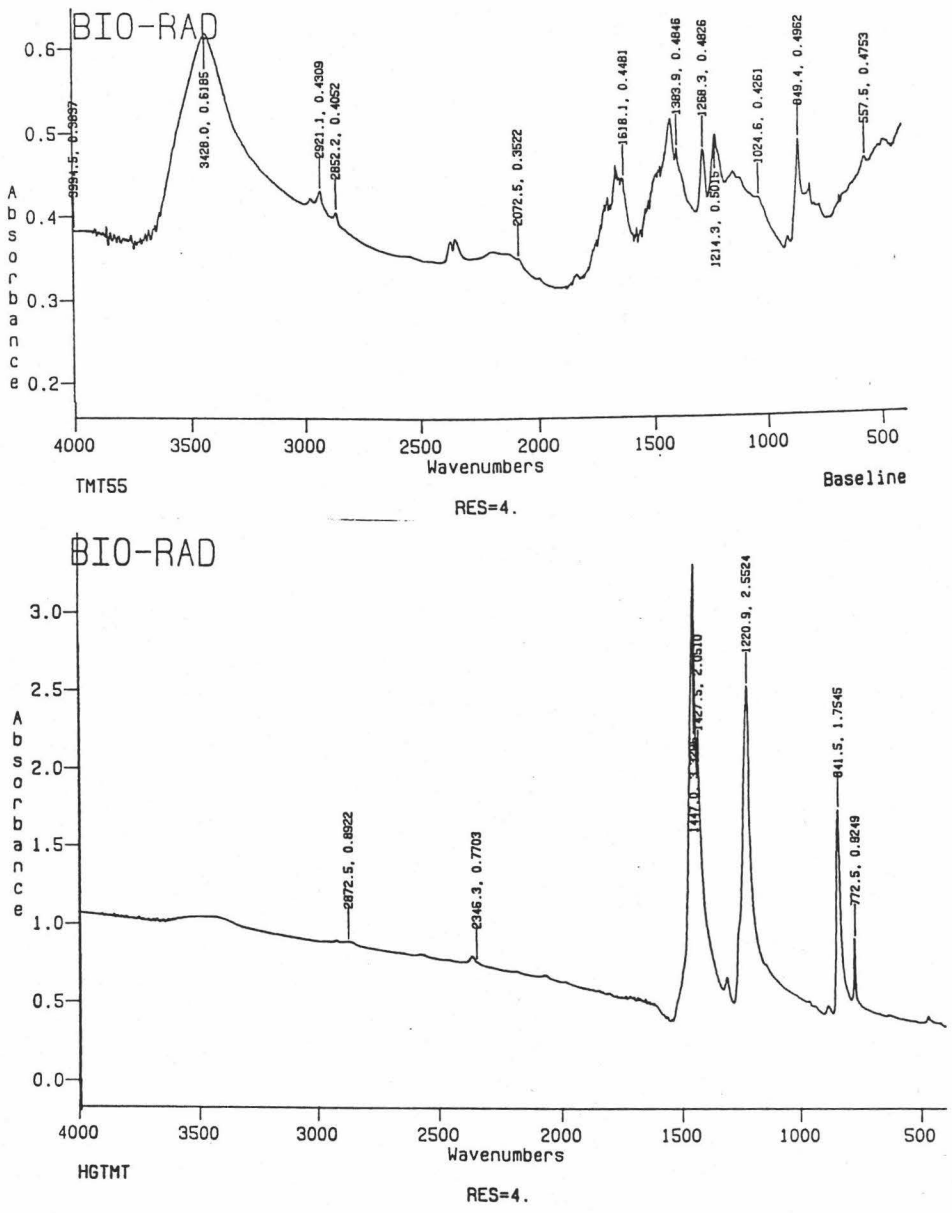

Figure 5. Infrared spectra of TMT-55 (top) and white HgTMT (bottom) made from 11.91 g of $HgCl_2$ (Table 19). The y axes are in units of absorbance, whereas the x axes have units of wave numbers (cm^{-1}). The 3400 cm^{-1} region shows the presence of water in TMT-55, but almost none in the HgTMT. A Raman spectrum of TMT-55 was similar, but no water peaks were detected in the 3400 cm^{-1} region for white HgTMT.

The concentrations of the measured parameters of the white HgTMT sample (Table 20) and their summation (including water) to nearly 100 percent suggests that impurities, such as $H_3C_3N_3S_3$, $HgCl_2$, TMT-55 or NaCl, are probably not abundant in the sample. Powder XRD scans of several white samples produced from $HgCl_2$ also do not contain any evidence of crystalline impurities, such as: $H_3C_3N_3S_3$, $HgCl_2$, TMT-55 or NaCl. Amorphous humps are either absent from XRD scans of white HgTMT or clearly are weaker than those in scans of the yellow variety (Figure 4).

The chemical analysis of the white HgTMT in Table 20 shows that the number of moles of carbon, sulfur, and nitrogen are approximately equal, which is consistent with the presence of $(C_3N_3S_3)^{3-}$. However, the reason(s) for the large number of moles of nonaqueous hydrogen is unknown. While the chemical analysis of the "pale cream colored" HgTMT described by Chudy and Dalziel (1975) is consistent with $(Hg^{2+})_3(C_3N_3S_3)_2$, the results in Table 20 show only 2 Hg for every $(C_3N_3S_3)^{3-}$. Table 21 compares the analysis of the white HgTMT (normalized without water) to various possible formulas containing one or two $(C_3N_3S_3)^{3-}$ units. The analysis from Chudy and Dalziel (1975) is included as another comparison. If the white HgTMT represents one pure compound rather than a mixture of compounds as the XRD analyses suggest, then the analytical data for the white HgTMT in Table 21 are consistent with three formulas, all of which contain mercury(I) (*i.e.*, $Hg^{2+}Hg^{1+}[C_3N_3S_3]$, $[Hg^{1+}]_2H[C_3N_3S_3]$, or $[Hg^{2+}][Hg^{1+}]_3H[C_3N_3S_3]_2$).

Table 21. The chemical analysis of the white HgTMT compound listed in Table 20 (normalized without water) is compared with likely chemical formulas. The analysis is most consistent with three formulas containing Hg^{1+} (*i.e.*, $Hg^{1+}Hg^{2+}[C_3N_3S_3]$, $[Hg^{2+}][Hg^{1+}]_3H[C_3N_3S_3]_2$, or $[Hg^{1+}]_2H[C_3N_3S_3]$).

Analysis or Ideal Formula	Mercury (wt%)	Carbon (wt%)	Nitrogen (wt%)	Sulfur (wt%)	Nonaqueous Hydrogen (wt%)
Analysis from Table 20	69.22	6.27	6.99	17.05	0.47
Analysis from Chudy and Dalziel (1975)	63.2	7.76	8.92	20.15	–
$(Hg^{1+})_3(C_3N_3S_3)$	77.55	4.64	5.41	12.39	0.00
$(Hg^{1+})_5H(C_3N_3S_3)_2$	74.16	5.33	6.21	14.22	0.07
$(Hg^{1+})_2H(C_3N_3S_3)$	69.60	6.25	7.29	16.69	0.17
$(Hg^{1+})_3H_3(C_3N_3S_3)_2$	63.13	7.56	8.82	20.18	0.32
$(Hg^{1+})H_2(C_3N_3S_3)$	53.23	9.56	11.15	25.52	0.53
$(Hg^{1+})H_5(C_3N_3S_3)_2$	36.20	13.01	15.17	34.72	0.91
$Hg^{2+}Hg^{1+}(C_3N_3S_3)$	69.72	6.26	7.30	16.72	0.00
$(Hg^{2+})(Hg^{1+})_4(C_3N_3S_3)_2$	77.55	4.64	5.41	12.39	0.00
$(Hg^{2+})(Hg^{1+})_3H(C_3N_3S_3)_2$	69.66	6.26	7.30	16.70	0.09
$(Hg^{2+})(Hg^{1+})_2H_2(C_3N_3S_3)_2$	63.19	7.57	8.83	20.20	0.21
$(Hg^{2+})(Hg^{1+})H_3(C_3N_3S_3)_2$	53.30	9.57	11.17	25.56	0.40
$(Hg^{2+})H(C_3N_3S_3)$	53.37	9.59	11.18	25.59	0.27
$(Hg^{2+})H_4(C_3N_3S_3)_2$	36.27	13.03	15.19	34.78	0.73
$(Hg^{2+})_2(Hg^{1+})H(C_3N_3S_3)_2$	63.26	7.58	8.83	20.22	0.11
$(Hg^{2+})_3(C_3N_3S_3)_2$	63.33	7.58	8.84	20.24	0.00

Mercury(I) compounds, such as mercurous chloride, actually consist of pairs of bonded Hg^{1+}, that is, Hg_2^{2+} (Nebergall et al., 1976, p. 846). Thus, the formula for mercury(I) chloride is really Hg_2Cl_2 rather than HgCl. Mercury(I) does not form very many stable compounds with organic ligands (Cotton and Wilkinson, 1972, p. 510). One of the few known compounds is $Hg_2N_2(COCH_3)_2$ (Bailar et al., 1973, p. 293) and by analogy with this compound, the following structure should be present in white HgTMT:

20) ...C-N ring - S - Hg - Hg - S - C-N ring ...

The mercury(II) structure, if present in white HgTMT, should be:

21) ...C-N ring - S - Hg - S - C-N ring ...

Mercury Concentrations of Other Varieties of HgTMT

Limited chemical data are available on other varieties of HgTMT. Gray, bright yellow, and amorphous greenish yellow samples, whose powder XRD patterns are shown in Figure 4, were analyzed for mercury (Table 22). Table 22 also includes results from a medium yellow specimen (1.61 g of $HgCl_2$; Table 19) and an originally white, but currently light gray, sample that was made from 2.49 g of red HgO (Table 19). An XRD analysis of the light gray sample contained peaks with *d*-values that were commonly found in some darker gray varieties of HgTMT made from $HgCl_2$ (see discussions below), whereas an XRD scan of the medium yellow sample was very similar to the scan of the bright yellow specimen in Figure 4.

Table 22. Mercury and other analyses of greenish yellow, yellow, gray, and light gray HgTMT. Figure 4 shows the powder XRD patterns of some of the samples.

HgTMT Sample	Mercury Compound Used to Produce the Sample	Mercury (wt%)	Carbon (wt%)	Water (wt%)
Bright yellow produced from exposure of white HgTMT to air	$HgCl_2$	38.6	–	–
Medium yellow produced from exposure of white HgTMT to water (XRD is not in Figure 4)	$HgCl_2$	63.5	6.62	1.08
Light gray produced from exposure of white HgTMT to air (XRD is not in Figure 4)	HgO	46.7	8.28	5.50
Dark Gray	$HgCl_2$	36.2	–	–
Resinous greenish yellow	$HgCl_2$	28.7	–	–

Potential contamination of analytical equipment by mercury vapor, high costs, and analytical interferences between mercury and oxygen often prevented the analysis of oxygen, water, carbon, nitrogen, and sulfur in the samples. The limited data in Table 22 verify that the compounds contain abundant mercury.

The mercury concentrations of the bright and medium yellow samples in Table 22 are very different. The discrepancy may be due to the amount of water in the samples or how the samples were analyzed. Personnel at ORNL analyzed the bright yellow, dark gray and resinous greenish yellow samples, whereas the other two samples with higher mercury concentrations were analyzed at ME&T Corporation.

The mercury concentration of the medium yellow HgTMT sample (63.5 wt%; Table 22) is very close to the results from the probable $(Hg^{2+})_3(C_3N_3S_3)_2$ in Chudy and Dalziel (1975) (63.2 wt% in Table 21). However, the carbon analysis (6.62 wt%; Table 22) is much lower than the expected value of 7.58 wt% for $(Hg^{2+})_3(C_3N_3S_3)_2$ (Table 21) and without nitrogen, sulfur, and oxygen analyses for the sample, an accurate description of its composition is not possible.

Crystalline Structure of White HgTMT

Many attempts were made to slow the crystallization of white HgTMT so that significantly large single crystals could be produced to determine the space group and other structural information by single-crystal XRD. However, no solvents or techniques were successful and the space group and other important information on the crystalline structure are still unknown.

Several powder XRD patterns of white HgTMT consistently provided 16 different *d*-values. The *d*-values were calibrated with silicon, corundum and fluorophlogopite standards (Table 23). The relative intensities of the white HgTMT peaks were determined from XRD analyses of three Vaseline® mounts without any standards. To reduce background noise, three point boxcar smoothing was applied to the scans from the relative intensity mounts.

The *d*-values listed in Table 23 were entered into TREOR90 (an updated version of Werner et al., 1985) and DICVOL91 (Boultif and Louer, 1991) to obtain independent unit cell solutions. Both programs obtained nearly the same solution and the solution

rejected none of the 16 peaks. The solution was verified and refined with PIRUM version 930101 (an update of Werner, 1969) and Table 24 shows the final unit cell results.

The unit cell of white HgTMT is much smaller than those for TMT-55 or the barium TMT compounds (compare Tables 13 and 24 with information in Chapter 7). Furthermore, the area of the unit cell represented by $a = 5.904$ Å and $b = 6.966$ Å (41.13 Å^2) is barely large enough to contain two mercury cations and one of the $(C_3N_3S_3)^{3-}$ ring structures. The sulfur to sulfur distances on the ring structure are about 5.6 Å as calculated from the TMT-55 25°C single crystal data in the Appendix. The atomic radii of Hg^{1+} and Hg^{2+} are typically 0.97 and 1.02 Å, respectively (Bloss, 1971, p. 211).

XRD Patterns of Gray HgTMT

The XRD patterns of one light gray and two darker gray HgTMT samples were compared. Table 25 shows the conditions used to produce the samples. The sample from October 25, 1995 was produced on October 19-25 from a relatively large dose of $HgCl_2$. The precipitated white gel was washed to remove any NaCl and then air dried. In seven days, the sample dried to a gray solid with minor amounts of yellow and white HgTMT. An XRD scan with the Scintag diffractometer was obtained on October 26, 1995. Figure 4 shows the scan. The sample contains 36.2 wt% mercury (Table 22).

Table 23. A list of measured *d*-values and corresponding 2θ values (based on $CuK_{\alpha 1}$ radiation) for peaks from powder XRD scans of white HgTMT samples. The *d*-values were calibrated with silicon, corundum and fluorophlogopite standards. Intensities were measured from three other mounts without any standards. The calculated data and *hkl* values are from PIRUM version 930101 (update of Werner, 1969).

Measured *d*-values (Å)	Measured 2θ (degrees)	Measured Relative Intensities	Calculated *d*-values (Å)	Calculated 2θ (degrees)	*hkl*
6.98	12.67	17,15,15	6.97	12.70	010
5.71	15.51	26,28,28	5.71	15.51	100
4.42	20.08	100,100,100	4.42	20.07	001
4.03	22.04	18,14,12	4.03	22.04	-101
3.734	23.81	22,20,17	3.732	23.82	011
3.486	25.53	60,54,57	3.488	25.52	-111
3.127	28.52	25,23,22	3.128	28.51	101
2.974	30.02	16,9,10	2.973	30.03	-120
2.853	31.33	24,19,21	2.853	31.32	111
2.736	32.71	17,21,28	2.736	32.71	021
2.322	38.76	14,7,10[a]	2.322	38.75	030
2.154	41.90	20,18,17	2.155	41.90	-112
2.011	45.04	13,7,18[a]	2.012	45.02	-131
1.8642	48.81	8,8,12[a]	1.8645	48.81	131
1.7441	52.42	–[b]	1.7441	52.42	-222
1.6204	56.77	–[b]	1.6204	56.77	041

[a] Three point box car smoothing eliminated some peaks on the third intensity mount. The intensities from the unsmoothed peaks are listed.

[b] The peaks were not seen on any of the intensity scans after smoothing and were not even present on all of the scans before smoothing. However, they were detected on some *d*-value calibration scans.

Table 24. Unit cell solution for white HgTMT.

Parameter	Value
Crystal System	Monoclinic
Crystal Class	Unknown
Space Group	Unknown
Length of *a* axis (Å)	5.904(3)
Length of *b* axis (Å)	6.966(1)
Length of *c* axis (Å)	4.572(1)
β angle (degrees)	104.85(2)
V (Å^3)	181.79
M_{16}	65
F_{16}	37 (0.0082, 53)

A sample of white HgTMT was produced on November 10-20, 1995 by dissolving 1.56 g of $HgCl_2$ in gently warmed distilled and deionized water. The water had been previously purged with ultrapure nitrogen gas for 24 hours. TMT-55 (1.40 g) rather than TMT-15 was directly added to the $HgCl_2$ solution and a white precipitate immediately formed. The precipitate was recovered, rinsed with distilled and deionized water, and slowly dried by gentle heating under a nitrogen purge from November 10-20, 1995. The dried sample remained white and gave the usual white HgTMT XRD pattern.

A total of 0.8128 g of the November 10-20, 1995 white HgTMT was placed in 100.16 g of distilled and deionized water on December 30, 1995. The sample leached in the distilled and deionized water for more than four months. By March 1996, the sample

had turned gray. The formerly white, gray HgTMT sample was removed from the water on May 14, 1996 and air dried.

White HgTMT was produced on May 19-23, 1996 by adding 38.56 g of TMT-15 to 2.49 g of red HgO. The white gel was allowed to air dry from May 23-25, 1996. The sample dried bright white, but over the next year it turned light gray in the presence of air.

Table 25. Conditions used to produce one light gray (5/97) and two darker gray (10/25/95 and 5/14/96) HgTMT samples.

Date Sample Produced	g of $HgCl_2$ (or red HgO)	ml of Distilled Water After TMT Added	g of TMT-55 in TMT-15	$Hg/(C_3N_3S_3)^{3-}$ Molar Ratio of Solution	Other Notes:
10/25/95	20.17	1100	15.00	2.0	No heat or nitrogen purge.
5/14/96	1.56	100	1.40 as TMT-55	1.7	Heated under nitrogen purge. Originally white, turned gray after three months of leaching in water.
5/97	2.49 (HgO)	39	5.78	0.81	No heat or nitrogen purge. Originally white, turned very light gray in air after one year.

In 1997, more extensive XRD analyses were done on the three gray HgTMT samples with two Philips diffractometers. Each of the three samples was analyzed at least twice, once to identify the intensities of the peaks and again to calibrate the *d*-values with a fluorophlogopite standard. Table 26 lists the *d*-values down to 2.0 Å seen in at least two separate analyses of one of the three samples.

The number of detected peaks in the October 25, 1995 sample was much greater when it was run on the Philips diffractometers than when the sample was originally scanned on a Scintag DMS 2000 diffractometer in 1995 (compare Figure 4 [a Scintag XRD scan from 1995] with the list of peaks in Table 26 [derived from Philips scans in 1997]). The increase in the number of peaks may be due to greater sensitivity in the Philips diffractometers or to the development of one or more additional crystalline compounds in the sample during the roughly two year period.

The XRD data in Table 26 show that the crystalline compound(s) in the October 25, 1995 sample is mostly different from the compound(s) in the other two samples. Unlike the May 1996 and 1997 samples, the gray HgTMT in the October 25, 1995 sample was produced in only seven days. Except for the presence of white HgTMT, the corrected *d*-values of the three samples in Table 26 do not consistently match $H_3C_3N_3S_3$ or any inorganic or organic compounds in the ICDD databases. Careful comparisons were also made between the list of *d*-values in Table 26 and many crystalline compounds that could possibly exist in the three samples. The *d*-values in Table 26 did not match within ±0.003 Å any of the most intense (intensities of 15 or greater) *d*-values of trithiocyanuric acid ($H_3C_3N_3S_3$), cinnabar (red HgS, PDF 6-0256 and 3-0396), metacinnabar (black HgS,

Table 26. A list of corrected *d*-values (above 2.0 Å) commonly seen in three light gray to gray HgTMT samples. The *d*-values were corrected with a fluorophlogopite standard. The relative intensities of the peaks in the samples are listed in the appropriate column.

d-values (Å)	Gray HgTMT (10/25/95)	Gray HgTMT (5/14/96)	Light Gray HgTMT (5/97)	Identity of Peak
10.90	43			Unknown
7.97		84	100	Unknown
7.26	10			Unknown
7.09		31	25	Unknown
6.78	40			Unknown
6.57	100	18		Unknown
6.05			5	Unknown
5.95	12			Unknown
5.82		21	14	Unknown
5.71	21	29		White HgTMT
5.65	33			Unknown
5.48		14	17	Unknown
5.11		25	27	Unknown
4.95		60	55	Unknown
4.63	10			Unknown
4.54		30	17	Cyanuric acid? (PDF 23-1637)
4.45	28			Unknown
4.42	24	100		White HgTMT
4.20	24			Unknown
4.01	6	16		Unknown
3.945		16	23	Cyanuric acid? (PDF 23-1637)

Table 26 cont.

3.875	16			Unknown
3.734	18	30		White HgTMT
3.703		18	13	Unknown
3.645	18			Unknown
3.634		60	40	Unknown
3.542			7	Unknown
3.478		93	16	Unknown
3.385	21	24	12	Cyanuric acid dihydrate? (PDF 31-1632); Mercury(II) sulfate? (PDF 31-867)
3.224	36			Unknown
3.189	51			Unknown
3.127		53	12	White HgTMT
3.070		50	49	Unknown
2.888		31	16	Unknown
2.853		38		White HgTMT; HgO? (PDF 2-0305)
2.790			15	Unknown
2.774		25	16	Unknown
2.747		32		Mercury oxide carbonate? (PDF 32-0657)
2.736		66	20	Unknown
2.663	30		21	Unknown
2.638		33	16	Unknown

Table 26 cont.

2.606		10	7	Unknown
2.558	20	10		Unknown
2.453	28			Unknown
2.369			18	Mercury(II) sulfate? (PDF 31-867)
2.262			9	Unknown
2.244			12	Unknown
2.210			11	Sodium cyanurate? (PDF 36-1812); Cyanuric acid? (PDF 24-1712 and 3-0202)
2.196			9	Unknown
2.154		49		White HgTMT
2.146	13			Unknown
2.137	10			Hg_2O? (PDF 13-0140); Sodium cyanurate? (PDF 36-1812)
2.103	14			Unknown
2.085	19			Unknown
2.063	27		8	Unknown
2.011	9			White HgTMT?

PDF 06-0261), halite (NaCl, PDF 5-628), s-triazine ($H_3C_3N_3$, PDF 31-1954), sodium cyanurate ($Na_3C_3N_3O_3$, PDF 31-1880), 4-nitroimidazole ($H_3C_3N_3O_2$, PDF 36-1677 and 34-1604), 6-azauracil ($H_3C_3N_3O_2$, PDF 26-1613), and various mercury (II) oxides (HgO, PDF 1-0896, 2-0305, 5-0596, 9-0381, 11-0584, and 37-1469). There were matches within ± 0.003 Å for one or two of the most intense peaks of mercury oxide carbonate ($HgCO_3$•2HgO, PDF 32-0657), cyanuric acid ($H_3C_3N_3O_3$, PDF 03-0202, 23-1637, and 24-1712), cyanuric acid dihydrate ($H_3C_3N_3O_3$•$2H_2O$, PDF 31-1632), mercury(II) sulfate ($HgSO_4$, PDF 31-867), sodium cyanurate ($Na_3C_3N_3O_3$, PDF 36-1812) and mercury(I) oxide (Hg_2O, PDF 13-0140) (Table 26). However, the numbers of matched peaks were not significant enough to state conclusively that any of the compounds were present in any of the gray HgTMT samples. The low number of intense peaks in many cyclic organic compounds especially hindered the characterization of the three HgTMT samples. For example, s-triazine (PDF 31-1954) only has two peaks with relative intensities of greater than four. The inability to identify any compounds in gray HgTMT except for white HgTMT means that more detailed and sophisticated analytical studies are required. For example, sieving the samples or extracting them with solvents that are chemically inert may concentrate some of the compounds and allow them to be identified by XRD. Furthermore, many of the PDF patterns are more than 30 years old and the accuracy of their *d*-values should be verified with modern methods.

Unknown compounds may be identified by entering their *d*-values into TREOR90 (an updated version of Werner et al., 1985) or PIRUM (an updated version of Werner, 1969). Any solution with an M_{20} value of 20 or higher could suggest that the peaks are

associated with one compound and the unit cell dimensions from such a solution could help in identifying the compound. The *d*-values unique to the October 25, 1995 sample were entered into TREOR90 and PIRUM. No solution was found. Peaks unique to both the May 1996 and 1997 samples were also evaluated with TREOR90. Again, no solutions with M_{20} values of 20 or higher were obtained.

Batch Leaching Studies of HgTMT and Metacinnabar

Introduction

Batch leaching tests are laboratory procedures used to determine the types and concentrations of contaminants (*e.g.*, mercury) that may dissolve out of a solid sample (*e.g.*, HgTMT) when it comes into contact with a leaching solution, usually water or dilute acids (Henke et al., 1993, p. 53). Typically, the tests consist of placing a specific mass of a solid sample into a bottle with a given volume of leaching solution, agitating or tumbling the mixture for at least 18 hours, filtering the mixture, and then analyzing the filtrate for any organic or inorganic contaminants. The concentrations of any contaminants may be compared with U.S. EPA standards for contaminants in wastes (40 CFR 268.40) or other regulatory standards that establish maximum acceptable levels of inorganic and organic contaminants in water. The Toxicity Characteristic Leaching Procedure (TCLP) is one of the better known batch leaching tests and is used in the United States to evaluate the toxic hazardousness of a solid or liquid waste (40 CFR 261).

Leaching studies were done on metacinnabar and several varieties of HgTMT to determine how much mercury would leach from the compounds in distilled and deionized

water. The tests may be useful in predicting whether substantial mercury may leach out of different varieties of HgTMT if the compounds come into contact with rain water or low TDS ground water.

Materials and Methods

Samples of Aldrich (lot 04609T2) metacinnabar and different varieties of HgTMT made from $HgCl_2$ were ground and dry sieved at either 118 or 243 μm. Glass vials (50 ml) were washed and baked for at least six hours at 500°C to remove any trace amounts of mercury. Samples of the sieved materials were placed in the vials and weighed. After weighing, the samples were thoroughly rinsed three times with distilled and deionized water to remove any water-soluble coatings, such as mercury(II) sulfate on the metacinnabar. Except for vials 5, 6, and 7 (Table 27), the vials were completely filled with a known mass of distilled and deionized water. Vials 5-7 were filled with approximately 41 ml of distilled and deionized water, which left a head space of approximately 6 ml of air. In the initial experiments, the leaching water was thoroughly bubbled with ultrapure nitrogen gas to reduce the amount of carbonic acid prior to the leaching tests. However, the nitrogen purge was discontinued after no differences were noticed between mercury analyses with bubbled and unbubbled water. The vials and their contents were thoroughly mixed for one week on end-over-end tumblers. After mixing, portions of the leachates were filtered at 0.45 and sometimes 0.20 μm. The remaining unfiltered leachates were measured for pH. The filtered aliquots, including duplicates of every fifth sample, were placed in ultraclean Teflon® bottles and diluted to 100 ml with distilled and deionized

water. The exact mass of the dilution was measured and recorded to the nearest 0.01 g. Distilled and deionized water blanks were also included with the samples. BrCl (0.50 ml) was added to each diluted leachate and blank to oxidize or "digest" any mercury to the +2 valence state.

The BrCl digestions were allowed to sit at room temperature for 24 hours before analysis. After 24 hours, 0.20 ml of a 30% aqueous solution of hydroxylamine (NH_2OH) was added to each digestion to eliminate the excess BrCl so that the sample could easily be reduced by stannous chloride during the subsequent mercury analysis. At least five

Table 27. Batch leaching results on metacinnabar and white, yellow, and gray varieties of HgTMT.

HgTMT or Metacinnabar (black HgS)	Vial #	g of Solid	μm Sieved	g of Water	pH	μg/l of Total Hg in Leachate	μm Filter
White	2	0.1197	243	46.0018	4.10	3900	0.45
White	3	0.0827	243	47.0419	4.25	3000	0.45
White	4	0.1036	243	46.6305	4.16	3800	0.45
White	5	0.0929	243	40.7001[a]	4.19	3800	0.45
White	6	0.0920	243	41.7673[a]	4.27	3200	0.45
White	7	0.1248	243	40.8420[a]	4.18	3800	0.45
White	17	0.0103	118	46.6101	5.46	280	0.45
White	18	0.0228	118	46.4585	5.14	650	0.45
Light Yellow	32	0.0555	243	47.2665	4.72	1300	0.45
Light Yellow	33	0.2435	243	47.2578	3.96	3500	0.45
Light Yellow	34	0.1352	243	45.7513	4.17	3100	0.45

Table 27 cont.

Light Yellow	39	0.0218	243	46.2888	5.01	490	0.45
Light Yellow	39	0.0218	243	46.2888	5.01	490	0.20
Light Yellow	40	0.4258	243	45.9029	3.70	6600	0.45
Medium Yellow	35	0.0569	243	45.8140	5.03	210	0.45
Medium Yellow	36	0.0665	243	46.3737	4.94	240	0.45
Medium Yellow	38	0.0232	243	46.3635	5.21	76	0.45
Medium Yellow	38	0.0232	243	46.3635	5.21	70	0.20
Bright Yellow	25	0.0180	243	46.2215	6.96	13	0.45
Bright Yellow	25	0.0180	243	46.2215	6.96	3.3	0.20
Bright Yellow	27	0.0279	243	48.1043	7.03	22	0.45
Bright Yellow	27	0.0279	243	48.1043	7.03	5.9	0.20
Gray	29	0.0574	243	45.9903	9.99	53	0.45
Gray	30	0.0267	243	46.0757	9.42	24	0.45
Gray	31	0.0309	243	46.1573	9.55	39	0.45
Gray	31	0.0309	243	46.1573	9.55	22	0.20
Metacinnabar	22	0.2188	243	46.2487	5.94	35	0.45
Metacinnabar	22	0.2188	243	46.2487	5.94	26	0.20
Metacinnabar	23	0.0917	243	46.2873	6.56	12	0.45
Metacinnabar	24	0.0777	243	46.7236	6.26	22	0.45
Metacinnabar	24	0.0777	243	46.7236	6.26	21	0.20

[a] Approximately 41 ml of water were placed in these three vials, which left head spaces of approximately 6 ml of air. The other vials were completely filled with water.

minutes after adding NH_2OH, an aliquot of each digestion was analyzed for mercury with a rapid, effective and inexpensive method developed by Dr. Ralph R. Turner at ORNL (Kriger and Turner, 1995; Šolc et al., 1997). The method involves adding 0.10 to 1.00 ml of the digestion to 100 ml of distilled and deionized water in a previously unused one liter plastic bottle. Five ml of stannous chloride solution is then added to the bottle. The bottle is quickly capped and hand shaken for one minute, which reduces the mercury and distributes the vapor between the head space and the water of the bottle according to Henry's Law (Kriger and Turner, 1995; Faure, 1991, p. 244). An Arizona Instrument Inc. Jerome Model 431-X mercury vapor analyzer is used to measure the concentration of the mercury vapor in the head space of the bottle. Duplicates are done on every fifth analysis and blanks and standards are run after no more than 10 analyses. By using mercury standards and blanks, the mercury concentrations from the vapor analyzer may be converted to μg/l of total mercury in the original filtered leachates.

Leaching Results and Discussion

Table 27 lists the leaching results on various masses of metacinnabar and white, yellow, and gray HgTMT samples. The resinous brownish yellow to brownish green variety could not be produced in large enough quantities for leaching studies.

As shown in Table 27, mercury concentrations of the 0.20 μm leachates are usually lower than those in the corresponding 0.45 μm samples. This trend is expected because finer filters should remove more of the "dissolved" mercury.

The mercury concentrations released by the bright yellow and gray HgTMT samples are similar to metacinnabar (Table 27). The leaching data also show that white and light yellow HgTMT release much more mercury in water than metacinnabar, gray HgTMT, or more yellow HgTMT. The mercury released by the white and light yellow varieties exceeds the 0.2 mg/l (200 μg/l) mercury standard for toxic hazardousness (40 CFR 268.40) and may even exceed 6000 μg/l (Table 27). Furthermore, the mercury concentrations in the leachates of the white and light yellow varieties show no evidence of approaching saturation. The leaching of mercury from white and light yellow HgTMT, however, may be reduced by the tendencies of the compounds to transform under atmospheric conditions to the less leachable bright yellow or gray varieties.

Information on the chemistry of white HgTMT (Table 20) and the data in Table 27 show that only 0.36 to 0.49% of the mercury in the white samples actually dissolves in water. Periodic pH measurements of the distilled and deionized water before it was mixed with the mercury compounds obtained values of around 5.7, which are consistent with water in equilibrium with atmospheric carbon dioxide at 25°C (Krauskopf, 1979, p. 33). For every mole of mercury that dissolved from white HgTMT into pH 5.7 water, there was a net increase of 1.05 to 3.98 moles of H^+. Currently, the chemical formula of white HgTMT and the strengths of the bonds in the compound are too uncertain to derive reliable reactions to explain the decrease in pH with the aqueous leaching of mercury from the compound.

MINTEQA2 (Allison et al., 1991) was used to model the pH and mercury concentrations for two of the leached metacinnabar samples: 0.2188 g of metacinnabar in

46.2487 g of water (0.0203 moles of HgS/liter of water) and 0.0777 g of metacinnabar in 46.7236 g of water (0.0071 moles/liter) (Table 27). If the pH of the water is 7.00, MINTEQA2 calculations suggest that the addition of metacinnabar should not affect pH and should release an undetectable amount of mercury into the water at 25°C (1.7×10^{-19} moles/kilogram or 4.0×10^{-11} μg/l as $Hg[OH]_2^0$ for both leachates). The consideration of 0.21 atmospheres of oxygen and 0.0003 atmospheres of carbon dioxide (Faure, 1991, p. 175, 217) in the model reduces the pH values of both mixtures to 5.68, but the mercury concentrations remain extremely low at 1.7×10^{-19} moles/kilogram or 4.0×10^{-11} μg/l as $Hg(OH)_2^0$. The measured mercury concentrations (as Hg^{2+}) in the water leachates of the metacinnabar samples are much higher (Table 27). Metacinnabar may decompose in water through the following thermodynamically favored reaction, which is analogous to the oxidation of pyrite in acid mine drainage (Faure, 1991, p. 312-313):

22) $HgS + 2O_2^0 + 4H_2O \rightarrow Hg(OH)_2^0 + SO_4^{2-} + 2H_3O^+$, $\Delta G = -13.12$ kcal/mol

There are at least three possible explanations for the discrepancies between the calculated MINTEQA2 results and measured values in Table 27: 1) rinsing with distilled and deionized water does not entirely remove leachable coatings of mercury(II) sulfate or other mercury compounds from the surfaces of the HgS; 2) the solubility products and modeling conditions in MINTEQA2 are inadequate; and 3) colloids of metacinnabar are sometimes observed when the compound is mixed with water. Colloids may pass through 0.20 or 0.45 μm filters to produce anomalously high mercury concentrations. Although the cause(s) of the discrepancies is unknown, the leaching conditions of HgS in a natural environment are probably more adequately modeled by laboratory studies with actual

water and HgS mixtures than with MINTEQA2 simulations that only consider a limited number of chemical and physical processes that might affect leaching.

The volume of liquid that is present often affects the leaching properties of a solid sample. For example, the pH and mercury concentration of a leachate resulting from the addition of 1.00 g of white HgTMT to 40 ml of distilled and deionized water may be different from the values associated with 1.00 g of white HgTMT in 1000 ml of water. Liquid to solid ratios may be derived to compare leachates that have different masses of solids and/or leaching solutions. The liquid to solid ratios of the leachates in Table 27 may be calculated by dividing the mass of water in each vial by the mass of the associated mercury compound.

When the mercury concentrations, pH values, and liquid to solid ratios of the 0.45 μm leachates in Table 27 are plotted against each other on graphs, some important relationships become apparent, at least for some HgTMT samples (Figures 6-8). Visual observations of Figure 8 and especially Figure 6 suggest that the data roughly fall on a logarithmic curve. The curve is more distinct if only the white and light yellow HgTMT samples are considered. Although the data points in Figure 7 are relatively scattered with compared with Figures 6 and 8, a logarithmic distribution also may be seen if only the white, light yellow, and medium yellow HgTMT samples are considered.

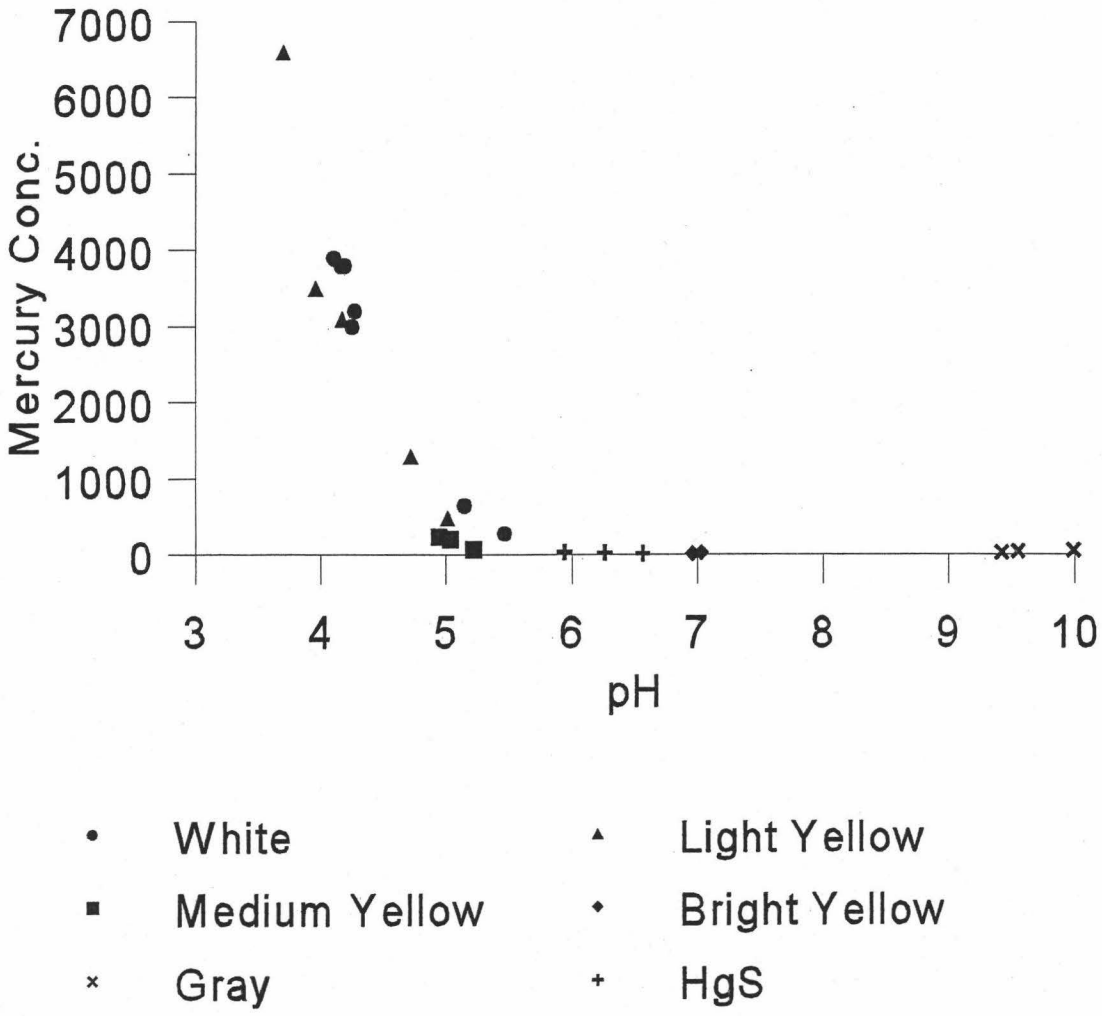

Figure 6. A plot of mercury concentrations in μg/l (y axis) versus pH values (x axis) of 0.45 μm distilled and deionized water leachates of metacinnabar and HgTMT samples (Table 27). Tables 28-30 list the statistical results.

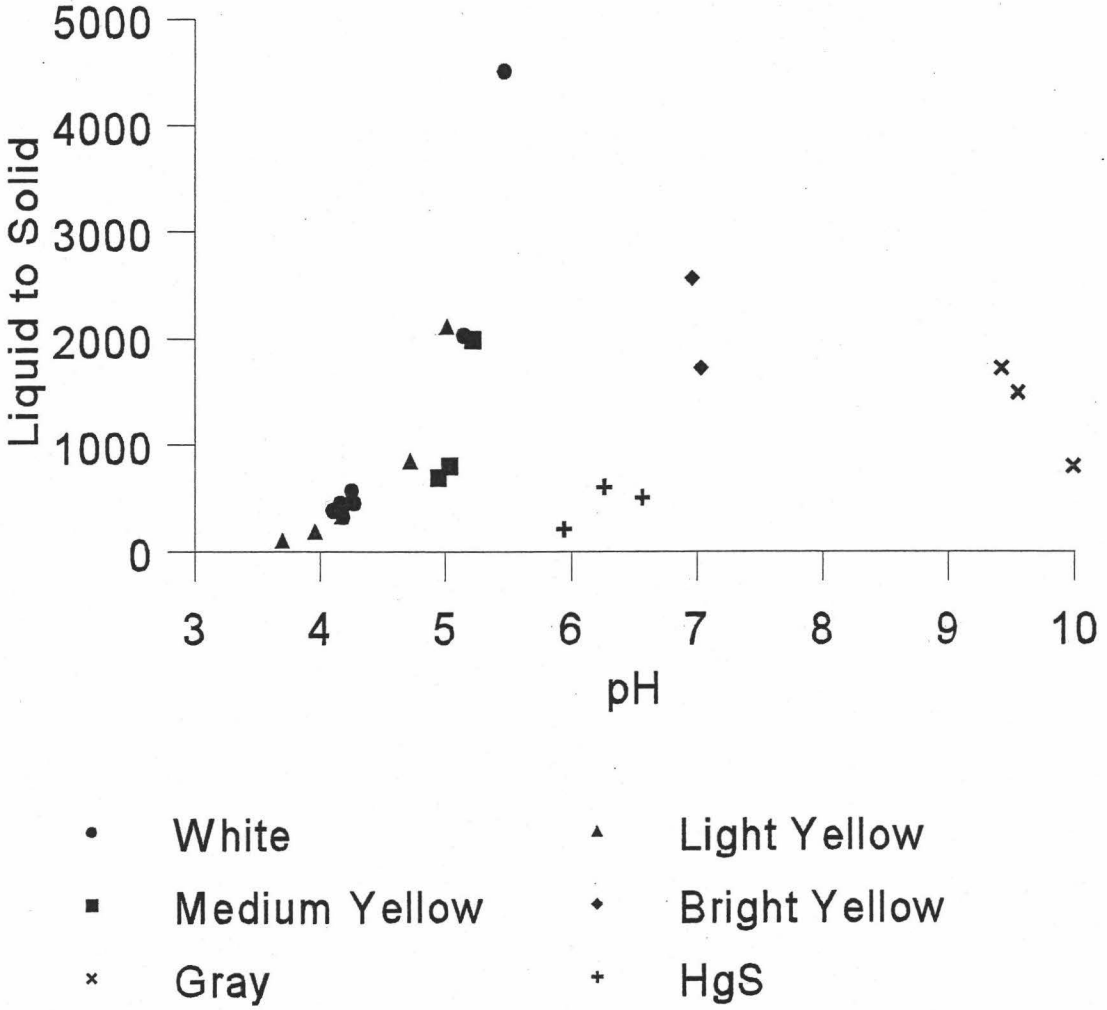

Figure 7. A plot of the liquid to solid ratios of 0.45 μm metacinnabar and HgTMT distilled and deionized water leachates (y axis) versus their pH values (x axis) (Table 27). Tables 28-30 list the statistical results.

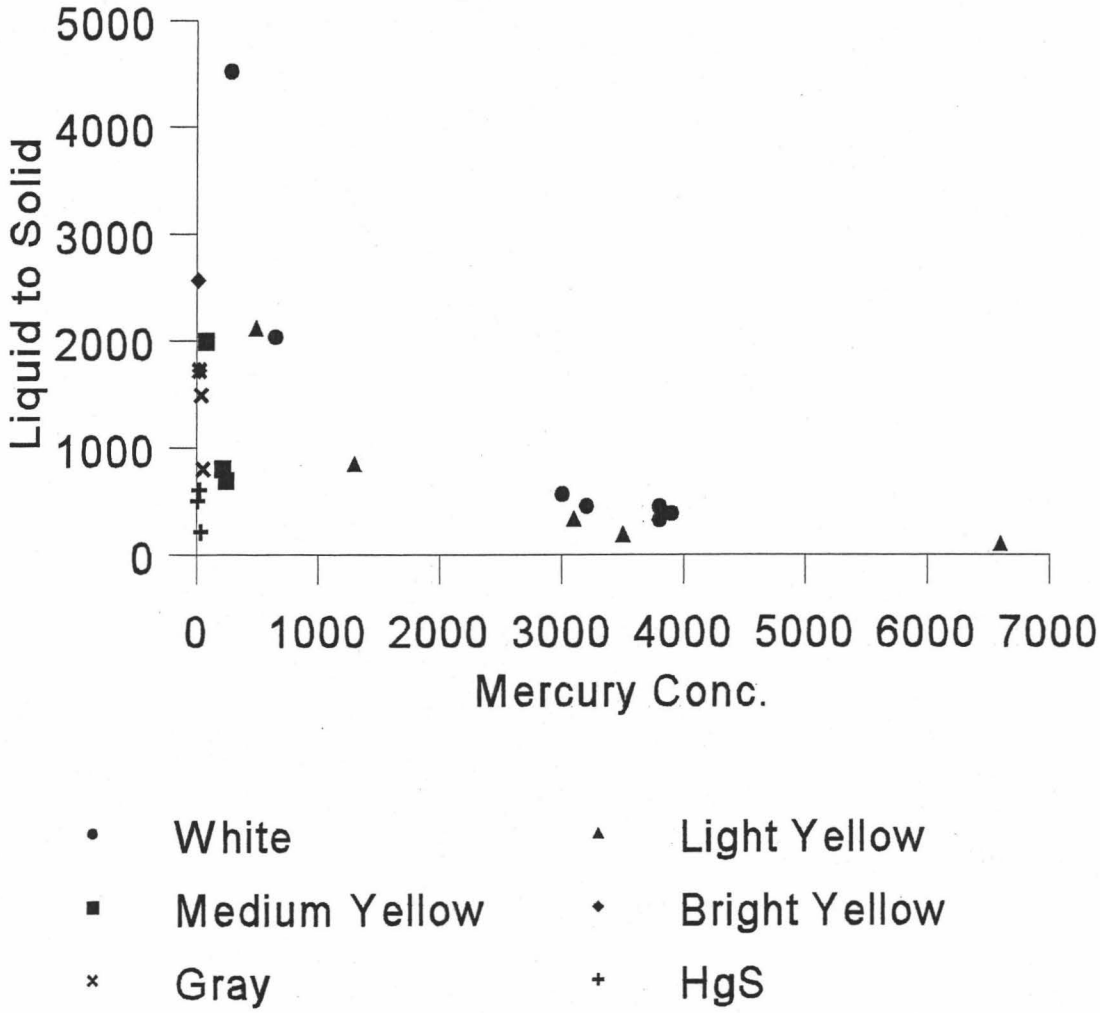

Figure 8. A plot of the liquid to solid ratios of 0.45 μm metacinnabar and HgTMT distilled and deionized water leachates (y axis) versus their mercury concentrations in μg/l (x axis) (Table 27). Tables 28-30 list the statistical results.

The 0.20 μm data from Table 27 are not included in Figures 6-8 and subsequent statistical calculations. Except for mercury concentrations, the 0.20 μm leaching data are duplicated by 0.45 μm samples (Table 27) and inclusion of the 0.20 μm data would bias the statistical results.

The linearity of the relationships in Figures 6-8 may be described with Pearsonian product-moment correlation coefficients ® values) (Davis, 1986, p. 34-41, 97). The range of possible r values is -1.00 to 1.00, where 1.00 represents a perfect direct linear relationship between two variables, zero signifies no relationship, and -1.00 represents a perfect inverse linear relationship (Davis, 1986, p. 38). Pearsonian *r* values and many other statistical parameters require that samples have normal distributions (Davis, 1986, p. 66). However, the number of samples in Table 27 is small and may not be normalized. Converting the data to log values may produce near-normal distributions (Davis, 1986, p. 87-92). The pH values are already in a log format, but the mercury concentrations and liquid to solid ratios must be converted to log values before the *r* values can be calculated. Table 28 shows the *r* values for various groups of the mercury compounds and their 0.45 µm leachates. When only the white HgTMT samples are considered, the *r* values show either strong inverse or direct correlations for all three comparisons. The *r* values decrease as data for the yellow varieties, gray variety and metacinnabar are added (Table 28). The decreases in the *r* values as the different mercury compounds are considered are probably due to differences in the solubilities of the various HgTMT forms and metacinnabar, as well as differences in the pH values of their leachates. For example, white HgTMT leachates are acidic, whereas the gray HgTMT samples produce alkaline leachates.

Table 28. Pearsonian product-moment correlation coefficients (r) for HgTMT and metacinnabar 0.45 μm leaching data from Table 27. For various groups of the HgTMT samples and metacinnabar, the r values describe the linearity of relationships between the log values of the liquid to solid ratios, pH values, and the log values of the mercury concentrations of the leachates.

Group	Number of Samples	r of log Liquid to Solid Ratio versus pH	r of log Liquid to Solid ratio versus log Mercury Concentration	r of pH versus log Mercury Concentration
White HgTMT	8	0.988	-0.993	-0.997
White and light yellow HgTMT	13	0.982	-0.956	-0.982
White and all yellow HgTMT	18	0.787	-0.779	-0.953
All HgTMT	21	0.520	-0.756	-0.831
All HgTMT and HgS	24	0.496	-0.515	-0.787

The statistical significance of the 15 r values in Table 28 may be evaluated to determine if the linearity is illusory (*i.e.,* only due to random fluctuations) or if the relationships are real and an analysis of any of the three variables (*i.e.*, the log of the liquid to solid ratio, pH, or the log value of the mercury concentration of the leachate) may be used to estimate the values of the other two (Davis, 1986, p. 66-67). Because inverse relationships are possible between any of the two variables, two tailed tests were used to evaluate the significance of the r values in Table 28. The α level of the evaluations was set at 0.0125 instead of the usual value of 0.05. Evaluations of the 15 different Pearsonian

r values at $\alpha = 0.05$ may create a serious "family wise" error (Keppel, 1991, p. 164-170). That is, the chance of having a Type I error could become high when 15 related r values are evaluated at $\alpha = 0.05$. The probability of making a Type I error may be reduced by lowering α to 0.02 or 0.01. However, the chances of making a Type II error increase when α is lowered. A Type II error states that the null hypothesis has been retained when it is false. The use of $\alpha = 0.0125$ with two tailed tests should be a reasonable compromise to avoid both Type I and II errors.

For each of the 15 evaluations, the following null and alternative hypotheses were used:

Null Hypothesis (H_o): The Pearsonian r value is not significant. There is no relationship between the two evaluated parameters for the given group of mercury compounds in Table 28. The linearity is due to random fluctuations.

Alternative Hypothesis (H_a): The Pearsonian r value is significant. There is a linear relationship between the two evaluated variables for the given group of mercury compounds in Table 28. The linear relationship states that if the value of one of the evaluated parameters is known, the value of the other may be reasonably predicted.

The significance of the 15 r values was tested with the following equation (Davis, 1986, p. 67):

23) $t = r\,(n\text{-}2)^{½} / (1\text{-}r^2)^{½}$

where:

t = test statistic

n = sample number

r = Pearsonian r value.

The degrees of freedom in Equation 23 are n-2. The calculated test statistic from the equation was compared with critical t values from a table in Davis (1986, p. 62). Table 29 shows the results of the 15 evaluations. The null hypothesis was rejected for all 15 evaluations, which means that at $\alpha = 0.0125$ any of the three parameters are capable of estimating the values of the other two for any of the groups of mercury compounds in Table 28. The estimations may be obtained from equations in the form of $y = mx + b$, which are derived from least squares methods (Davis, 1986, p. 176-186). Table 30 lists the equations for different combinations of mercury compounds and pairs of leaching variables.

Table 29. Evaluation of the statistical significance at $\alpha = 0.0125$ (two tailed tests) of the 15 r values from Table 28. The critical t values are from Davis (1986, p. 62) and the degrees of freedom are shown in parentheses. The degrees of freedom are equal to two less than the number of samples.

Sample Group	Critical t Value at α = 0.0125 (Degrees of Freedom)	Test Statistic for r of log Liquid to Solid Ratio versus pH	Test Statistic for r of log Liquid to Solid Ratio versus log Mercury Concentration	Test Statistic for r of pH versus log Mercury Concentration
White HgTMT	± 2.447 (6)	15.67	-20.59	-31.55
White and light yellow HgTMT	± 2.201 (11)	17.24	-10.81	-17.24
White and all yellow HgTMT	± 2.120 (16)	5.102	-4.970	-12.58
All HgTMT	± 2.093 (19)	2.654	-5.034	-6.512
All HgTMT and HgS	± 2.074 (22)	2.679	-2.818	-5.983

Table 30. Equations in the form of $y = mx + b$ to describe the linear relationships between the log values of the liquid to solid ratios, pH, and the log values of the mercury concentrations of the leachates for different groups of HgTMT samples and metacinnabar (Table 27).

Sample Group	log Liquid to Solid Ratio versus pH	log Liquid to Solid Ratio versus log Mercury Concentration	pH versus log Mercury Concentration
White HgTMT	log liquid to solid ratio = 1.263 pH + 0.872	log liquid to solid ratio = -1.068 log Hg + 6.363	pH = -1.185 log Hg + 8.405
White and light yellow HgTMT	log liquid to solid ratio = 1.130 pH + 1.289	log liquid to solid ratio = -0.901 log Hg + 5.813	pH = -1.198 log Hg + 8.393
White and all yellow HgTMT	log liquid to solid ratio = 1.718 pH - 0.118	log liquid to solid ratio = -1.502 log Hg + 7.207	pH = -1.079 log Hg + 7.938
All HgTMT	log liquid to solid ratio = 2.467 pH - 1.656	log liquid to solid ratio = -1.669 log Hg + 7.553	pH = -1.784 log Hg + 10.34
All HgTMT and HgS	log liquid to solid ratio = 2.108 pH - 0.442	log liquid to solid ratio = -1.242 log Hg + 6.095	pH = -1.490 log Hg + 9.374

CHAPTER 7

CHEMISTRIES, AQUEOUS SOLUBILITIES, AND CRYSTALLINE STRUCTURES OF BARIUM 2,4,6-TRIMERCAPTOTRIAZINE COMPOUNDS

Introduction

The U.S. EPA classifies barium as a toxic hazard (40 CFR 141, 261.24, and 268.40). Barium is used in rat poisons, fireworks, paints, and as heat-stabilizers in plastics (Harte et al., 1991; Henke and Atwood, in press). $BaCO_3$ and $Ba(OH)_2 \bullet nH_2O$ compounds may irritate the eyes, nose, throat, and skin (Sittig, 1985, p. 105). When ingested, water-soluble barium compounds may damage muscle and nerve cells by disrupting the flow of potassium ions (Harte et al., 1991; Henke and Atwood, in press). Barium compounds may also slow heart rate, cause intestinal peristalsis, and unwanted bladder contraction (Sittig, 1985, p. 105). Ultimately, barium behaves like calcium and accumulates in bone (Harte et al., 1991; Henke and Atwood, in press). Because of human health and environmental concerns, information on the removal of barium contaminants from water is clearly important.

Degussa Corporation (1993) does not contain any information on the precipitation of dissolved barium from water with TMT-55 or the properties of any barium 2,4,6-trimercaptotriazine (BaTMT) compounds. BaTMT compounds are known to exist and

were first reported by Claësson (Klason) (1884, p. 9) (*i.e.*, $BaHC_3N_3S_3 \bullet nH_2O$) and Hofmann (1885, p. 2204-2205) (*i.e.*, $BaH_4[C_3N_3S_3]_2 \bullet nH_2O$). However, a literature review found no published studies on their properties and chemical structures.

Studies of BaTMT compounds were initiated to determine if TMT-55 could be used to remove barium contaminants from water. Furthermore, by studying BaTMT compounds, predictions may be made regarding the chemistry of the TMT ligand with other alkaline earths, especially radium. Radium is a potential radiation hazard in some ground waters (Fetter, 1993, p. 287). Because radium is radioactive and research with the element requires extensive training, regulatory permits and safety procedures, studies with BaTMT and other alkaline earth TMT compounds (*e.g.*, Henke and Atwood, in press) may cheaply and safely provide some preliminary information on whether TMT-55 might precipitate radium and whether research with radium and TMT-55 is warranted.

Preparation of BaTMT Compounds

Two different BaTMT compounds were produced in aqueous solutions: $Ba_3(C_3N_3S_3)_2 \bullet 8H_2O$ and $BaH_4(C_3N_3S_3)_2 \bullet 4.5H_2O$. $Ba_3(C_3N_3S_3)_2 \bullet 8H_2O$ slowly precipitates when aqueous solutions of highly soluble TMT-55 and $BaCl_2 \bullet 2H_2O$ are mixed at a $Ba/(C_3N_3S_3)$ molar ratio of 3:2. Specifically, the compound may be prepared by first dissolving 4.88 g (0.0200 moles) of $BaCl_2 \bullet 2H_2O$ in 200 ml of distilled water (0.100 M). A separate solution of 5.40 g (0.0133 moles) of TMT-55 dissolved in 200 ml of distilled water (0.067 M) is also prepared. The two solutions are then mixed and 1.36 g of $Ba_3(C_3N_3S_3)_2 \bullet 8H_2O$ will precipitate within 48 hours. After precipitation and recovery, the

crystals should be lightly washed with distilled water to remove any sodium and chloride. The purity of the $Ba_3(C_3N_3S_3)_2 \bullet 8H_2O$ may be confirmed with a powder XRD analysis. The yield of 1.36 g is only 22.4% of what would be expected if all of the barium and $(C_3N_3S_3)^{3-}$ reacted and precipitated as $Ba_3(C_3N_3S_3)_2 \bullet 8H_2O$ according to the following general reactions in water:

24) $BaCl_2 \bullet 2H_2O + H_2O \rightarrow Ba^{2+} + 2Cl^-$

25) $Na_3C_3N_3S_3 \bullet 9H_2O + H_2O \rightarrow (C_3N_3S_3)^{3-} + 3Na^+$

26) $3Ba^{2+} + 6Cl^- + 2(C_3N_3S_3)^{3-} + 6Na^+ \rightarrow Ba_3(C_3N_3S_3)_2 \bullet 8H_2O\downarrow + 6Cl^- + 6Na^+$

The low recovery is probably due to the slow reaction time and high solubility of $Ba_3(C_3N_3S_3)_2 \bullet 8H_2O$ in water (see below). Higher yields may be obtained by increasing the reaction time to 72 or more hours or decreasing the volume of water through heating.

$Ba_3(C_3N_3S_3)_2 \bullet 8H_2O$ crystals are white and fibrous. They often grow in radial bundles that resemble zeolite "flowers." Although crystal fibers are usually abundant, they are too fine-grained for optical studies or single-crystal XRD analyses. Many attempts to increase their size have been unsuccessful.

$BaH_4(C_3N_3S_3)_2 \bullet 4.5H_2O$ precipitates when solid $H_3C_3N_3S_3$ is added to a suspension of $Ba(OH)_2 \bullet 8H_2O$ in water. While highly pure $Ba_3(C_3N_3S_3)_2 \bullet 8H_2O$ is easily produced, the preparation of $BaH_4(C_3N_3S_3)_2 \bullet 4.5H_2O$ requires more sophisticated methods to avoid the formation of substantial $H_3C_3N_3S_3$ and/or barium carbonate ($BaCO_3$) impurities in the precipitate. $BaH_4(C_3N_3S_3)_2 \bullet 4.5H_2O$ is prepared by adding fresh and noncarbonated $Ba(OH)_2 \bullet 8H_2O$ (3.10 g or 0.00983 moles) to one liter of deionized water. The $Ba(OH)_2 \bullet 8H_2O$ is stirred for one hour under a nitrogen purge. $H_3C_3N_3S_3$ (3.48 g or

0.0196 moles) is then added to the suspension and stirred under nitrogen. Once the $H_3C_3N_3S_3$ and $Ba(OH)_2 \cdot 8H_2O$ have essentially dissolved, usually within 48 hours, the solution is filtered in air. Unless some $BaH_4(C_3N_3S_3)_2 \cdot 4.5H_2O$ precipitates, the unfilterable material typically totals no more than 0.03 g and mostly consists of undissolved $H_3C_3N_3S_3$. To avoid the precipitation of $H_3C_3N_3S_3$ or $BaCO_3$ impurities, the filtered solution should be boiled in air until the volume decreases to about 50 ml. As the solution air-cools to room temperature, abundant and nearly pure white $BaH_4(C_3N_3S_3)_2 \cdot 4.5H_2O$ crystals will rapidly precipitate. The crystals should be removed from the solution before the remaining solution evaporates in air and possibly contributes impurities to the precipitates. The crystals should be lightly washed with distilled water to remove possible trace impurities of $Ba(OH)_2 \cdot H_2O$ (monohydrate, PDF 26-154). The purity of the $BaH_4(C_3N_3S_3)_2 \cdot 4.5H_2O$ may be confirmed with powder XRD analyses. A total of 5.50 g of product is expected with a yield of 98.0%.

As with $Ba_3(C_3N_3S_3)_2 \cdot 8H_2O$, $BaH_4(C_3N_3S_3)_2 \cdot 4.5H_2O$ crystals are clear to white needles. $BaH_4(C_3N_3S_3)_2 \cdot 4.5H_2O$ does not grow in bundles as frequently as $Ba_3(C_3N_3S_3)_2 \cdot 8H_2O$ and individual $BaH_4(C_3N_3S_3)_2 \cdot 4.5H_2O$ needles are sometimes thick enough for single crystal XRD analyses. Otherwise, unless chemical or XRD analyses are done, $BaH_4(C_3N_3S_3)_2 \cdot 4.5H_2O$ may be difficult to distinguish from $Ba_3(C_3N_3S_3)_2 \cdot 8H_2O$.

Chemistry of BaTMT Compounds

Methods

Personnel at ME&T Corporation analyzed both BaTMT compounds for water of hydration and, when possible, barium and sulfur. The water of hydration values were determined with a modification of a Karl Fischer method (ASTM D4017) (ASTM, 1992). The modification consisted of a pretreatment step at 150°C to remove moisture from the surfaces of the samples. Chemical preparations for barium and sulfur analyses were done in accordance with ASTM C809 (ASTM, 1992), followed by analyses with an ICP. Because the samples often would not entirely dissolve in acids or "digest" during chemical preparation, reliable analyses could not always be obtained for barium and sulfur.

Results

Tables 31 and 32 list the chemical results, which suggest that the compounds are $Ba_3(C_3N_3S_3)_2 \cdot 8H_2O$ and $BaH_4(C_3N_3S_3)_2 \cdot 4.5H_2O$. The chemical composition of $BaH_4(C_3N_3S_3)_2 \cdot 4.5H_2O$ is also consistent with single crystal XRD results, as discussed below.

Chemical differences in the two BaTMT compounds are due to the chemistries of the reactants, as well as the pH values and $Ba/(C_3N_3S_3)$ molar ratios of the BaTMT-precipitating solutions. Because $H_3C_3N_3S_3$ is a triprotic acid, four different dissolved species could exist in an aqueous solution (*i.e.*, $[C_3N_3S_3]^{3-}$, $[HC_3N_3S_3]^{2-}$, $[H_2C_3N_3S_3]^{-}$, and $H_3C_3N_3S_3{}^0$). The concentrations of the different $H_3C_3N_3S_3$ species would vary with pH and would affect the chemistries of any precipitating BaTMT compounds. Currently,

changes in the concentrations of the different $H_3C_3N_3S_3$ species with pH are poorly understood. Hirt et al. (1961) contain two dissociation constants or pK_a values for $H_3C_3N_3S_3$:

27) $H_3C_3N_3S_3 = (H_2C_3N_3S_3)^- + H^+$, $pK_a = 4.96$

28) $(H_2C_3N_3S_3)^- = (HC_3N_3S_3)^{2-} + H^+$, $pK_a = 8.0$

29) $(HC_3N_3S_3)^{2-} = (C_3N_3S_3)^{3-} + H^+$, pK_a is unknown.

Table 31. Chemical results of $Ba_3(C_3N_3S_3)_2 \bullet 8H_2O$ made from $BaCl_2 \bullet 2H_2O$ and TMT-55. A reliable sulfur analysis could not be obtained. The results were normalized on the ideal sulfur concentration.

Parameter	Measured Concentration (wt%)	Ideal Concentration (wt%)
Barium	45.05	45.55
Carbon	8.00[a]	7.97
Nitrogen	8.61[b]	9.29
Sulfur	21.26 (not analyzed)	21.26
Water of hydration	15.43	15.93
Total	98.35	100.00
Formula	$Ba_{3.0}(C_{3.0}N_{2.8}S_{3.0})_2 \bullet 7.75H_2O$	$Ba_3(C_3N_3S_3)_2 \bullet 8H_2O$

[a] The average results of two carbon analyses of 8.06 and 7.93 wt%.

[b] The average results of two nitrogen analyses of 8.41 and 8.81 wt%.

Table 32. Chemical results of $BaH_4(C_3N_3S_3)_2 \cdot 4.5H_2O$ made from $Ba(OH)_2 \cdot 8H_2O$ and $H_3C_3N_3S_3$. A reliable barium analysis could not be obtained. The results are normalized on the ideal barium concentration.

Parameter	Measured Concentration (wt%)	Ideal Concentration (wt%)
Barium	24.06 (not analyzed)	24.06
Carbon	12.74[a]	12.62
Hydrogen	0.61 (nonaqueous only)	0.71
Nitrogen	14.46[b]	14.72
Sulfur	30.95	33.69
Water of hydration	14.47	14.20
Total	97.29	100.00
Formula	$BaH_{3.5}(C_{3.0}N_{3.0}S_{2.5})_2 \cdot 4.58H_2O$	$BaH_4(C_3N_3S_3)_2 \cdot 4.5H_2O$

[a] The average results of two carbon analyses of 12.99 and 12.50 wt%.

[b] The average results of two nitrogen analyses of 14.69 and 14.22 wt%.

Precipitation Reactions of $Ba_3(C_3N_3S_3)_2 \cdot 8H_2O$

When 0.067 M (pH 12) TMT-55 and 0.100 M (pH 7.5) $BaCl_2 \cdot 2H_2O$ aqueous solutions are mixed, a pH 12 solution results and $Ba_3(C_3N_3S_3)_2 \cdot 8H_2O$ slowly precipitates. Based on pK_a values from Hirt et al. (1961), a pH 12 aqueous solution probably contains much more $(C_3N_3S_3)^{3-}$ than $(H_2C_3N_3S_3)^-$, $(HC_3N_3S_3)^{2-}$, or $H_3C_3N_3S_3{}^0$. That is, once the $(C_3N_3S_3)^{3-}$ from the TMT-55 solution enters the $BaCl_2 \cdot 2H_2O$ solution, the anion would preferentially react with the relatively abundant dissolved barium (0.0200 moles in 400 ml or 0.05 M) to precipitate $Ba_3(C_3N_3S_3)_2 \cdot 8H_2O$ rather than with much less abundant

(approximately pH 12 or 1 x 10^{-12} M) H^+ to form $BaH_4(C_3N_3S_3)_2 \bullet 4.5H_2O$, $BaHC_3N_3S_3 \bullet nH_2O$, or $H_3C_3N_3S_3$.

Precipitation Reactions of $BaH_4(C_3N_3S_3)_2 \bullet 4.5H_2O$

Separately, $H_3C_3N_3S_3$ and $Ba(OH)_2 \bullet 8H_2O$ are not very soluble in water. When mixed with one liter of water, 0.00983 moles of $Ba(OH)_2 \bullet 8H_2O$ partially dissolves to form a pH 12 solution. The addition of 0.0196 moles of solid $H_3C_3N_3S_3$ to the $Ba(OH)_2 \bullet 8H_2O$ solution while stirring under a nitrogen purge causes the pH to decline to 7 and both $H_3C_3N_3S_3$ and $Ba(OH)_2 \bullet 8H_2O$ dissolve entirely, usually within 48 hours. The dissolution of $Ba(OH)_2 \bullet 8H_2O$ releases OH^- through this reaction:

30) $Ba(OH)_2 \bullet 8H_2O \rightarrow Ba^{2+} + 2\ OH^-$

The OH^- leads to the dissolution of $H_3C_3N_3S_3$. Because the pH of the $H_3C_3N_3S_3$ and $Ba(OH)_2 \bullet 8H_2O$ solution is 7, pK_a values from Hirt et al. (1961) state that $(H_2C_3N_3S_3)^-$ should be the dominant dissolved $H_3C_3N_3S_3$ species. $(H_2C_3N_3S_3)^-$ would form from $H_3C_3N_3S_3$ through this reaction:

31) $H_3C_3N_3S_3 + OH^- \rightarrow H_2C_3N_3S_3^- + H_2O$

The consumption of OH^- by Reaction 31 would lower the pH and increase the solubility of $Ba(OH)_2 \bullet 8H_2O$ by forcing Reaction 30 to the right through Le Chatelier's Principle. Reaction 31 would consume the OH^- until all of the solid $H_3C_3N_3S_3$ dissolves.

The filtered $Ba(OH)_2 \bullet 8H_2O$ and $H_3C_3N_3S_3$ solution is heated to reduce its volume and then cooled, which produces $BaH_4(C_3N_3S_3)_2 \bullet 4.5H_2O$ saturation and precipitation.

That is, the $H_2C_3N_3S_3^-$ and dissolved barium produced by Reactions 30 and 31 would react to precipitate $BaH_4(C_3N_3S_3)_2 \bullet 4.5H_2O$ through this reaction:

32) $Ba^{2+} + 2\ H_2C_3N_3S_3^- \rightarrow BaH_4(C_3N_3S_3)_2 \bullet 4.5H_2O\downarrow$

Solubility of $BaH_4(C_3N_3S_3)_2 \bullet 4.5H_2O$ and $Ba_3(C_3N_3S_3)_2 \bullet 8H_2O$ in Water

Pure samples of both BaTMT compounds were weighed and separately mixed in various volumes of distilled water. Each sample was hand shaken for one minute and then allowed to sit undisturbed for 24 hours at approximately 25°C. After 24 hours, the mixtures were filtered and the undissolved portions of the compounds were separately air dried and weighed. To calculate the solubilities, the masses of the undissolved samples were compared with the original masses. The solubility results for $Ba_3(C_3N_3S_3)_2 \bullet 8H_2O$ were reasonably consistent and are shown in Table 33. However, results from duplicated studies with $BaH_4(C_3N_3S_3)_2 \bullet 4.5H_2O$ varied from 4.02 to 5.68 g/l. Reasonably consistent results were only obtained after the leaching time was extended to 48 hours (Table 33). As shown in Table 33, both BaTMT compounds have solubilities of approximately 5 g/l. The average solubility of 4.56 g/l for $BaH_4(C_3N_3S_3)_2 \bullet 4.5H_2O$ is lower than the 5.50 g that normally remains dissolved after filtering a one liter solution of $H_3C_3N_3S_3$ and $Ba(OH)_2 \bullet 8H_2O$. The discrepancy may result from the fact that the preparation of $BaH_4(C_3N_3S_3)_2 \bullet 4.5H_2O$ occurs under a nitrogen purge with constant stirring. In contrast, the solubility studies were done under an ambient atmosphere without constant stirring or agitation. Extensive stirring or agitation of an aqueous $BaH_4(C_3N_3S_3)_2 \bullet 4.5H_2O$ mixture in the presence of carbon dioxide in the air could result in $BaCO_3$ precipitation, which would

confound the solubility measurements. Although stirring the mixture under a nitrogen purge could hinder the precipitation of $BaCO_3$, commercial treatment of barium in waste waters may occur in the presence of air and solubility measurements with a nitrogen purge may not be appropriate for such commercial applications.

Table 33. The solubilities and experimental conditions used to determine the solubilities of $BaH_4(C_3N_3S_3)_2 \cdot 4.5H_2O$ and $Ba_3(C_3N_3S_3)_2 \cdot 8H_2O$ in water. The leaching time for $Ba_3(C_3N_3S_3)_2 \cdot 8H_2O$ was 24 hours, whereas $BaH_4(C_3N_3S_3)_2 \cdot 4.5H_2O$ required 48 hours to obtain consistent results.

BaTMT Compound	Mass of Compound (g)	Mass of Distilled Water (g)	Mass of Dissolved Compound (g)	Solubility in Water (g/l)
$Ba_3(C_3N_3S_3)_2 \cdot 8H_2O$	0.34	40.56	0.23	5.67
$Ba_3(C_3N_3S_3)_2 \cdot 8H_2O$	0.19	25.43	0.14	5.51
$Ba_3(C_3N_3S_3)_2 \cdot 8H_2O$	0.34	49.23	0.28	5.69
Average				5.62
$BaH_4(C_3N_3S_3)_2 \cdot 4.5H_2O$	0.84	99.73	0.44	4.41
$BaH_4(C_3N_3S_3)_2 \cdot 4.5H_2O$	0.75	89.19	0.41	4.60
$BaH_4(C_3N_3S_3)_2 \cdot 4.5H_2O$	0.72	85.39	0.40	4.68
Average				4.56

The U.S. EPA requires that waste waters with 100 mg/l or more of barium be treated before being discharged into the environment (40 CFR 268.40). The solubilities of both BaTMT compounds are obviously not low enough to achieve this level and TMT-55 probably would not be effective in removing barium from contaminated waters.

Structures of BaTMT Compounds from Powder and Single Crystal XRD Analyses

Powder XRD Results for $Ba_3(C_3N_3S_3)_2 \cdot 8H_2O$

XRD analyses were done on both BaTMT compounds. Because $Ba_3(C_3N_3S_3)_2 \cdot 8H_2O$ crystals are too small for single crystal XRD analyses, information is currently unavailable on the space group, atomic positions and bond lengths of this compound. Powder XRD analyses with silicon and fluorophlogopite standards identified 102 possible peaks for $Ba_3(C_3N_3S_3)_2 \cdot 8H_2O$ from scans between 3 and 140° 2θ (based on $CuK_{\alpha 1}$ radiation) (Table 34). The 102 *d*-values were initially entered into the computer program TREOR90 (an updated version of Werner et al., 1985), which used 100 of them to derive two possible solutions for the crystal system of $Ba_3(C_3N_3S_3)_2 \cdot 8H_2O$: one hexagonal and the other orthorhombic. The solutions were confirmed and refined with PIRUM (an updated version of Werner, 1969; Table 35). The refined results from PIRUM were further verified by LSUCRI (Garvey, 1986 after Appleman and Evans, 1973).

Table 34. The *d*-values and corresponding 2θ values (based on $CuK_{\alpha 1}$ radiation) of measured peaks from powder XRD scans of $Ba_3(C_3N_3S_3)_2 \cdot 8H_2O$.

Measured *d*-values	Measured 2θ Based on $CuK_{\alpha 1}$ Radiation	Measured Intensities
7.03	12.58	66
6.21	14.26	100
5.37	16.48	8
5.16	17.16	16
4.65	19.06	18
4.27	20.78	33
4.11	21.60	8
4.06	21.85	52
3.761	23.64	10
3.724	23.87	6
3.586	24.81	7
3.522	25.27	14
3.346	26.62	71
3.218	27.70	5
3.082	28.94	31
3.063	29.13	54
3.001	29.75	3
2.984	29.92	17
2.841	31.47	4
2.762	32.39	7
2.689	33.29	51
2.674	33.49	28
2.661	33.65	13
2.584	34.69	6

Table 34 cont.

2.546	35.22	5
2.523	35.56	1
2.468	36.38	68
2.394	37.54	2
2.385	37.68	2
2.347	38.32	13
2.328	38.64	29
2.301	39.12	2
2.276	39.56	64
2.234	40.34	7
2.224	40.54	4
2.209	40.82	2
2.180	41.38	11
2.137	42.26	4
2.120	42.60	4
2.096	43.13	20
2.076	43.57	8
2.043	44.30	3
2.026	44.69	8
1.9523	46.48	44
1.9312	47.02	43
1.8916	48.06	8
1.8792	48.40	2
1.8626	48.86	3
1.8512	49.18	6
1.8486	49.25	6

Table 34 cont.

1.8353	49.63	6
1.8000	50.67	3
1.7877	51.05	6
1.7682	51.65	9
1.7601	51.91	5
1.7224	53.13	8
1.7147	53.39	2
1.6937	54.10	4
1.6731	54.83	12
1.6622	55.22	4
1.6558	55.45	8
1.6523	55.58	8
1.6433	55.91	4
1.6155	56.96	12
1.6064	57.31	5
1.5910	57.91	3
1.5806	58.33	4
1.5660	58.93	2
1.5564	59.33	1
1.5526	59.49	4
1.5384	60.09	3
1.5311	60.41	9
1.5165	61.05	4
1.4888	62.32	8
1.4677	63.31	3
1.4583	63.77	6

Table 34 cont.

1.4528	64.04	3
1.4478	64.29	5
1.4416	64.60	1
1.4329	65.04	7
1.4205	65.68	7
1.4140	66.02	4
1.3847	67.60	9
1.3641	68.76	3
1.3550	69.29	13
1.3436	69.96	3
1.3406	70.14	8
1.3365	70.39	3
1.3304	70.76	4
1.3272	70.96	1
1.3140	71.78	5
1.3070	72.22	2
1.2959	72.94	3
1.2914	73.24	4
1.2828	73.81	1
1.2748	74.35	2
1.2644	75.07	8
1.2595	75.41	2
1.2527	75.89	2
1.2418	76.68	2

Table 35. Two possible unit cell solutions from PIRUM (version 93101, updated from Werner, 1969) for $Ba_3(C_3N_3S_3)_2 \cdot 8H_2O$. One standard deviation in the value of the last digit is shown in parentheses.

Parameter	Hexagonal Solution	Orthorhombic Solution
a (Å)	21.5106(6)	18.629(1)
b (Å)	-	10.7557(7)
c (Å)	4.4474(3)	4.4474(3)
V (Å^3)	1782.14	891.11
M_{20}	46	37
F_{30}	110 (0.00635, 43)	82 (0.00620, 59)
Number of d-values	102	102
Number of indexed d-values	100	100
Unindexed d-values (Å)	1.3436, 1.7147	1.3436, 1.7147

The unit cell volume and most other aspects of the hexagonal solution are very different from the orthorhombic solution (Table 35). However, the lengths of the c axes for both solutions are identical (4.4474[3] Å). The M_{20} values in Table 35 favor the hexagonal solution over the orthorhombic alternative, whereas $/\Delta 2\theta/$ in the F_{30} value for the orthorhombic solution is slightly lower than the hexagonal value. For both solutions, all of the 100 measured 2θ values are within acceptable limits (*i.e.*, $\pm 0.03^\circ$ 2θ) of the calculated 2θ values (Table 36). Both solutions rejected two relatively weak peaks (Tables 35 and 36). The 1.3436 Å peak (69.96° 2θ based on $CuK_{\alpha 1}$ radiation) had a relative intensity of 3, whereas the peak at 1.7147 Å (53.39° 2θ based on $CuK_{\alpha 1}$ radiation) had an intensity of 2. The peaks may have originated from background noise, unidentified

impurities, or miscalibrations. Review of the ICDD data file and XRD powder data for $H_3C_3N_3S_3$ were unable to find matches for several possible impurities, including various $BaCO_3$ and $Ba(OH)_2 \cdot nH_2O$ polymorphs and $H_3C_3N_3S_3$.

Table 36. Measured and calculated 2θ values (based on $CuK_{\alpha 1}$ radiation) for both the hexagonal and orthorhombic solutions for $Ba_3(C_3N_3S_3)_2 \cdot 8H_2O$. The calculated 2θ and *hkl* values are from PIRUM (version 930101).

Measured 2θ	Calc. 2θ, Hex.	Difference 2θ	*hkl* Hex.	Calc. 2θ, Orth.	Difference 2θ	*hkl* Orth.
12.58	12.56	0.02	210	12.56	0.02	210
14.26	14.25	0.01	300	14.25	0.01	300
16.48	16.47	0.01	220	16.47	0.01	020, 310
17.16	17.15	0.01	310	17.15	0.01	120
19.06	19.04	0.02	400	19.04	0.02	220, 400
20.78	20.77	0.01	320	20.77	0.01	410
21.60	21.60	0.00	111	21.60	0.00	011
21.85	21.85	0.00	410	21.84	0.01	320
23.64	23.64	0.00	211	23.64	0.00	211
23.87	23.86	0.01	500	23.86	0.01	500
24.81	24.82	-0.01	330	24.81	0.00	030
25.27	25.28	-0.01	420	25.28	-0.01	130, 420, 510
26.62	26.62	0.00	510	26.62	0.00	230
27.70	27.71	-0.01	401	27.71	-0.01	221, 401

Table 36 cont.

28.94	28.95	-0.01	321	28.95	-0.01	411
29.13	29.14	-0.01	430	29.14	-0.01	520
29.75	29.75	0.00	411	29.75	0.00	321
29.92	29.93	-0.01	520	29.93	-0.01	610
31.47	31.47	0.00	610	31.46	0.01	430
32.39	32.41	-0.02	421	32.41	-0.02	131, 421, 511
33.29	33.30	-0.01	440	33.29	0.00	040, 620
33.49	33.49	0.00	511	33.49	0.00	231
33.65	33.65	0.00	700	33.65	0.00	140, 700
34.69	34.70	-0.01	620	34.70	-0.01	240, 530, 710
35.22	35.22	0.00	601	35.22	0.00	331, 601
35.56	35.56	0.00	431	35.56	0.00	521
36.38	36.38	0.00	710	36.38	0.00	340
37.54	37.54	0.00	611	37.54	0.00	431
37.68	37.68	0.00	540	37.68	0.00	720
38.32	38.32	0.00	630	38.32	0.00	630
38.64	38.64	0.00	800	38.63	0.01	440, 800
39.12	39.12	0.00	441	39.12	0.00	041, 621
39.56	39.57	-0.01	720	39.57	-0.01	810

Table 36 cont.

40.34	40.34	0.00	621	40.34	0.00	241, 531, 711
40.54	40.53	0.01	002	40.54	0.00	002
40.82	40.84	-0.02	102	40.84	-0.02	102
41.38	41.38	0.00	810	41.38	0.00	540
42.26	42.26	0.00	640	42.26	0.00	150, 730, 820
42.60	42.60	0.00	212	42.60	0.00	212
43.13	43.13	0.00	730	43.12	0.01	250
43.57	43.57	0.00	631	43.57	0.00	631
44.30	44.31	-0.01	312	44.31	-0.01	122
44.69	44.69	0.00	721	44.69	0.00	811
46.48	46.46	0.02	910	46.46	0.02	450, 830
47.02	47.00	0.02	740	47.00	0.02	920
48.06	48.06	0.00	830	48.06	0.00	740
48.40	48.38	0.02	422	48.38	0.02	512
48.86	48.85	0.01	10 00	48.85	0.01	10 00
49.18	49.16	0.02	512	49.16	0.02	232
49.25	49.25	0.00	821	49.25	0.00	351, 641, 911
49.63	49.63	0.00	920	49.62	0.01	10 10
50.67	50.69	-0.02	432	50.69	-0.02	522
51.05	51.04	0.01	911	51.04	0.01	451, 831

Table 36 cont.

51.65	51.65	0.00	10 10	51.65	0.00	650
51.91	51.90	0.01	840	51.90	0.01	260, 840, 10 20
53.13	53.14	-0.01	930	53.14	-0.01	360
53.39	–	–	–	–	–	–
54.10	54.11	-0.01	11 00	54.11	-0.01	11 00
54.83	54.83	0.00	10 20	54.83	0.00	460, 750, 11 10
55.22	55.20	-0.02	661	55.20	-0.02	061, 931
55.45	55.44	0.01	751	55.44	0.01	161
55.58	55.59	-0.01	712	55.59	-0.01	342
55.91	55.92	-0.01	10 11	55.91	0.00	651
56.96	56.96	0.00	11 10	56.96	0.00	560, 11 20
57.31	57.32	-0.01	931	57.32	-0.01	361
57.91	57.93	-0.02	722	57.93	-0.02	812
58.33	58.35	-0.02	10 30	58.35	-0.02	850
58.93	58.94	-0.01	10 21	58.94	-0.01	461, 751, 11 11
59.33	59.31	0.02	812	59.31	0.02	542
59.49	59.50	-0.01	12 00	59.50	-0.01	660, 12 00
60.09	60.08	0.01	851	60.07	0.02	941
60.41	60.40	0.01	860	60.40	0.01	170, 10 40, 11 30

Table 36 cont.

61.05	61.08	-0.03	950	61.08	-0.03	270
62.32	62.31	0.01	10 31	62.31	0.01	851
63.31	63.33	-0.02	912	63.33	-0.02	452, 832
63.77	63.77	0.00	742	63.77	0.00	922
64.04	64.07	-0.03	11 21	64.06	-0.02	071, 12 11
64.29	64.28	0.01	861	64.28	0.01	171, 10 41, 11 31
64.60	64.58	0.02	303	64.58	0.02	303
65.04	65.03	0.01	13 00	65.03	0.01	11 40, 13 00
65.68	65.68	0.00	12 20	65.68	0.00	570, 860, 13 10
66.02	66.01	0.01	10 41	66.01	0.01	371, 951, 12 21
67.60	67.60	0.00	11 40	67.60	0.00	13 20
68.76	68.77	-0.01	13 01	68.77	-0.01	11 41, 13 01
69.29	69.29	0.00	12 30	69.28	0.01	960
69.96	–	–	–	–	–	–
70.14	70.12	0.02	970	70.12	0.02	180
70.39	70.37	0.02	10 22	70.37	0.02	462, 752, 11 12
70.76	70.75	0.01	14 00	70.75	0.01	13 30, 14 00

Table 36 cont.

70.96	70.93	0.03	523	70.93	0.03	613
71.78	71.78	0.00	11 50	71.78	0.00	380
72.22	72.23	-0.01	11 12	72.23	-0.01	562, 11 22
72.94	72.92	0.02	12 31	72.92	0.02	961
73.24	73.22	0.02	12 40	73.22	0.02	480, 10 60, 14 20
73.81	73.83	-0.02	14 10	73.83	-0.02	870
74.35	74.35	0.00	14 01	74.35	0.00	281, 771, 11 51, 13 31, 14 01
75.07	75.05	0.02	13 30	75.05	0.02	580, 13 40
75.41	75.44	-0.03	543	75.44	-0.03	723
75.89	75.90	-0.01	952	75.90	-0.01	272
76.68	76.67	0.01	15 00	76.67	0.01	15 00

Single Crystal XRD Results for $BaH_4(C_3N_3S_3)_2 \cdot 4.5H_2O$

A suitable sample of $BaH_4(C_3N_3S_3)_2 \cdot 4.5H_2O$ was collected for a single crystal XRD analysis at 25°C. Tables 37-39 show selected information from the single crystal analysis and the Appendix lists the complete data. The compound is monoclinic and its formula is consistent with the chemical results in Table 32. When compared with TMT-55 (Table 13), the unit cell volume of $BaH_4(C_3N_3S_3)_2 \cdot 4.5H_2O$ is approximately 1000 $Å^3$ larger (Table 37). The unit cell volume is also much larger than the solutions for

$Ba_3(C_3N_3S_3)_2 \bullet 8H_2O$ (Table 35) and white HgTMT (Table 24), but much smaller than the 5882 Å^3 for $(Os_3H[CO]_{10})_3(C_3N_3S_3)$ (Ainscough et al., 1993).

The errors associated with the single crystal analysis (*R1* values of 0.0427 and 0.0501 in Table 37) are acceptable. Errors could be lowered by running the analysis at -110°C, but the lower temperature probably would significantly shorten the bond lengths and the unit cell volume (Table 13 and compare the 25°C and -110°C data for TMT-55 in the Appendix).

The structure of $BaH_4(C_3N_3S_3)_2 \bullet 4.5H_2O$ is shown in two diagrams in Figure 9. The single crystal XRD analysis was not sensitive enough to find the hydrogen atoms and their estimated positions are not shown in Figure 9. The barium atoms (*e.g.*, Ba1 in the diagram on the right side of Figure 9) have tenfold coordination with three sulfurs (*i.e.*, S1, S6 and S9 for Ba1 in Figure 9), two nitrogens (*i.e.*, N3 and N9 for Ba1), and five water molecules (*i.e.*, O1, O2, O3, O4 and O5 for Ba1). Two pairs of waters bridge each barium atom (O1 and O2 and O3 and O5 for Ba1 in Figure 9; Ba-O at 2.789[5] to 2.983[5] Å, Table 38). The barium atoms and water units form a continuous zigzagging chain that is situated between stacks of TMT rings (left diagram in Figure 9, Henke and Atwood, in press).

In Table 38, the lengths of various bonds and atomic distances in $BaH_4(C_3N_3S_3)_2 \bullet 4.5H_2O$ are compared with corresponding values from other compounds. Overall, the lengths in $BaH_4(C_3N_3S_3)_2 \bullet 4.5H_2O$ are somewhat longer and more variable than related distances in compounds from the literature. However, the differences are still minor and expected.

Variations in bond lengths between a given pair of atoms from one compound to another are mostly due to: 1) whether the covalent bonds are single, double or variable because of resonance, that is, the number of s and p orbitals that are present and 2) any differences in the valence states and coordination numbers of the atoms in the bonds (March, 1985, p. 18-20; Bloss, 1971, p. 203-218).

Table 37. Selected crystalline properties of $BaH_4(C_3N_3S_3)_2 \cdot 4.5H_2O$ at 25°C. One standard deviation in the value of the last digit is shown in parentheses. The Appendix lists more detailed results.

Parameter	Value
Crystal System	Monoclinic
Crystal Class	2/m
Space Group	$P2_1/c$
Z	4
Density (calculated) (g/cm^3)	2.077
a (Å)	8.5576(4)
b (Å)	21.028(1)
c (Å)	20.276(1)
β (degrees)	96.440(1)
V ($Å^3$)	3625.6(3)
Final $R1$ ($I>2\sigma[I]$)	0.0427
$R1$ (all data)	0.0501

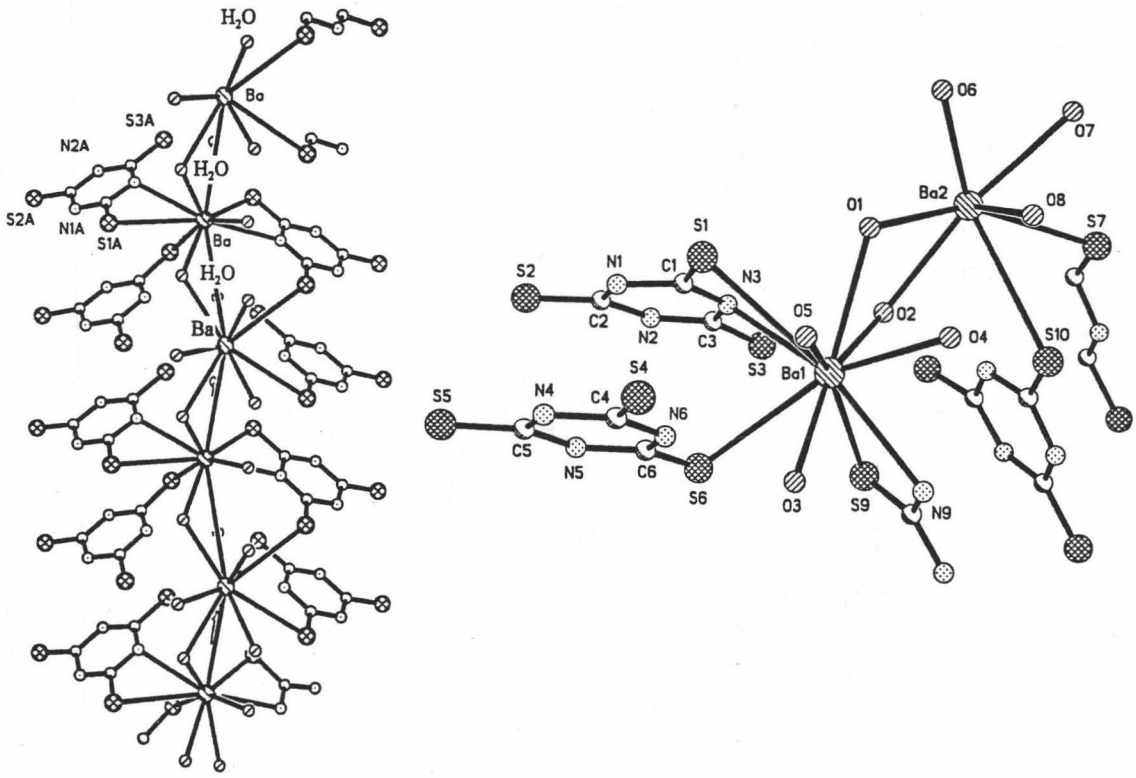

Figure 9. Ball and stick representations of the extended structure of $BaH_4(C_3N_3S_3)_2 \cdot 4.5H_2O$. Hydrogen atoms are not shown. The diagram on the left shows a zigzagging chain of barium and water units passing between rings of TMT. The diagram on the right shows the distribution of atoms around a barium atom labeled as Ba1.

Table 38. Comparisons of selected bond lengths and atomic distances in Å and bond angles in degrees between $BaH_4(C_3N_3S_3)_2 \bullet 4.5H_2O$ and other compounds at 25°C. Except for hydrogen, Figure 9 shows the location of the atoms in $BaH_4(C_3N_3S_3)_2 \bullet 4.5H_2O$. One standard deviation in the value(s) of the last digit(s) is shown in parentheses. The Appendix lists the complete results for $BaH_4(C_3N_3S_3)_2 \bullet 4.5H_2O$.

Bond or Atomic Distance	Length (Å)	Bond Length or Atomic Distance in Related Compound (Å)	Related Compound
Ba-O	2.789(5) to 2.983(5)	2.844 to 2.887	$BaCl_2 \bullet 2H_2O$[a]
Ba-O	2.789(5) to 2.983(5)	2.726(2) to 2.814(2)	$Ba(OH)_2 \bullet 8H_2O$[b]
Ba..N	2.993(6) to 3.050(6)	2.899(4) to 2.914(5)	$Ba(SCN)_2 \bullet 3H_2O$[c]
Ba-S	3.396(2) to 3.629(2)	3.391(2)	$Ba(SCN)_2 \bullet 3H_2O$[c]
Ba..Ba	4.7779(7) to 4.8059(7)	3.90(1)	$Ba_2L_4(H_2O)_{1.81}$[d]
Ba..Ba	4.7779(7) to 4.8059(7)	4.382(2) to 5.457(3)	$Ba_5(thd)_9Cl(H_2O)_7$[e]
Ba..Ba	4.7779(7) to 4.8059(7)	4.195 to 5.170	$Ba_6(thd)_{12}(H_2O)_{13}$[f]
S-C	1.652(8) to 1.695(8)	1.733(6)	TMT-55[g]
S-C	1.652(8) to 1.695(8)	1.649(8) to 1.662(9)	$Ba(SCN)_2 \bullet 3H_2O$[c]
N-C	1.326(9) to 1.414(10)	1.350(5) to 1.356(5)	TMT-55[g]
N-C	1.326(9) to 1.414(10)	1.347 to 1.365	pyrazole[h]
N-C	1.326(9) to 1.414(10)	1.319 to 1.347	pyrazine[h]

Table 38 cont.

Bond angle	Degrees	Bond Angle in related compound	Related compound
C(1)-N(1)-C(2)	121.9(7)	116.5(4)	TMT-55[g]
N(1)-C(1)-N(3)	120.1(7)	123.5(5)	TMT-55[g]
S(1)-C(1)-N(1)	118.4(6)	118.3(3)	TMT-55[g]
S(1)-C(1)-N(3)	121.4(6)	118.1(3)	TMT-55[g]

[a] Padmanabhan et al. (1978).

[b] Sacerdoti et al. (1990).

[c] Mereiter and Preijinger (1982).

[d] L = 2-methoxy-2,6,6-trimethylheptane-3-5-dionate. Ivanov et al. (1997).

[e] thd = dipivaloylmethanate or 2,2,6,6-tetramethylheptanedionate. Drozdov et al. (1994a).

[f] thd = dipivaloylmethanate or 2,2,6,6-tetramethylheptanedionate. Drozdov et al. (1994b).

[g] Results at 25°C, see the Appendix.

[h] Allen et al., 1987.

With covalent bonds, sp^2 double bonds tend to be shorter than sp^3 single bonds. For example, a carbon-nitrogen single bond (sp^3) has a typical length of 1.47 Å, whereas the double bond (sp^2) has an average length of only 1.28 Å (March, 1985, p. 19). The shortening may be due to the higher "s character" of the double bonds when compared with sp^3 single bonds, that is, while sp^3 single bonds have three p bonds, the sp^2 double bonds only have two. As the s character increases from a single to a double bond, the hybrid orbital becomes more like a typical s orbital. That is, the electrons are held more

tightly to the nucleus than electrons in the p orbitals and the bond length becomes shorter (March, 1985, p. 18-20; Cotton and Wilkinson, 1972, p. 117).

The lengths of the carbon-nitrogen bonds in the $C_3N_3S_3$ rings of $BaH_4(C_3N_3S_3)_2 \bullet 4.5H_2O$ are relatively variable (1.326[9] to 1.414[10] Å) when compared with those in TMT-55 (1.350[5] to 1.356[5] Å) and other heterocyclic aromatic amines (*e.g.*, pyrazole, about 1.347 to 1.365 Å and pyrazine, about 1.319 to 1.347 Å, Allen et al., 1987, Table 38). While the carbon-nitrogen single bond (sp^3) has a typical length of 1.47 Å and the double bond (sp^2) has an average length of 1.28 Å, a carbon-nitrogen single bond where the carbon atom is double bonded to another atom (sp^2) typically has an intermediate value of 1.36 Å (March, 1985, p. 19). The average length of the carbon-nitrogen bonds in $BaH_4(C_3N_3S_3)_2 \bullet 4.5H_2O$ is 1.370 Å, which is consistent with the expected length of a carbon-nitrogen single bond in a $C_3N_3S_3$ ring, where the carbon atom is double bonded to a second nitrogen atom (Figure 2).

The distance between two atoms is also affected by the coordination numbers and valence states of the two atoms and the identities and arrangements of surrounding atoms. All else being equal, bond lengths usually increase with an increase in the coordination number of one of the bonded atoms and decrease with an increase in the valence number (Bloss, 1971, p. 203-218). For example, a Fe^{2+}-O bond should be longer than a Fe^{3+}-O bond (Bloss, 1971, p. 211). Differences in the coordination numbers of barium may also explain why the Ba-O bond lengths are generally longer in $BaH_4(C_3N_3S_3)_2 \bullet 4.5H_2O$ (2.789[5] to 2.983[5] Å, Table 38), where barium has a coordination number of 10, when

compared with $Ba(OH)_2 \cdot 8H_2O$ (2.726[2] to 2.814[2] Å; Sacerdoti et al., 1990, p. 114; Table 38), where barium only has eightfold coordination.

The arrangement of nitrogen and sulfur atoms around each carbon in a $C_3N_3S_3$ ring may be described as a trigonal planar relationship (Figure 2; Brown, 1988, p. 15-17). Ideally, all of the angles between S(1)-C(1)-N(1), S(1)-C(1)-N(3), N(1)-C(1)-N(3), and C(1)-N(1)-C(2) on any $C_3N_3S_3$ ring in any TMT compound should be 120.0° (Figures 2 and 9). The values in Table 38 for $BaH_4(C_3N_3S_3)_2 \cdot 4.5H_2O$ range from 118.4° to 121.9°, which are typical deviations. In comparison, the bond angles around the trigonal carbons in formaldehyde and ethylene similarly vary from 118° to 121° (Brown, 1988, p. 15-16). The deviations usually result because of differences in the electronegativities of the atoms that bond to the trigonal carbons (*e.g.*, nitrogen versus sulfur in the $C_3N_3S_3$ ring) or repulsive forces from unshared pairs of electrons (*e.g.*, the repulsion from two pairs of unshared electrons on oxygen in water, which reduces the H-O-H bond angle from the predicted value of 109.5° to 104.5°) (March, 1985, p. 20-21; Brown, 1988, p. 14-15).

The consistency of the angle measurements for S(1)-C(1)-N(1), S(1)-C(1)-N(3), and N(1)-C(1)-N(3) in Table 38 may be easily checked by summing their values. Because the three angles form a trigonal planar relationship, the angles should add up to 360.0°. The actual sum is 359.9°, which is a reasonable result.

Calculated and Measured Powder XRD Results for $BaH_4(C_3N_3S_3)_2 \cdot 4.5H_2O$

A theoretical XRD powder pattern for $BaH_4(C_3N_3S_3)_2 \cdot 4.5H_2O$ may be calculated from the single crystal XRD data in the Appendix. The calculated powder pattern may be

compared with actual analyses to detect preferred orientations, possible impurities, and other features in the measured patterns.

The unit cell parameters, atomic positions, and other single crystal data for $BaH_4(C_3N_3S_3)_2 \cdot 4.5H_2O$ (Table 37, the Appendix) were entered into Micro-POWD version 2.31 (Smith and Smith, 1993) to calculate the peak intensities and *d*-values for a theoretical powder XRD pattern generated by a Philips diffractometer. The Micro-POWD calculations assumed a variable slit, stripping of α_2 peaks, and a diffracted beam monochromator at 26.630 2θ, but no incident beam monochromator. The *x*, *y*, and *z* positions of the hydrogen atoms were unavailable for entry into Micro-POWD. The Micro-POWD program was only capable of calculating a pattern up to 42° 2θ (based on Cu Kα_1 radiation with $\lambda = 1.54060$ Å).

Table 39 lists the Micro-POWD results. Micro-POWD also calculated the density of $BaH_4(C_3N_3S_3)_2 \cdot 4.5H_2O$ at 2.043 g/cm^3, which is similar to the value of 2.077 g/cm^3 obtained from the single crystal analysis (Table 37). The *d*-values calculated by Micro-POWD were confirmed by also entering the unit cell parameters from the single crystal XRD data (Table 37) into LSUCRI (Garvey, 1986).

Powder XRD analyses on several $BaH_4(C_3N_3S_3)_2 \cdot 4.5H_2O$ samples were done with two Philips diffractometers. Side, Vaseline® and acetone mounts were used. Silicon and fluorophlogopite standards were not effective in correcting most of the *d*-values because of several overlaps between the most intense *d*-values of the standards and $BaH_4(C_3N_3S_3)_2 \cdot 4.5H_2O$. One side mount of a sample that was precipitated on October 22,

1996 produced intensities and uncorrected *d*-values that were fairly close to the results predicted by Micro-POWD (Sample 10/22/96, Table 39).

Table 39. Calculated and measured powder XRD intensities of $BaH_4(C_3N_3S_3)_2 \cdot 4.5H_2O$. Calculated *d*-values, *hkl* values, and calculated intensities are from Micro-POWD version 2.31 (Smith and Smith, 1993).

Calculated *d*-values	*hkl*	Calc. Int.	Measured Intensities, 10/22/96 sample	Measured Intensities, 6/17/97 Sample
10.51	020	13	19	29
10.07	002	54	66	86
9.08	012	2	5	–
7.27	022	47	34	63
6.89	-102	7	19	4
6.55	-112	11	16	8
6.45	-121	3	6	–
6.17	102, 121	13	12	17
5.92	112	2	–	–
5.76	-122, 032	26	21	32
5.66	023	3	8	–
5.32	-131, 122	25	15	–
5.26	040	11	11	14
5.09	041	2	2	–
5.04	004	2	3	4
4.91	-132	10	9	7
4.66	042	10	11	16
4.56	-104	7	6	–
4.54	024, 123	8	7	6

Table 39 cont.

4.46	-114	27	28	17	
4.37	-133	2	2		–
4.31	141	6	4		–
4.25	200	7	9	8	
4.19	-124, -142, -211, 210	39	33	29	
4.14	043, 104	24	17		–
4.09	034	8	4		–
4.01	-212, 142, 211	36	29	20	
3.942	220	13	7		–
3.881	052	18	12		–
3.848	124	27	13		–
3.825	-134, -222	22	14		–
3.795	221	13	8		–
3.769	202	10	11		–
3.739	-151,-213	20	32	9	
3.710	212	11	7		–
3.635	230, 143	24	17		–
3.565	-223, 053	86	100	57	
3.529	-232, 231	43	32	24	
3.505	060, 035	29	18		–
3.446	-144	5	3		–
3.400	-214	11	8		–
3.379	213	13	–		–
3.359	-153, 006	27	42		–

Table 39 cont.

3.334	-233	45	61		–
3.319	232, 062	99	69[a]	83	
3.255	223, 144	34	15	19	
3.228	054	30	–		–
3.221	-161, 241	30	21	12	
3.212	-116	30	–		–
3.178	161	19	22		–
3.076	233, -243, -215	100	69	86	
3.028	036	31	31	23	
3.010	106	15	12		–
2.992	-251, 250	20	10[a]		–
2.980	116, -225	22	16		–
2.958	224, -136	25	12	8	
2.930	-252, 251	14	5		–
2.894	126	24	9[a]		–
2.877	064, 163	35	22	20	
2.838	-235, 300, 046	54	49	52	
2.819	-171,-253, 252	15	12		–
2.791	171, -312, -164	6	9		–
2.766	136	3	6		–
2.706	-261, 260	10	9		–
2.682	225, 164, -245	24	25		–

Table 39 cont.

2.660	-262, 261, 253	58	27	53	
2.631	312, 080, 330	22	19		-
2.620	-137, 146, -332	15	8		-
2.598	-304	8	8		-
2.579	235, -314, -263	31	25	9	
2.572	-156, 262	28	8		-
2.543	082	33	35	21	
2.522	-324, 008	42	53	18	
2.509	-174	26	-		-
2.502	-181, 018, -255	47	37	100	
2.482	181, 332, -342, -118	35	21	18	
2.455	-271, 270, 245, 028, 263, 083, 156	34	16	17	
2.436	-334, 226	20	15		-
2.420	-272, 182, 271	12	5		-
2.408	075	7	4		-
2.375	057, 038, -237, 342	35	42	12	
2.360	-351, 304, 147	24	-		-
2.351	350, 272, -138, 314, -157, 108	29	16		-

Table 39 cont.

2.330	084, 118, -344, 183	13	13[a]		–
2.310	351	9	4		–
2.302	324	11	7		–
2.297	-306	12	7	7	
2.288	128, -353, 166, -316, -208, -184	27	15		–
2.259	246, 217	10	–		–
2.246	-191, -326, 352	23	14		–
2.237	-281, 334, 280, 191, -228	30	18	8	
2.223	138, -345, 184, 227	13	6		–
2.213	-192, -354, -176, 085	16	13	5	
2.193	-362	6	8		–
2.183	-336	10	4		–
2.170	-238	5	7		–
2.161	058, -257, -275, 237	14	11	3	
2.144	-158, 148	7	9		–
2.129	-402	33	25		–

[a] The $BaH_4(C_3N_3S_3)_2 \cdot 4.5H_2O$ *d*-values overlap the most intense d-values of minor impurities of $Ba(OH)_2 \cdot H_2O$ (PDF 26-154).

$Ba(OH)_2 \cdot H_2O$ (PDF 26-154) is an impurity in the October 22, 1996 sample. Some *d*-values of the impurity overlap the *d*-values for $BaH_4(C_3N_3S_3)_2 \cdot 4.5H_2O$ and may have affected the intensities of the $BaH_4(C_3N_3S_3)_2 \cdot 4.5H_2O$ peaks, as stated in Table 39. The most intense peak of $Ba(OH)_2 \cdot H_2O$ (4.70 Å) had a relative intensity of 15 in the October 22, 1996 sample.

Most of the measured intensities from the powder XRD scans of other $BaH_4(C_3N_3S_3)_2 \cdot 4.5H_2O$ samples were significantly different from the calculated Micro-POWD results or the measured results from the October 22, 1996 sample. Table 39 lists the measured intensities of a typical example from the larger group. The sample was produced on June 17, 1997 and was sieved at 60 mesh onto a Vaseline® mount. No impurities, such as $BaCO_3$ or $Ba(OH)_2 \cdot H_2O$, were detected in the June 17, 1997 sample.

When compared with the Micro-POWD results, the (002) peak (*d*-value of 10.07) is consistently more intense in the October 22, 1996, June 17, 1997 and all other measured samples (Table 39). In the June 17, 1997 sample, peaks with *hkl* values of (020), (022), and possibly (018) (*i.e.*, *d*-values of 10.51, 7.27, and 2.502, respectively [Table 39]) were also more intense than predicted. The four *d*-values (*i.e.*, 10.51, 10.07, 7.27, and 2.502) would parallel the [100] zone and the higher intensities may suggest a preferred orientation in that direction possibly resulting from insufficient grinding of $BaH_4(C_3N_3S_3)_2 \cdot 4.5H_2O$ needles.

CHAPTER 8

SUMMARY, CONCLUSIONS AND RECOMMENDATIONS ON THE USE OF THIO-RED® AND TMT-55

Summary

Thio-Red® (manufactured and distributed by ETUS, Inc. of Sanford, Florida) and 2,4,6-trimercaptotriazine, trisodium salt (TMT-55 or $Na_3C_3N_3S_3 \bullet 9H_2O$, a product of Degussa Corporation USA of Allendale, New Jersey) are commercial products that are widely used to remove divalent heavy metals from water. The chemistries of the two products were investigated along with the chemistries and crystalline structures of selected heavy metal precipitates that result from their use.

Thio-Red® is an aqueous solution of sodium and/or potassium thiocarbonate ($[Na,K]_2CS_3 \bullet nH_2O$, where $n \geq 0$). The results of titration experiments, XRD, and chemical analyses suggest that CS_3^{2-}, HS^-, and S^{2-} are the dominant sulfur species in Thio-Red® and that these species are responsible for precipitating heavy metals from aqueous solutions. ETUS, Inc. (1994) states that Thio-Red® removes dissolved heavy metals from water by precipitating them as stable metal thiocarbonates (MCS_3, where $M = Pb^{2+}$, Cu^{2+}, Ni^{2+}, Cd^{2+}, Zn^{2+} and other divalent heavy metals). The results of extensive laboratory studies with aqueous solutions of mercury, zinc, lead, and copper salts,

however, demonstrate that Thio-Red® ultimately removes dissolved metals through the formation of stable metal sulfides (*e.g.*, CuS, HgS, PbS, and ZnS). Although $PbCS_3$ or $ZnCS_3$ may briefly form in solutions treated with Thio-Red®, their overall importance is minor when compared with the far more stable and abundant metal sulfides.

Trace amounts of highly poisonous and flammable carbon disulfide (CS_2) have been detected in Thio-Red®. Additional CS_2 could form from reactions between dissolved heavy metals and CS_3^{2-}. CS_2, as well as H_2S, could create contamination problems if large quantities of undiluted Thio-Red® are injected into low oxygen aquifers or sediments for *in situ* restoration. If the pH of a waste water treatment system can be controlled to minimize the formation of H_2S and if the CS_2 concentration of a batch of Thio-Red® is known to be extremely low, then small volumes of Thio-Red® might be used in the system to precipitate heavy metal contaminants. Peyton et al. (1976) contain useful information on the hazards and stability of CS_2.

The chemistry and crystalline structure of TMT-55 have not been previously studied. The results of chemical and single crystal XRD analyses demonstrate that TMT-55 contains 40 wt% water of hydration (*i.e.*, $Na_3C_3N_3S_3 \bullet 9H_2O$). XRD and optical data on TMT-55 now allow for rapid and inexpensive identification of the compound. TMT-55 crystals are uniaxial negative with indices of refraction (25°C) of $n_\epsilon = 1.520$ and $n_\omega = 1.675$. The crystal data at 25°C are: $R\bar{3}$, $Z = 6$, $a = 17.600(1)$ Å, $c = 9.720(2)$ Å, $V = 2607.5(5)$ Å^3, and a density of 1.55 g/cm^3. The most intense peak from the powder pattern for TMT-55 has a *d*-value of 4.63 Å and an *hkl* value of (012). Two peaks with

hkl values of (303) (d = 2.733 Å) and (330) (d = 2.935 Å) vary as the second- and third-most intense values.

The precipitation of divalent mercury with TMT-55 is more complex than described in Degussa Corporation (1993). Mercury is initially precipitated as a white gel. The gel dries to white mercury 2,4,6-trimercaptotriazine (HgTMT) or to one or more previously unidentified compounds, including yellow, gray, or resinous greenish yellow to greenish brown varieties. The white variety probably contains mercury(I) and has a chemical composition that is consistent with $Hg^{1+}Hg^{2+}(C_3N_3S_3)$, $(Hg^{2+})(Hg^{1+})_3H(C_3N_3S_3)_2$, or $(Hg^{1+})_2H(C_3N_3S_3)$. White HgTMT is monoclinic and its unit cell has the following parameters at 25°C: a = 5.904(3) Å, b = 6.966(1) Å, c = 4.572(1) Å, β = 104.85(2)°, and V = 181.79 Å^3. Many attempts were made to slow the crystallization of white HgTMT so that significantly large single crystals could be produced to determine the space group and other information about the crystalline structure. However, no solvents or techniques were successful and the space group and related information are still unknown.

The yellow variety contains the same major peaks as the white form. However, unlike white HgTMT, the yellow variety also contains a broad amorphous "hump" centered around 4.7 Å (22° 2θ for $CoK_{\alpha 1}$ radiation or 19° 2θ for $CuK_{\alpha 1}$ radiation). The resinous greenish yellow to greenish brown variety is entirely amorphous. Powder XRD patterns of gray HgTMT samples suggest that the variety consists of mixtures of different compounds that result from the decomposition of white and/or yellow HgTMT. Except for minor amounts of white HgTMT, the powder XRD peaks of the gray samples do not match any known organic or inorganic crystalline compounds.

White HgTMT does not have long-term stability. It may convert to the yellow variety within three months in the presence of air at ambient temperatures. Continued exposure to air may result in the conversion of the yellow form to gray HgTMT within a year. If white HgTMT is left in water, it may alter to yellow HgTMT within a few days or to the gray variety within three months.

Batch leaching studies with distilled and deionized water were done on metacinnabar and samples of the gray, yellow, and white varieties of HgTMT. The mercury concentrations in leachates from white HgTMT easily exceeded the 0.2 mg/l mercury standard for toxic hazardousness (40 CFR 268.40). In comparison, mercury concentrations in water leachates of the gray and bright yellow samples were relatively low and resembled the leaching results of metacinnabar (*i.e.*, 3.3 - 53 μg/l). Although the mercury concentrations are low in water leachates of the gray and bright yellow HgTMT samples, the samples may contain other unidentified deleterious compounds that could easily leach into water. Extensive chemical analyses and leaching studies are still required on the gray, yellow and greenish brown varieties.

Studies of barium 2,4,6-trimercaptotriazine (BaTMT) compounds were initiated to determine if TMT-55 could be used to remove barium contaminants from water. Additionally, information on the solubility of BaTMT and other alkaline earth TMT compounds may suggest if TMT-55 could be used to precipitate radium from water.

Two different BaTMT compounds were produced in aqueous solutions: $Ba_3(C_3N_3S_3)_2 \cdot 8H_2O$ and $BaH_4(C_3N_3S_3)_2 \cdot 4.5H_2O$. Both compounds have solubilities of about 5 g/l in water. To be effective, waste water treatment techniques must reduce

barium concentrations in water to below 100 mg/l (40 CFR 268.40). The solubilities of both BaTMT compounds are obviously not low enough to achieve this level and, therefore, TMT-55 probably would not be effective in precipitating barium from water.

Although crystal fibers of $Ba_3(C_3N_3S_3)_2 \cdot 8H_2O$ are usually abundant, they are too fine-grained for optical studies or single crystal XRD analyses. Powder XRD analyses at 25°C provide two possible solutions for the unit cell of $Ba_3(C_3N_3S_3)_2 \cdot 8H_2O$, one hexagonal ($a$ = 21.5106[6] Å, c = 4.4474[3] Å, and V = 1782.14 Å^3) and the other orthorhombic (a = 18.629[1] Å, b = 10.7557[7]Å, c = 4.4474[3] Å, and V = 891.11 Å^3). The results of a single crystal analysis of $BaH_4(C_3N_3S_3)_2 \cdot 4.5H_2O$ at 25°C state that the compound is monoclinic ($P2_1/c$) and the unit cell parameters are Z = 4, calculated density = 2.077 g/cm^3, a = 8.5576(4) Å, b = 21.028(1) Å, c = 20.276(1) Å, β = 96.440(1)°, and V = 3625.6(3) Å^3.

Conclusions and Recommendations

The following conclusions and recommendations may be made:

1. Large volumes of undiluted Thio-Red® should not be injected into subsurface environments for *in situ* restoration until studies eliminate the possibility of CS_2 or H_2S contamination or metal sulfide oxidation. If gallons of Thio-Red® are used at once in waste water treatment facilities, the air in the facilities should be monitored for CS_2 and H_2S.

2. If any ground waters, soils or sediments have undergone *in situ* restoration with Thio-Red®, the pH, chemistry and reduction/oxidation conditions of the ground

waters or other associated waters should be monitored to detect any evidence of the oxidation of sulfide precipitates or the presence of undesirable concentrations of CS_2 or H_2S.

3. Additional research is required on the chemistry and leaching properties of the different HgTMT varieties, including the pH and mercury concentrations of leachates over a greater range of liquid to solid ratios. Further research is also needed to identify the HgTMT varieties that are likely to form in low oxygen subsurface environments. Usually, the treatment of mercury wastes with TMT-15 would allow for the recovery of the resulting HgTMT precipitates. The precipitates could be rendered harmless by extracting the mercury in the elemental form with "roasting and retorting" methods (Henke et al., 1993, p. 22). If *in situ* restoration is the only feasible option at a mercury-contaminated site, TMT-15 should not be used until studies have demonstrated that the resulting HgTMT precipitates have long-term stability in subsurface environments and are essentially unleachable with respect to mercury or any other contaminants.

4. Unless additional methods can be developed to produce suitable single crystals of white HgTMT, Rietveld analyses (Rietveld, 1967, 1969) are necessary to determine the space group, atomic coordinates, and other information on the crystalline structure of the compound.

5. Mercury(I) sulfide (Hg_2S) may rapidly decompose into elemental mercury and HgS (Nebergall et al., 1976, p. 847). Mercury(I) in white HgTMT may decompose through the same process, which could explain the break down of the

white HgTMT crystalline structure to form the partially amorphous yellow variety. Additional experimental evidence is needed to understand the origin of the yellow variety and to determine if this decomposition reaction is occurring in HgTMT.

6. Additional XRD and other studies are required to identify the crystalline compounds in gray HgTMT. Observations with a binocular microscope suggest that gray HgTMT samples contain metacinnabar (HgS). During the conversion of white or yellow HgTMT to the gray variety, the sulfur and mercury complexes may be separating from the TMT ring to form metacinnabar. Hydroxides then could combine with the carbons on the ring to produce cyanuric acid ($H_3C_3N_3O_3$). Current XRD studies have not detected HgS or $H_3C_3N_3O_3$ in gray HgTMT. If the compounds are present in gray HgTMT, longer aqueous leaching studies with white and gray HgTMT samples may produce enough HgS and $H_3C_3N_3O_3$ to be detected by XRD or other methods. Although substantial mercury did not leach from the gray and yellow varieties, additional leaching and chemical studies are needed to evaluate them for the possible presence of other leachable deleterious compounds, in particular organic compounds.

7. TMT-55 probably would not be effective in precipitating barium from waste waters and contaminated ground waters.

8. TMT-55 reacts with calcium and strontium hydroxides (Henke and Atwood, in press), as well as solutions of barium hydroxide and barium chloride. As with calcium, strontium, and barium sulfates, the solubilities of alkaline earth TMT compounds in the form of $MH_4(C_3N_3S_3)_2 \bullet nH_2O$ ($M = Ba^{2+}$, Sr^{2+}, and Ca^{2+})

decrease with increasing atomic numbers in the alkaline earth group (*i.e.*, calcium > strontium > barium) (Henke and Atwood, in press). These studies suggest that radium 2,4,6-trimercaptotriazine (RaTMT) compounds may form in water and that their solubilities should be less than those of the investigated BaTMT compounds. Preliminary studies should be conducted to confirm the formation of RaTMT compounds and to determine their solubilities in water. If the solubilities of RaTMT are extremely low, TMT-15 may be effective in removing radium from water.

9. Because of the new information on the water content of TMT-55 and how TMT-55 and Thio-Red® react with dissolved heavy metal contaminants, the dosage formulas for the two products should be evaluated with laboratory studies and, if necessary, revised to precipitate heavy metals more effectively.

APPENDIX: SINGLE CRYSTAL X-RAY DIFFRACTION RESULTS ON 2,4,6-TRIMERCAPTOTRIAZINE COMPOUNDS

$Na_3C_3N_3S_3 \bullet 9H_2O$ at -110°C

Table 40. Crystal data and structure refinement for 2,4,6-trimercaptotriazine, trisodium salt, nonahydrate at -110°C. Terms in this table are defined in textbooks on single crystal XRD, such as Stout and Jensen (1989).

Identification code:	NaTMT
Empirical formula:	$C_3H_{18}N_3Na_3O_9S_3$
Formula weight:	405.35
Temperature:	163(2) K (-110°C)
Wavelength:	0.71073 Å
Crystal system:	Rhombohedral
Space group:	R-3
Unit cell dimensions:	
	a: = 17.530(2) Å $\quad \alpha$: = 90°
	b: = 17.530(2) Å $\quad \beta$: = 90°
	c: = 9.6312(13) Å $\quad \gamma$: = 120°
Volume, Z:	2563.1(5) Å^3, 6
Density (calculated):	1.576 g/cm^3
Absorption coefficient:	0.548 mm^{-1}
F(000):	1260
Crystal size:	0.37 x 0.16 x 0.14 mm
Gq range for data collection:	2.32 to 27.46°
Limiting indices:	$-12 \le h \le 19$, $-10 \le k \le 19$, $-12 \le l \le 12$
Reflections collected:	1918
Independent reflections:	1308 (R_{int} = 0.0215)
Absorption correction:	None
Refinement method:	Full-matrix least-squares on F^2
Data / restraints / parameters:	1308 / 24 / 83
Goodness-of-fit on F^2:	1.051
$R1$ [$F^2 > 2\sigma F^2$] (obs. reflect.):	0.0276
$wR2$ (F^2) (all reflections):	0.0747
Largest diff. peak and hole:	0.382 and -0.231 eÅ^{-3}

Table 41. Atomic coordinates (x 10^4) and equivalent isotropic displacement parameters ($Å^2$ x 10^3) for 2,4,6-trimercaptotriazine, trisodium salt, nonahydrate at -110°C. *U(eq)* is defined as one third of the trace of the orthogonalized U_{ij} tensor.

	x	*y*	*z*	*U(eq)*
S	2009(1)	872(1)	7467(1)	15(1)
Na	2401(1)	-589(1)	7619(1)	19(1)
O(1)	2220(1)	-2020(1)	7502(1)	20(1)
O(2)	1248(1)	-1255(1)	5863(1)	22(1)
O(3)	3218(1)	-395(1)	9740(1)	21(1)
C	876(1)	382(1)	7409(2)	13(1)
N	393(1)	-509(1)	7401(1)	14(1)

Table 42. Bond lengths (Å) and angles (degrees) for 2,4,6-trimercaptotriazine, trisodium salt, nonahydrate at -110°C.

S-C	1.727(2)
S-Na	2.9694(9)
Na-O(3)#1	2.357(2)
Na-O(1)	2.368(2)
Na-O(3)	2.420(2)
Na-O(2)	2.438(2)
Na-O(1)#2	2.461(2)
Na-Na#2	3.6142(14)
Na-Na#3	4.0573(8)
Na-Na#1	4.0573(8)
O(1)-Na#2	2.461(2)
O(3)-Na#3	2.357(2)
C-N#4	1.352(2)
C-N	1.354(2)
N-C#5	1.352(2)
C-S-Na	106.08(6)
O(3)#1-Na-O(1)	103.11(5)
O(3)#1-Na-O(3)	90.20(3)
O(1)-Na-O(3)	86.88(5)
O(3)#1-Na-O(2)	106.26(5)
O(1)-Na-O(2)	79.62(5)

Table 42 cont.

O(3)-Na-O(2)	160.65(5)
O(3)#1-Na-O(1)#2	170.96(6)
O(1)-Na-O(1)#2	83.10(5)
O(3)-Na-O(1)#2	83.52(5)
O(2)-Na-O(1)#2	81.16(5)
O(3)#1-Na-S	89.86(4)
O(1)-Na-S	160.95(4)
O(3)-Na-S	107.24(4)
O(2)-Na-S	83.41(4)
O(1)#2-Na-S	85.82(4)
O(3)#1-Na-Na#2	145.18(5)
O(1)-Na-Na#2	42.53(4)
O(3)-Na-Na#2	83.54(4)
O(2)-Na-Na#2	77.13(4)
O(1)#2-Na-Na#2	40.57(3)
S-Na-Na#2	124.72(3)
O(3)#1-Na-Na#3	85.72(4)
O(1)-Na-Na#3	118.16(4)
O(3)-Na-Na#3	31.39(3)
O(2)-Na-Na#3	156.35(4)
O(1)#2-Na-Na#3	85.54(4)
S-Na-Na#3	76.17(3)
Na#2-Na-Na#3	104.85(2)
O(3)#1-Na-Na#1	32.32(3)
O(1)-Na-Na#1	78.90(4)
O(3)-Na-Na#1	109.98(4)
O(2)-Na-Na#1	81.11(4)
O(1)#2-Na-Na#1	156.67(4)
S-Na-Na#1	107.02(2)
Na#2-Na-Na#1	119.94(4)
Na#3-Na-Na#1	116.05(2)
Na-O(1)-Na#2	96.90(5)
Na#3-O(3)-Na	116.29(6)
N#4-C-N	122.9(2)
N#4-C-S	118.74(12)
N-C-S	118.34(12)
C#5-N-C	117.1(2)

Symmetry transformations used to generate equivalent atoms:
#1 -y+1/3,x-y-1/3,z-1/3 #2 -x+1/3,-y-1/3,-z+5/3 #3 -x+y+2/3,-x+1/3,z+1/3
#4 -y,x-y,z #5 -x+y,-x,z

Table 43. Anisotropic displacement parameters ($Å^2 \times 10^3$) for 2,4,6-trimercaptotriazine, trisodium salt, nonahydrate at -110°C. The anisotropic displacement factor exponent takes the form: $-2\pi^2 [(ha^*)^2U_{11} + ... + 2hka^*b^*U_{12}]$.

	U11	*U22*	*U33*	*U23*	*U13*	*U12*
S	12(1)	15(1)	18(1)	1(1)	0(1)	6(1)
Na	18(1)	18(1)	20(1)	1(1)	1(1)	9(1)
O(1)	25(1)	25(1)	15(1)	1(1)	0(1)	17(1)
O(2)	28(1)	26(1)	17(1)	-1(1)	0(1)	18(1)
O(3)	20(1)	21(1)	24(1)	-1(1)	0(1)	11(1)
C	13(1)	14(1)	11(1)	0(1)	0(1)	6(1)
N	12(1)	13(1)	19(1)	1(1)	0(1)	7(1)

Table 44. Hydrogen coordinates ($\times 10^4$) and isotropic displacement parameters ($Å^2 \times 10^3$) for 2,4,6-trimercaptotriazine, trisodium salt, nonahydrate at -110°C.

	x	*y*	*z*	*U(eq)*
H(1A)	2249(14)	-2138(13)	6728(13)	29
H(1B)	2512(12)	-2163(13)	7900(19)	29
H(2A)	951(12)	-1085(14)	6184(20)	32
H(2B)	1284(14)	-1129(14)	5087(13)	32
H(3A)	3574(11)	-520(13)	9550(21)	31
H(3B)	2866(11)	-806(11)	10153(21)	31

$Na_3C_3N_3S_3 \cdot 9H_2O$ at 25°C

Table 45. Crystal data and structure refinement for 2,4,6-trimercaptotriazine, trisodium salt, nonahydrate at 25°C. Terms in this table are defined in single crystal XRD textbooks, such as Stout and Jensen (1989).

Identification code:	NaTMT
Diffractometer Used:	Siemens R3m/V
Monochromator:	Highly oriented graphite crystal
Empirical formula:	$C_3H_{18}N_3Na_3O_9S_3$
Formula weight:	405.4
Temperature:	298 K (25°C)
Wavelength:	MoKα (0.71073 Å)
Crystal system:	Rhombohedral
Space group:	R-3
Unit cell dimensions:	
	a: = 17.5950(10) Å α: = 90°
	b: = 17.5950(10) Å β: = 90°
	c: = 9.7190(10) Å γ: = 120°
Volume, Z:	2605.8(5) Å^3, 6
Density (calculated):	1.550 g/cm^3
Absorption coefficient:	0.539 mm^{-1}
F(000):	1260
Crystal size:	0.05 x 0.05 x 0.2 mm
2θ range:	7.0 to 45.0°
Scan type:	ω
Scan speed:	Variable; 8.00 to 60.00°/min. in ω
Scan range (ω):	0.34°
Background Measurement:	Stationary crystal and stationary counter at beginning and end of scan, each for 0.5% of total scan time
Standard Reflections:	3 measured every 97 reflections
Limiting indices:	$-1 \le h \le 23$, $-24 \le k \le 12$, $-11 \le l \le 13$
Reflections collected:	2141
Independent reflections:	1645 (R_{int} = 0.0256)
Observed Reflections: 1048 (F . 4.0σ[F])	
Absorption correction:	None
Solution system:	Siemens SHELXTL PLUS (PC Version)
Solution:	Direct Methods
Refinement method:	Full-matrix least-squares
Quantity Minimized:	$\sum w(F_o - F_c)^2$

Table 45 cont.

Hydrogen Atoms:	Riding model, fixed isotropic U
Weighing Scheme:	$w^{-1} = \sigma^2(F) + 99.0000F^2$
No. of Refined Parameters:	64
Final *R* Indices (obs. data):	*R1* = 5.81 %, *wR2* = 6.03%
R Indices (all data):	*R1* = 9.40 %, *wR2* = 8.56%
Goodness-of-fit on F^2:	3.71
Data-to-Parameter ratio:	16.4:1
Largest diff. peak and hole:	0.47 and -0.70 eÅ^{-3}

Table 46. Atomic coordinates (x 10^4) and equivalent isotropic displacement parameters (Å^2 x 10^3) for 2,4,6-trimercaptotriazine, trisodium salt, nonahydrate at 25°C. *U(eq)* is defined as one third of the trace of the orthogonalized U_{ij} tensor.

	x	*y*	*z*	*U(eq)*
S(1)	7543(1)	2206(1)	862(1)	27(1)
C(1)	7046(3)	2844(3)	920(4)	21(1)
N(1)	6158(2)	2433(2)	923(4)	25(1)
Na	6313(1)	-941(1)	4048(2)	34(1)
O(2)	5350(2)	916(2)	9140(3)	35(1)
O(3)	4592(2)	-843(2)	-2478(4)	40(2)
O(4)	6274(2)	-278(2)	-1408(4)	39(1)

Table 47. Bond lengths (Å) and angles (degrees) for 2,4,6-trimercaptotriazine, trisodium salt, nonahydrate at 25°C.

S(1)-C(1)	1.733 (6)
S(1)-NaD	2.980 (2)
C(1)-N(1)	1.356 (5)
C(1)-N(1A)	1.350 (5)
N(1)-C(1A)	1.350 (5)
Na-S(1A)	2.980 (3)
Na-NaA	3.630 (5)
Na-NaB	4.097 (1)

Table 47 cont.

Na-NaD	4.097 (1)
Na-O(2A)	2.498 (4)
Na-O(2B)	2.391 (5)
Na-O(3A)	2.469 (4)
Na-O(4A)	2.447 (4)
Na-O(4B)	2.373 (4)
O(2)-NaE	2.497 (4)
O(2)-NaF	2.391 (3)
O(3)-NaG	2.469 (5)
O(4)-NaC	2.373 (4)
O(4)-NaD	2.447 (4)
C(1)-S(1)-NaD	105.7(1)
S(1)-C(1)-N(1)	118.3(3)
S(1)-C(1)-N(1A)	118.1(3)
N(1)-C(1)-N(1A)	123.5(5)
C(1)-N(1)-C(1A)	116.5(4)
S(1A)-Na-NaA	125.2(1)
S(1A)-Na-NaB	107.3(1)
NaA-Na-NaB	119.4(1)
S(1A)-Na-NaD	76.3(1)
NaA-Na-NaD	104.7(1)
NaB-Na-NaD	116.0(1)
S(1A)-Na-O(2A)	86.0(1)
NaA-Na-O(2A)	40.9(1)
NaB-Na-O(2A)	156.8(1)
NaD-Na-O(2A)	85.2(1)
S(1A)-Na-O(2B)	161.6(1)
NaA-Na-O(2B)	43.2(1)
NaB-Na-O(2B)	77.6(1)
NaD-Na-O(2B)	118.1(1)
O(2A)-Na-O(2B)	84.1(1)
S(1A)-Na-O(3A)	83.5(1)
NaA-Na-O(3A)	77.5(1)
NaB-Na-O(3A)	81.0(1)
NaD-Na-O(3A)	156.7(1)
O(2A)-Na-O(3A)	81.8(1)
O(2B)-Na-O(3A)	79.7(1)
S(1A)-Na-O(4A)	107.3(1)
NaA-Na-O(4A)	83.2(1)

Table 47 cont.

NaB-Na-O(4A)	109.8(1)
NaD-Na-O(4A)	31.3(1)
O(2A)-Na-O(4A)	83.1(1)
O(2B)-Na-O(4A)	86.9(1)
O(3A)-Na-O(4A)	160.7(2)
S(1A)-Na-O(4B)	90.1(1)
NaA-Na-O(4B)	144.4(1)
NaB-Na-O(4B)	32.3(1)
NaD-Na-O(4B)	85.7(1)
O(2A)-Na-O(4B)	170.7(2)
O(2B)-Na-O(4B)	101.8(1)
O(3A)-Na-O(4B)	106.2(1)
O(4A)-Na-O(4B)	90.0(1)
NaE-O(2)-NaF	95.9(1)
NaC-O(4)-NaD	116.4(1)

Table 48. Anisotropic displacement parameters ($Å^2$ x 10^3) for 2,4,6-trimercaptotriazine, trisodium salt, nonahydrate at 25°C. The anisotropic displacement factor exponent takes the form: $-2\pi^2 [(ha^*)^2 U_{11} + ... + 2hka^*b^* U_{12}]$

	U11	*U22*	*U33*	*U23*	*U13*	*U12*
S(1)	26(1)	25(1)	35(1)	16(1)	-1(1)	-1(1)
C(1)	23(2)	19(2)	23(2)	11(2)	1(2)	0(2)
N(1)	19(2)	19(2)	36(2)	10(1)	-1(1)	-3(1)
Na	31(1)	30(1)	42(1)	15(1)	1(1)	-1(1)
O(2)	38(2)	27(2)	35(2)	12(1)	-2(1)	-3(1)
O(3)	44(2)	34(2)	34(2)	13(2)	3(2)	-4(1)
O(4)	35(2)	32(2)	46(2)	15(1)	5(2)	3(2)

Table 49. Hydrogen coordinates (x 10^4) and isotropic displacement parameters ($Å^2$ x 10^3) for 2,4,6-trimercaptotriazine, trisodium salt, nonahydrate at 25°C.

	x	*y*	*z*	*U(eq)*
H(2A)	4773	638	9537	50
H(2B)	5776	1254	9831	50
H(3A)	4168	-713	-2089	50
H(3B)	4343	-1217	-3265	50
H(4A)	5757	-389	-1841	50
H(4B)	6039	-909	-1231	50

$BaH_4(C_3N_3S_3)_2 \bullet 4.5H_2O$

Table 50. Crystal data and structure refinement for $BaH_4(C_3N_3S_3)_2 \bullet 4.5H_2O$ at 25°C. Terms in this table are defined in single crystal XRD textbooks, such as Stout and Jensen (1989).

Identification code:	BaTMT
Empirical formula:	$C_{12}H_{26}N_{12}Ba_2O_9S_{12}$
Formula weight:	1133.78 for empirical formula
Temperature:	298 K (25°C)
Wavelength:	MoKα (0.71073 Å)
Crystal system:	Monoclinic
Space group:	$P2_1/c$
Unit cell dimensions:	
	a: = 8.5576(4)Å $\quad \alpha$: = 90°
	b: = 21.0284(10) Å $\quad \beta$: = 96.4400(10)°
	c: = 20.2756(10) Å $\quad \gamma$: = 90°
Volume, *Z*:	3625.6(3) $Å^3$, 4
Density (calculated):	2.077 g/cm^3
Absorption coefficient:	2.908 mm^{-1}
F(000):	2200
Crystal size:	0.02 x 0.04 x 1.0 mm
θ range:	1.40 to 21.00°
Limiting indices:	$-11 \le h \le 11, -28 \le k \le 27, -26 \le l \le 20$
Reflections collected:	11942
Independent reflections:	3872 (R_{int} = 0.1116)

Table 50 cont.

Refinement method:	Full-matrix least-squares on F^2
Data / restraints / parameters	3861 / 0 /424
Goodness-of-fit on F^2:	1.028
Final R Indices ($I>2\sigma[I]$):	$R1$ = 4.27 %, $wR2$ = 13.05%
R Indices (all data):	$R1$ = 5.01 %, $wR2$ = 14.19%
Largest diff. peak and hole:	0.917 and -0.947 eÅ^{-3}

Table 51. Atomic coordinates (x 10^4) and equivalent isotropic displacement parameters (Å^2 x 10^3) for $BaH_4(C_3N_3S_3)_2 \cdot 4.5H_2O$ at 25°C. *U(eq)* is defined as one third of the trace of the orthogonalized U_{ij} tensor.

	x	*y*	*z*	*U(eq)*
Ba(1)	3454(1)	7372(1)	274(1)	24(1)
Ba(2)	8206(1)	7734(1)	-728(1)	31(1)
S(1)	3231(2)	5801(1)	-223(1)	30(1)
S(2)	4697(3)	4354(1)	1884(1)	38(1)
S(3)	7179(3)	6649(1)	1769(1)	35(1)
S(4)	8342(2)	6026(1)	-278(1)	32(1)
S(5)	9618(3)	4488(1)	1773(1)	35(1)
S(6)	2370(3)	6737(1)	1761(1)	35(1)
S(7)	10727(2)	9096(1)	-340(1)	29(1)
S(8)	11900(3)	10442(1)	1842(1)	34(1)
S(9)	4685(2)	8218(1)	1662(1)	29(1)
S(10)	6033(3)	9119(1)	-274(1)	36(1)
S(11)	-3131(3)	10535(1)	1888(1)	34(1)
S(12)	-277(3)	8308(1)	1819(1)	33(1)
N(1)	4036(7)	5153(3)	885(3)	25(2)
N(2)	5851(7)	5516(3)	1725(3)	25(2)
N(3)	5165(7)	6175(3)	810(3)	23(2)
N(4)	9128(7)	5324(3)	788(3)	26(2)
N(5)	10853(7)	5641(3)	1694(3)	27(2)
N(6)	10317(8)	6339(3)	776(3)	29(2)
N(7)	11444(7)	9674(3)	806(3)	27(2)
N(8)	3226(7)	9325(3)	1656(3)	25(2)
N(9)	2685(7)	8693(3)	684(3)	23(2)
N(10)	6542(7)	9752(3)	865(3)	28(2)
N(11)	-1781(7)	9414(3)	1758(3)	22(2)

Table 51 cont.

N(12)	-2154(7)	8763(3)	806(3)	22(2)
C(1)	4242(8)	5713(3)	533(4)	21(2)
C(2)	4855(10)	5035(4)	1479(4)	31(2)
C(3)	6014(9)	6096(4)	1402(4)	26(2)
C(4)	9354(9)	5901(4)	478(4)	23(2)
C(5)	9886(9)	5177(3)	1400(4)	23(2)
C(6)	1095(9)	6224(4)	1378(4)	26(2)
C(7)	11708(9)	9137(3)	422(4)	23(2)
C(8)	12223(9)	9777(4)	1418(4)	25(2)
C(9)	3463(8)	8759(4)	1303(4)	26(2)
C(10)	6878(8)	9209(4)	510(4)	24(2)
C(11)	-2783(9)	9867(4)	1492(4)	25(2)
C(12)	-1461(9)	8846(3)	1433(3)	21(2)
O(1)	5263(6)	7014(3)	-831(3)	37(1)
O(2)	6723(6)	7553(2)	442(2)	26(1)
O(3)	275(6)	7576(2)	424(3)	26(1)
O(4)	3158(7)	8124(3)	-894(3)	49(2)
O(5)	1012(6)	7011(3)	-830(3)	33(1)
O(6)	7737(7)	6952(3)	-1844(3)	56(2)
O(7)	9917(7)	8134(3)	-1788(3)	48(2)
O(8)	5845(7)	8230(3)	-1689(3)	46(2)
O(9)	2828(9)	7082(5)	-1944(4)	89(3)

Table 52. Bond lengths (Å) and angles (degrees) for $BaH_4(C_3N_3S_3)_2 \cdot 4.5H_2O$ at 25°C.

Ba(1)-O(3)	2.804(5)
Ba(1)-O(2)	2.806(5)
Ba(1)-O(4)	2.834(6)
Ba(1)-O(1)	2.960(5)
Ba(1)-O(5)	2.983(5)
Ba(1)-N(9)	2.993(6)
Ba(1)-N(3)	3.050(6)
Ba(1)-S(9)	3.396(2)
Ba(1)-S(1)	3.453(2)
Ba(1)-S(6)	3.517(2)
Ba(1)-Ba(2)#1	4.7779(7)
Ba(1)-Ba(2)	4.8059(7)
Ba(2)-O(3)#2	2.789(5)

Table 52 cont.

Ba(2)-O(6)	2.789(6)
Ba(2)-O(2)	2.839(5)
Ba(2)-O(8)	2.842(6)
Ba(2)-O(7)	2.858(6)
Ba(2)-O(5)#2	2.870(5)
Ba(2)-O(1)	2.926(5)
Ba(2)-S(7)	3.618(2)
Ba(2)-S(10)	3.629(2)
Ba(2)-Ba(1)#2	4.7779(7)
S(1)-C(1)	1.685(8)
S(2)-C(2)	1.663(8)
S(3)-C(3)	1.652(8)
S(4)-C(4)	1.695(8)
S(5)-C(5)	1.662(7)
S(6)-C(6)	1.663(8)
S(7)-C(7)	1.674(8)
S(8)-C(8)	1.681(7)
S(9)-C(9)	1.659(8)
S(10)-C(10)	1.683(8)
S(11)-C(11)	1.661(8)
S(12)-C(12)	1.656(7)
N(1)-C(2)	1.347(10)
N(1)-C(1)	1.399(9)
N(2)-C(2)	1.381(10)
N(2)-C(3)	1.399(10)
N(3)-C(1)	1.335(9)
N(3)-C(3)	1.342(10)
N(4)-C(5)	1.371(10)
N(4)-C(4)	1.388(9)
N(5)-C(5)	1.371(9)
N(5)-C(6)#2	1.411(10)
N(6)-C(4)	1.336(10)
N(6)-C(6)#2	1.345(10)
N(7)-C(8)	1.358(10)
N(7)-C(7)	1.405(10)
N(8)-C(8)#1	1.333(10)
N(8)-C(9)	1.414(10)
N(9)-C(7)#1	1.326(9)
N(9)-C(9)	1.359(10)
N(10)-C(11)#2	1.359(10)

Table 52 cont.

N(10)-C(10)	1.397(10)
N(11)-C(11)	1.352(10)
N(11)-C(12)	1.407(9)
N(12)-C(10)#1	1.347(10)
N(12)-C(12)	1.351(9)
C(6)-N(6)#1	1.345(10)
C(6)-N(5)#1	1.411(10)
C(7)-N(9)#2	1.326(9)
C(8)-N(8)#2	1.333(10)
C(10)-N(12)#2	1.347(10)
C(11)-N(10)#1	1.359(10)
O(3)-Ba(2)#1	2.789(5)
O(5)-Ba(2)#1	2.870(5)
O(3)-Ba(1)-O(2)	158.8(2)
O(3)-Ba(1)-O(4)	90.5(2)
O(2)-Ba(1)-O(4)	91.2(2)
O(3)-Ba(1)-O(1)	135.9(2)
O(2)-Ba(1)-O(1)	61.8(2)
O(4)-Ba(1)-O(1)	61.0(2)
O(3)-Ba(1)-O(5)	61.0(2)
O(2)-Ba(1)-O(5)	136.95(14)
O(4)-Ba(1)-O(5)	61.7(2)
O(1)-Ba(1)-O(5)	75.5(2)
O(3)-Ba(1)-N(9)	65.3(2)
O(2)-Ba(1)-N(9)	95.0(2)
O(4)-Ba(1)-N(9)	73.3(2)
O(1)-Ba(1)-N(9)	126.6(2)
O(5)-Ba(1)-N(9)	106.7(2)
O(3)-Ba(1)-N(3)	121.3(2)
O(2)-Ba(1)-N(3)	68.7(2)
O(4)-Ba(1)-N(3)	138.8(2)
O(1)-Ba(1)-N(3)	77.8(2)
O(5)-Ba(1)-N(3)	109.0(2)
N(9)-Ba(1)-N(3)	141.1(2)
O(3)-Ba(1)-S(9)	92.52(11)
O(2)-Ba(1)-S(9)	67.40(11)
O(4)-Ba(1)-S(9)	113.00(13)
O(1)-Ba(1)-S(9)	128.37(11)
O(5)-Ba(1)-S(9)	151.78(11)
N(9)-Ba(1)-S(9)	48.78(12)

Table 52 cont.

N(3)-Ba(1)-S(9)	92.55(12)
O(3)-Ba(1)-S(1)	98.95(11)
O(2)-Ba(1)-S(1)	100.79(11)
O(4)-Ba(1)-S(1)	107.05(13)
O(1)-Ba(1)-S(1)	63.38(11)
O(5)-Ba(1)-S(1)	61.72(11)
N(9)-Ba(1)-S(1)	164.17(12)
N(3)-Ba(1)-S(1)	47.41(12)
S(9)-Ba(1)-S(1)	138.13(5)
O(3)-Ba(1)-S(6)	67.18(11)
O(2)-Ba(1)-S(6)	107.61(11)
O(4)-Ba(1)-S(6)	157.02(13)
O(1)-Ba(1)-S(6)	139.70(12)
O(5)-Ba(1)-S(6)	108.43(11)
N(9)-Ba(1)-S(6)	91.53(12)
N(3)-Ba(1)-S(6)	62.80(12)
S(9)-Ba(1)-S(6)	64.86(5)
S(1)-Ba(1)-S(6)	82.84(5)
O(3)-Ba(1)-Ba(2)#1	31.24(11)
O(2)-Ba(1)-Ba(2)#1	155.07(10)
O(4)-Ba(1)-Ba(2)#1	64.17(12)
O(1)-Ba(1)-Ba(2)#1	105.40(11)
O(5)-Ba(1)-Ba(2)#1	34.50(10)
N(9)-Ba(1)-Ba(2)#1	75.24(11)
N(3)-Ba(1)-Ba(2)#1	132.36(11)
S(9)-Ba(1)-Ba(2)#1	117.29(4)
S(1)-Ba(1)-Ba(2)#1	90.56(4)
S(6)-Ba(1)-Ba(2)#1	95.70(4)
O(3)-Ba(1)-Ba(2)	154.03(11)
O(2)-Ba(1)-Ba(2)	31.85(10)
O(4)-Ba(1)-Ba(2)	63.85(12)
O(1)-Ba(1)-Ba(2)	35.03(10)
O(5)-Ba(1)-Ba(2)	106.15(10)
N(9)-Ba(1)-Ba(2)	101.15(11)
N(3)-Ba(1)-Ba(2)	83.47(11)
S(9)-Ba(1)-Ba(2)	93.96(4)
S(1)-Ba(1)-Ba(2)	92.86(4)
S(6)-Ba(1)-Ba(2)	137.71(4)
Ba(2)#1-Ba(1)-Ba(2)	126.49(2)
O(3)#2-Ba(2)-O(6)	129.0(2)

Table 52 cont.

O(3)#2-Ba(2)-O(2)	65.5(2)
O(6)-Ba(2)-O(2)	124.2(2)
O(3)#2-Ba(2)-O(8)	162.4(2)
O(6)-Ba(2)-O(8)	68.5(2)
O(2)-Ba(2)-O(8)	105.8(2)
O(3)#2-Ba(2)-O(7)	109.5(2)
O(6)-Ba(2)-O(7)	66.6(2)
O(2)-Ba(2)-O(7)	169.1(2)
O(8)-Ba(2)-O(7)	76.2(2)
O(3)#2-Ba(2)-O(5)#2	62.6(2)
O(6)-Ba(2)-O(5)#2	71.0(2)
O(2)-Ba(2)-O(5)#2	116.4(2)
O(8)-Ba(2)-O(5)#2	133.0(2)
O(7)-Ba(2)-O(5)#2	66.3(2)
O(3)#2-Ba(2)-O(1)	117.3(2)
O(6)-Ba(2)-O(1)	65.9(2)
O(2)-Ba(2)-O(1)	61.9(2)
O(8)-Ba(2)-O(1)	66.5(2)
O(7)-Ba(2)-O(1)	127.5(2)
O(5)#2-Ba(2)-O(1)	116.1(2)
O(3)#2-Ba(2)-S(7)	66.72(11)
O(6)-Ba(2)-S(7)	132.17(13)
O(2)-Ba(2)-S(7)	103.61(11)
O(8)-Ba(2)-S(7)	102.68(13)
O(7)-Ba(2)-S(7)	65.65(13)
O(5)#2-Ba(2)-S(7)	87.24(11)
O(1)-Ba(2)-S(7)	155.87(11)
O(3)#2-Ba(2)-S(10)	100.26(11)
O(6)-Ba(2)-S(10)	130.4(2)
O(2)-Ba(2)-S(10)	66.77(11)
O(8)-Ba(2)-S(10)	62.24(13)
O(7)-Ba(2)-S(10)	105.96(13)
O(5)#2-Ba(2)-S(10)	154.21(12)
O(1)-Ba(2)-S(10)	88.40(12)
S(7)-Ba(2)-S(10)	67.66(5)
O(3)#2-Ba(2)-Ba(1)#2	31.43(10)
O(6)-Ba(2)-Ba(1)#2	107.08(14)
O(2)-Ba(2)-Ba(1)#2	96.33(11)
O(8)-Ba(2)-Ba(1)#2	155.74(12)
O(7)-Ba(2)-Ba(1)#2	80.21(13)

Table 52 cont.

O(5)#2-Ba(2)-Ba(1)#2	36.08(11)
O(1)-Ba(2)-Ba(1)#2	135.08(11)
S(7)-Ba(2)-Ba(1)#2	61.60(3)
S(10)-Ba(2)-Ba(1)#2	120.26(4)
O(3)#2-Ba(2)-Ba(1)	96.58(11)
O(6)-Ba(2)-Ba(1)	101.41(12)
O(2)-Ba(2)-Ba(1)	31.44(10)
O(8)-Ba(2)-Ba(1)	77.15(12)
O(7)-Ba(2)-Ba(1)	153.30(13)
O(5)#2-Ba(2)-Ba(1)	134.50(11)
O(1)-Ba(2)-Ba(1)	35.50(11)
S(7)-Ba(2)-Ba(1)	123.05(4)
S(10)-Ba(2)-Ba(1)	62.47(4)
Ba(1)#2-Ba(2)-Ba(1)	126.49(2)
C(1)-S(1)-Ba(1)	80.4(3)
C(6)-S(6)-Ba(1)	93.9(3)
C(7)-S(7)-Ba(2)	117.8(2)
C(9)-S(9)-Ba(1)	82.7(3)
C(10)-S(10)-Ba(2)	98.7(3)
C(2)-N(1)-C(1)	121.9(7)
C(2)-N(2)-C(3)	124.1(6)
C(1)-N(3)-C(3)	121.4(6)
C(1)-N(3)-Ba(1)	102.3(4)
C(3)-N(3)-Ba(1)	127.7(5)
C(5)-N(4)-C(4)	122.0(7)
C(5)-N(5)-C(6)#2	122.2(6)
C(4)-N(6)-C(6)#2	120.2(6)
C(8)-N(7)-C(7)	122.8(7)
C(8)#1-N(8)-C(9)	122.7(6)
C(7)#1-N(9)-C(9)	121.3(7)
C(7)#1-N(9)-Ba(1)	133.7(5)
C(9)-N(9)-Ba(1)	104.6(5)
C(11)#2-N(10)-C(10)	122.4(7)
C(11)-N(11)-C(12)	124.0(6)
C(10)#1-N(12)-C(12)	120.8(6)
N(3)-C(1)-N(1)	120.1(7)
N(3)-C(1)-S(1)	121.4(6)
N(1)-C(1)-S(1)	118.4(6)
N(1)-C(2)-N(2)	115.2(6)
N(1)-C(2)-S(2)	122.5(6)

Table 52 cont.

N(2)-C(2)-S(2)	122.3(6)
N(3)-C(3)-N(2)	117.0(7)
N(3)-C(3)-S(3)	123.7(6)
N(2)-C(3)-S(3)	119.3(6)
N(6)-C(4)-N(4)	120.7(7)
N(6)-C(4)-S(4)	121.9(6)
N(4)-C(4)-S(4)	117.5(6)
N(4)-C(5)-N(5)	115.8(6)
N(4)-C(5)-S(5)	122.2(6)
N(5)-C(5)-S(5)	122.0(6)
N(6)#1-C(6)-N(5)#1	119.1(7)
N(6)#1-C(6)-S(6)	122.6(6)
N(5)#1-C(6)-S(6)	118.2(6)
N(9)#2-C(7)-N(7)	118.5(7)
N(9)#2-C(7)-S(7)	124.2(6)
N(7)-C(7)-S(7)	117.3(5)
N(8)#2-C(8)-N(7)	116.5(6)
N(8)#2-C(8)-S(8)	122.9(6)
N(7)-C(8)-S(8)	120.5(6)
N(9)-C(9)-N(8)	118.0(7)
N(9)-C(9)-S(9)	123.6(6)
N(8)-C(9)-S(9)	118.4(6)
N(12)#2-C(10)-N(10)	119.5(7)
N(12)#2-C(10)-S(10)	121.4(6)
N(10)-C(10)-S(10)	119.1(6)
N(11)-C(11)-N(10)#1	115.6(6)
N(11)-C(11)-S(11)	122.9(6)
N(10)#1-C(11)-S(11)	121.4(6)
N(12)-C(12)-N(11)	117.5(6)
N(12)-C(12)-S(12)	122.5(6)
N(11)-C(12)-S(12)	119.9(5)
Ba(2)-O(1)-Ba(1)	109.5(2)
Ba(1)-O(2)-Ba(2)	116.7(2)
Ba(2)#1-O(3)-Ba(1)	117.3(2)
Ba(2)#1-O(5)-Ba(1)	109.4(2)

Symmetry transformations used to generate equivalent atoms: #1 x-1, y, z #2 x+1, y, z

Table 53. Anisotropic displacement parameters ($Å^2$ x 10^3) for $BaH_4(C_3N_3S_3)_2 \cdot 4.5H_2O$. The anisotropic displacement factor exponent takes the form: $-2\pi^2$ [$(ha^*)^2 U_{11} + ... + 2hka^*b^* U_{12}$]

	U11	*U22*	*U33*	*U23*	*U13*	*U12*
Ba(1)	24(1)	21(1)	26(1)	-3(1)	-5(1)	2(1)
Ba(2)	26(1)	39(1)	25(1)	3(1)	-4(1)	2(1)
S(1)	39(1)	21(1)	27(1)	4(1)	-15(1)	-2(1)
S(2)	57(2)	22(1)	31(1)	7(1)	-14(1)	-13(1)
S(3)	46(1)	26(1)	30(1)	2(1)	-12(1)	-12(1)
S(4)	43(1)	24(1)	23(1)	8(1)	-13(1)	-5(1)
S(5)	54(2)	19(1)	27(1)	8(1)	-13(1)	-9(1)
S(6)	42(1)	26(1)	34(1)	2(1)	-10(1)	-12(1)
S(7)	40(1)	20(1)	22(1)	-4(1)	-14(1)	3(1)
S(8)	48(1)	19(1)	30(1)	-10(1)	-13(1)	9(1)
S(9)	36(1)	22(1)	26(1)	-1(1)	-9(1)	5(1)
S(10)	45(1)	35(1)	22(1)	-8(1)	-15(1)	6(1)
S(11)	50(1)	22(1)	27(1)	-6(1)	-11(1)	12(1)
S(12)	42(1)	26(1)	27(1)	0(1)	-5(1)	11(1)
N(1)	35(4)	17(4)	22(4)	6(3)	-6(3)	-1(3)
N(2)	36(4)	12(4)	24(4)	2(3)	-11(3)	-13(3)
N(3)	27(4)	18(4)	22(4)	3(3)	-9(3)	-3(3)
N(4)	38(4)	16(4)	22(4)	8(3)	-7(3)	0(3)
N(5)	37(4)	18(4)	24(4)	2(3)	-7(3)	-12(3)
N(6)	37(4)	22(4)	26(4)	6(3)	-2(3)	1(4)
N(7)	38(4)	23(4)	15(4)	-5(3)	-13(3)	-3(3)
N(8)	37(4)	10(3)	26(4)	-6(3)	-6(3)	5(3)
N(9)	25(4)	25(4)	18(4)	0(3)	-10(3)	4(3)
N(10)	36(4)	22(4)	25(4)	-6(3)	-5(3)	0(3)
N(11)	31(4)	12(3)	21(3)	-8(3)	-4(3)	9(3)
N(12)	32(4)	13(4)	22(4)	1(3)	0(3)	-1(3)
C(1)	17(4)	15(4)	30(5)	0(4)	0(4)	8(4)
C(2)	50(5)	22(5)	19(5)	9(4)	-1(4)	5(5)
C(3)	30(5)	17(5)	30(5)	5(4)	-7(4)	8(4)
C(4)	32(5)	19(5)	16(4)	1(4)	-2(4)	7(4)
C(5)	33(5)	16(4)	19(5)	0(4)	0(4)	1(4)
C(6)	37(5)	22(5)	17(5)	-5(4)	-3(4)	-5(4)
C(7)	33(5)	12(5)	24(5)	12(4)	-2(4)	-5(4)
C(8)	34(5)	15(5)	26(5)	-11(4)	-5(4)	-3(4)
C(9)	14(4)	25(5)	40(5)	7(4)	3(4)	-10(4)

Table 53 cont.

C(10)	20(4)	27(5)	24(5)	1(4)	-4(4)	-7(4)
C(11)	37(5)	21(5)	13(5)	-1(4)	-5(4)	-3(4)
C(12)	28(4)	18(5)	16(5)	3(3)	-8(4)	-3(4)
O(1)	36(3)	29(3)	44(4)	-8(3)	-1(3)	-7(3)
O(2)	32(3)	23(3)	19(3)	-2(2)	-6(2)	-2(2)
O(3)	24(3)	24(3)	28(3)	-1(2)	-3(2)	1(2)
O(4)	63(4)	25(4)	59(4)	3(3)	-1(3)	0(3)
O(5)	31(3)	30(3)	36(3)	6(3)	-4(3)	4(3)
O(6)	55(4)	64(5)	49(4)	-19(3)	10(3)	-17(4)
O(7)	54(4)	42(4)	49(4)	1(3)	8(3)	-7(3)
O(8)	44(4)	52(4)	40(4)	10(3)	0(3)	12(3)
O(9)	68(5)	154(8)	44(5)	-29(5)	1(4)	8(6)

REFERENCES CITED

REFERENCES CITED

Adewuyl, Y. G., and Carmichael, G. R., 1987, Kinetics of hydrolysis and oxidation of carbon disulfide by hydrogen peroxide in alkaline medium and application of carbonyl sulfide: Environmental Science & Technology, v. 21, no. 2, p.170-177.

Ainscough, E.W., Brodie, A.M., Coll, R.K., Mair, A.J.A., and Waters, J.M., 1993, The synthesis and single-crystal X-ray structure of $[\{Os_3H(CO)_{10}\}_3(S_3C_3N_3)]$; a novel osmium cluster containing three linked osmium triangles: Inorganica Chimica Acta, v. 214, p. 21-22.

Allen, F. H., Kennard, O., Watson, D. G., Brammer, L., Orpen, A. G., and Taylor, R., 1987, Tables of bond lengths determined by x-ray and neutron diffraction, Part 1: Bond lengths in organic compounds: Journal of the Chemical Society, Perkin Transactions, II, p. S1-S19.

Allison, J. D., Brown, D. S., and Novo-Gradac, K. J., 1991, MINTEQA2/PRODEFA2, a geochemical assessment model for environmental systems: version 3.0 user's manual. Environmental Research Laboratory, Office of Research and Development, U. S. Environmental Protection Agency, Athens, GA.

American Society for Testing and Materials (ASTM), 1991, Annual book of ASTM standards, Philadelphia, Pennsylvania.

American Society for Testing and Materials (ASTM), 1992, Annual book of ASTM standards, Philadelphia, Pennsylvania.

Anderson, A., ed., 1973, The Raman effect, volume 2, applications: Marcel Dekker, Inc., New York, p. 405-1033.

Andersson, A., 1979, Mercury in soils, in Nriagu, J. O., ed., The biochemistry of mercury in the environment: Elsevier/North-Holland Biomedical Press, Amsterdam, v. 3, p. 79-112.

Appleman, D. E. and Evans, H. T., 1973, Indexing and least squares refinement of powder diffraction data: U.S. Geological Survey Report PB 216188, U.S. Department of Commerce, National Technical Information Service, 5285 Port Royal Road, Springfield, Virginia 22151.

Ayoub, G. M., Koopman, B., Bitton, G., and Riedesel, K., 1995, Heavy metal detoxification by trimercapto-s-triazine (TMT) as evaluated by a bacterial enzyme assay: Environmental Toxicology and Chemistry, v. 14, no. 2, p. 193-196.

Bailar, J. C., Emeléus, H. J., Nyholm, R., and Trotman-Dickenson, A. F., 1973, Comprehensive inorganic chemistry: v. 1, Pergamon Press, Oxford, England, 1487p.

Bloss, F. D., 1971, Crystallography and crystal chemistry, an introduction: Holt, Rinehart and Winston, Inc., New York, 545p.

Boultif, A. and Louer, D., 1991, Indexing of powder diffraction patterns for low symmetry lattices by the successive dichotomy method: Journal of Applied Crystallography, v. 24, 987-993.

Brown, W.H., 1988, Introduction to organic chemistry, 4th ed., Brooks/Cole Publishing Co., Pacific Grove, California, 536p.

Chudy, J. C. and Dalziel, J. A. W., 1975, Metal complexes of 1,3,5-triazine-2,4,6-trithiol: Journal of Inorganic and Nuclear Chemistry, v. 37, p. 2459-2461.

Claësson (Klason), P., 1884, Öfver di- och trithiocyanursyra: Bihang Till K. Svenska Vet.-Akad. Handlingar, v. 9, no. 17, 21p.

Clesceri, L.S., A.E. Greenberg and R.R. Trussell, eds., 1989, Standard methods for the examination of water and wastewater: 17th ed., American Public Health Association. Washington, DC.

Clement Associates, 1989, Toxicological profile for mercury: National Technical Information Service, PB90-181256, Springfield, Virginia.

Code of Federal Regulations (CFR), U.S. Government Printing Office, Superintendent of Documents, Washington, DC.

Cole, H.S., Hitchcock, A.L., and Collins, R., 1992, Mercury warning - The fish you catch may be unsafe to eat: A study of mercury contamination in the United States: Clean Water Fund, Clean Water Action, 1320 18th Street, NW, Washington, DC 20036.

Cotton, F. A. and Wilkinson, G., 1972, Advanced inorganic chemistry: 3rd edition, Interscience Publishers, a Division of John Wiley & Sons, New York, 1145p.

Davis, J. C., 1986, Statistics and data analysis in geology: 2nd edition, John Wiley & Sons, New York, 646p.

Degussa Corporation, 1993, Data sheets on TMT-15 and TMT-55, Ridgefield Park, New Jersey 07660.

de Wolff, P. M., 1968, A simplified criterion for the reliability of a powder pattern indexing: Journal of Applied Crystallography, v. 1, p. 108-113.

Douglas, J., 1991, Mercury in the environment: EPRI Journal, p. 4-11.

Drozdov, A.A., Troyanov, S. I., Pisarevsky, A. P., and Struchkov, Yu. T., 1994a, New oligomeric mixed ligand barium chelates containing additional anionic ligands: Polyhedron, v. 13, no. 9, p. 1445-1452.

Drozdov, A.A., Troyanov, S. I., Pisarevsky, A. P., and Struchkov, Yu. T., 1994b, Synthesis and crystal structure of hydrated barium 2,2,6,6-tetramethylheptanedionate $[Ba_6(thd)_{12}(H_2O)_{13}]$: Polyhedron, v. 13, no. 15-16, p. 2459-2461.

Durst R. A., ed., 1969, Ion-selective electrodes., National Bureau of Standards Special Publication 314, Washington, DC.

Engler, R., and Gattow, G., 1972, Untersuchungen über Thioameisensäuren: 3. Darstellung und Eigenschaften der Dithioameisensäure: Zeitschrift für Anorganische und Allgemeine Chemie, v. 389, p. 145-150.

ETUS, Inc., 1994, Product information of Thio-Red®: Sanford, Florida, 32771.

Faure, G., 1991, Principles and applications of inorganic geochemistry: MacMillan, NewYork, 626p.

Fetter, C. W., 1993, Contaminant hydrogeology: Prentice Hall, Upper Saddle River, New Jersey 07458, 458p.

Garvey, R. G., 1986, LSUCRI least squares unit cell refinement for the personal computer: Powder Diffraction, v. 1, p. 114.

Gattow, G. and Krebs, B., 1963, Das Kohlenstoffsulfid-di-(Hydrogensulfid) $SC(SH)_2$ und das System H_2S-CS_2: 3. Trithiokohlensäure H_2CS_3 in wäßriger Lösung: Zeitschrift für Anorganische und Allgemeine Chemie, v. 323, p. 13-27.

Harte, J., Holdren, C., Schneider, R., and Shirley, C., 1991, Toxics A to Z, University of California Press, Berkeley, p. 229.

Henke, K. R. and Atwood, D. A., in press, Group 2 complexes of 2,4,6-trimercaptotriazine (TMT): Inorganic Chemistry.

Henke, K.R.; Bryan, J.C.; and Elless, M.P., 1997, Structure and powder diffraction pattern of 2,4,6-trimercapto-s-triazine, trisodium salt ($Na_3S_3C_3N_3 \cdot 9H_2O$): Powder Diffraction, v. 12, no. 1, March, p. 7-12.

Henke, K. R., Kühnel, V., Stepan, D. J., Fraley, R. H., Robinson, C. M., Charlton, D. S., Gust, H. M., and Bloom, N. S., 1993, Critical review of mercury contamination issues relevant to manometers at natural gas industry sites: GRI-93/0117, Gas Research Institute, Chicago, 110 p.

Hirt, R. C., Schmitt, R. G., Strauss, H. L., and Koren, J. G., 1961, Spectrophotometrically determined ionization constants of derivatives of symmetric triazine: Journal of Chemical and Engineering Data, v. 6, no. 4, p. 610-612.

Hofmann, A. W., 1885, Ueber die Sulfocyanursäure: Berichte der Deutschen Chemischen Gesellschaft, v. 18, p. 2196-2207.

Ingram, G., and Toms, B. A., 1957, The hydrolysis of sodium thiocarbonate and its reaction with ethanol: Journal of the Chemical Society (London), pt. 4, p. 4328-4344.

Ivanov, S., N. Snezko, A. Ilyukhin, and V. Sergienko, 1997, Synthesis and x-ray crystal structure of a barium complex with 2 methoxy 2,6,6 trimethylheptane 3,5 dionate: Polyhedron, v. 16, no. 14, p. 2527-2530.

Johri, K. N., Kaushik, N. K., and Singh, K., 1970, Thermogravimetric analysis of some metal thiocarbonates and sulfides obtained with potassium thiocarbonate (PTC) reagent: Journal of Thermal Analysis, v. 2, p. 37.

Keppel, G., 1991, Design and analysis, a researcher's handbook: 3rd edition, Prentice Hall, Englewood Cliffs, New Jersey 07632, 594p.

Krauskopf, K. B., 1979, Introduction to geochemistry: 2nd edition, McGraw-Hill Book Company, New York, 617 p.

Kriger, A. and Turner, R. R., 1995, Field analysis of mercury in water, sediment and soil using static headspace analysis: Water, Air and Soil Pollution, v. 80, n. 1-4, p. 1295-1304.

March, J., 1985, Advanced organic chemistry: reactions, mechanisms, and structure: 3rd ed., John Wiley & Sons, New York, 1346p.

Maurin, M., 1961, Contribution a l'étude des propriétés du trithiocarbonate de sodium CS_3Na_2 hydrates formés en présence de vapeur d'eau: Annales de Chimie, v. 6, series 13, p. 1221-1278.

Mereiter, K. and Preijinger, A., 1982, Barium thiocyanate trihydrate: Acta Crystallographica, v. B38, p. 382-385.

Mighell, A. D., Hubbard, C. R. and Stalick, J. K., 1981, NBS*AIDS80: a FORTRAN program for crystallographic data evaluation: National Bureau of Standards (USA) Technical Note 1141.

Moody, G. J., and Thomas, J. D. R., 1971, Selective ion sensitive electrodes, Merrow, Shildon Co. Durham, Great Britain.

Nakamoto, K., 1986, Infrared and Raman spectra of inorganic and coordination compounds: 4th edition, John Wiley & Sons, New York, 484 p.

Nebergall, W. H., Schmidt, F. C., and Holtzclaw, H. F., Jr., 1976, College chemistry: 5th edition, D.C. Heath and Company, Lexington, Massachusetts, 1058 p.

O'Donoghue, I. G., and Kahan, Z., 1906, Thiocarbonic acid and some of its salts: Journal of the Chemical Society (London), v. 89, p. 1812.

Orion Research Inc., 1991, Model 94-16 silver/sulfide electrode instruction manual: Boston, Massachusetts.

Padmanabhan, V.M., Busing, W. R., and Levy, H. A., 1978, Barium chloride dihydrate by neutron diffraction: Acta Crystallographica, v. B34, p. 2290-2292.

Peyton, T.O., Steele, R.V., and Mabey, W.R., 1976, Carbon disulfide, carbonyl sulfide: literature review and environmental assessment: Final Report, contract no. 68-01-2940, task 023, U.S. Environmental Protection Agency, Washington, DC 20460, 58p.

Ramamoorthy, S., Cheng, T.C., and Kushner, D.J., 1982, Effect of microbial life stages on the fate of methylmercury in natural waters: Bulletin of Environmental Contamination and Toxicology, v. 29, no. 2, p. 167-173.

Rietveld, H.M., 1967, Line profiles of neutron powder-diffraction peaks for structure refinement: Acta Crystallographica, v. 22, p. 151-152.

Rietveld, H.M., 1969, A profile refinement method for nuclear and magnetic structures: Journal of Applied Crystallography, v. 2, p. 65-71.

Sacerdoti, M., Bertolasi, V., Ferretti, V. and Accorsi, C. A., 1990, A redetermination of the crystal structure of barium hydroxide octahydrate $Ba(OH)_2 \cdot 8H_2O$: Zeitschrift für Kristallographie, v. 192, p. 111-118.

Siemens Industrial Automation, Inc., 1994, SHELXTL: version 5, Madison, Wisconsin.

Sittig, M., 1985, Handbook of toxic and hazardous chemicals and carcinogens: 2nd edition, Noyes Publications, Park Ridge, New Jersey, 950p.

Smith, G. S. and Snyder, R. L., 1979, F_N: a criterion for rating powder diffraction patterns and evaluating the reliability of powder-pattern indexing: Journal of Applied Crystallography, v. 12, p. 60-65.

Smith, K. L. and Smith, D. K., 1993, Micro-POWD: version 2.31, Materials Data Inc., Livermore, California.

Snoeyink, V.L. and Jenkins, D., 1980, Water chemistry: John Wiley & Sons, New York, 463 p.

Šolc, J., Harju, J. A. and Grisanti, A. A., 1997, Field analytical techniques for mercury in soils - technology evaluation: GRI-97/0146, Gas Research Institute, Chicago, 109 p.

Stolzenburg, T.R., Stanforth, R.R., and Nichols, D.G., 1986, Potential health effects of mercury in water supply wells: Journal of the American Water Works Association, v. 78, no. 1, p. 45-48.

Stout, G. H. and Jensen, L. H., 1989, X-ray structure determination: a practical guide: 2nd edition, John Wiley & Sons, New York, 467p.

Tarabocchia, J. and Karg, A., 1990, Printed circuit waste treatment removes metals, reduces costs: Plating and Surface Finishing, February, p. 24-26.

U. S. Environmental Protection Agency, 1990, Test methods for evaluating solid wastes: SW-846, November revision, Office of Solid Waste and Emergency Response, U. S. Environmental Protection Agency, Washington, DC 20460.

Werner, P.-E., 1969, A Fortran program for least-squares refinement of crystal-structure cell dimensions: Arkiv för Kemi, v. 31, no. 43, p. 513-516.

Werner, P.-E., Eriksson, L., and Westdahl, M., 1985, TREOR, a semi-exhaustive trial-and-error powder indexing program for all symmetries: Journal Applied Crystallography, v. 18, p. 367-370.